Development and Application of Non-iterative Methods for Calculation of Electric Response Properties within Density Functional Theory

THE THESIS SUBMITTED TO THE

UNIVERSITY OF PUNE

FOR THE DEGREE OF

DOCTOR OF PHILOSOPHY
IN CHEMISTRY

By

SAPANA VITTHAL SHEDGE

Dr. SOURAV PAL
(Research Guide)

Physical Chemistry Division

National Chemical Laboratory

Pune-411008

INDIA

May-2012

DECLARATION

I, Sapana Vitthal Shedge, hereby declare that the work incorporated in this thesis entitled,

Development and application of non-iterative methods for calculation of electric response properties within density functional theory

submitted by me for the degree of Doctor of Philosophy to the University of Pune is the record of the work I have carried out at the Physical Chemistry Division, National Chemical Laboratory, Pune – 411 008 from October, 2009 to December, 2011 under the supervision of Dr. Sourav Pal, is original and has not formed the basis of award of any degree or diploma.

I further declare that the material obtained from other sources has been duly acknowledged in this thesis.

Date:

_____

Sapana Vitthal Shedge
Physical Chemistry Division,
National Chemical Laboratory,
Pune – 411 008

Dedicated to

my parents

Acknowledgement

Take life slowly and deliberately,
making sure to acknowledge the people
who have helped you succeed along the way.
-Ted Levine

I would like to express my deepest gratitude to my advisor, Dr. Sourav Pal, who has supported me throughout my thesis with patience and guided me by his immense knowledge. I thank him for allowing and giving me opportunity to work independently and add value to the research work. His enthusiastic teaching of quantum chemistry and density functional theory has provided me a strong foundation of the subject. I was always motivated by his words "one should practice teaching for doing quality research". His trust and confidence in my knowledge and ability has been a motivating factor during my research work. Without his support and guidance this thesis would not have been possible. I am extremely thankful and proud to get an opportunity to work with him. Besides scientific discussions I have also enjoyed teatime gossips on various topics. One simply could not wish for a better and friendlier supervisor.

Many of the practical implementations of the work have been done by collaboration with Prof. Andreas Köster, Mexico. I benefited a lot from the discussions with him on many aspects of the present area of research. One of the major milestones in research work was introduction to deMon software at programming level. I am extremely thankful to him for giving me this opportunity and for his vital support at every juncture.

I take this opportunity to thank the Director of NCL for giving me the right place to pursue my research. I am also grateful to Dr. Anil Kumar, Head Physical Chemistry Division. I would like to thank the NCL library for providing the facility of reading various journals and books.

I acknowledge Prof. S. R. Gadre and Dr. S. P. Gejji for introducing me to quantum chemistry and computational chemistry. I would also like to record my sincere gratitude to department of chemistry where I took my first lesson of research.

I am grateful to Dr. Nayana Vaval for support and encouragement during my stay in laboratory. She was always a friend and well wisher. I also thank Dr. Sailaja Krishnamuthy for her healthy suggestions and fruitful discussions. I acknowledge Dr. Kumar Vanka and Dr. Neelanjana Sengupta for their valuable comments during group presentations which helped me improve at various levels. I thank all ESTG group members for their assistance.

I acknowledge the financial support from J. C. Bose Grant of Dr. Sourav Pal and Council of Science and Industrial Research for direct SRF. I also acknowledge DST-CONACYTE for Indo-Mexico project grant and foreign travel grant for supporting me to visit Mexico and Bremen, Germany.

My thanks goes to Mr. Deepak Jori, Miss Khare and Mrs. Asha Shinde, secretaries, director office, NCL for their kind help over many official issues. I can't forget to mention here Mr. Punekar and Mr. Gulab for their timely help and quick support where ever required.

In my daily work I have been blessed with a friendly and cheerful group of fellow students. I thank them all for their association and help. My special thanks to Sophy for her guidance in the early stage of my work. Thanks to my seniors Prashant, Arijit, Tuhina, Bhakti, Lalitha, Sumantra, Himadri (Sr.) for making me comfortable in lab. Special thanks to Subrata and Rahul for the discussions on various issues of chemistry and quantum chemistry. I thank Deepti for treating me more as a friend than a junior. I must thank Debarati, Mudit and Jitendra for their friendship. I enjoyed the nice time spent with Sayali. I thank her for always willing to help and cheering me in bad times, she is a wonderful friend. I also thank my juniors Kamalika, Anagha, Susanta, Achintya, Aarya, Himadri (Jr.) and Manzoor for their cheerful company. There are plenty of enjoyable moments and fun-full of memories which cannot be forgotten.

It is difficult to express in words my gratitude for my parents; they strongly supported me and encouraged me during my education. Their endless patience, encouragement and understanding gave me strength to stand firm in all circumstances. I can't forget to mention my brother for being a good friend. I thank my in-laws for understanding my aspirations and supporting me during the crucial period of my thesis writing. My special thanks go to my husband, Paritosh, who taught me to be positive in any situation. His love, support and faith always encouraged me to go ahead on my path. I dedicate this thesis to my mom, dad and Paritosh.

-Sapana

Contents

List of Abbreviations

The following abbreviations, in alphabetical order, have been used in this thesis:

ADFT	Auxiliary Density Functional Theory
ADPT	Auxiliary Density Perturbation Theory
AIMD	*Ab initio* molecular dynamics
BLYP	Becke, Lee, Yang and Parr
BOA	Born-Oppenheimer approximation
BOMD	Born-Oppenheimer molecular dynamics
BWPT	Brillouin-Weigner perturbation theory
CC	Coupled-cluster
CCD	Coupled-cluster doubles
CCSD	Coupled-cluster singles and doubles
CCSDT	Coupled-cluster singles, doubles and triples
CGTO	Cartesian Gaussian type of orbitals
CI	Configuration interaction
CID	Configuration interaction doubles
CIDi	Circular intensity difference
CISD	Configuration interaction singles and doubles
CISDT	Configuration interaction singles, doubles and triples
CISDT	Configuration interaction singles, doubles, triples and quadruples
CPMD	Car-Parrinello
CPHF	Couple-perturbed Kohn-Sham
CPKS	Coupled perturbed Kohn-Sham
deMon	density of Montréal
DFT	Density functional theory
EN	Epstein-Nebset
FCC	Full coupled-cluster
FF	Finite-field
GGA	Generalized gradient approximation
HF	Hartree-Fock

HK	Hohenberg-Kohn
KS	Kohn-Sham
LCGTO	Linear combination of Gaussian type of orbitals
LDA	Local density approximation
LR-TDDFT	linear response time-dependent density functional theory
MBPT	Many- body perturbation theory
MCSCF	Multi configuration self consistent field
MC	Monte-Carlo
MD	Molecular dynamics
MP	Møller-Plesset
NIA-CPKS	Non-iterative approximation to coupled-perturbed Kohn-Sham
NLO	Non-linear optical properties
PBE	Perdew, Burke and Ernzerhof
PES	Potential energy surface
PSPT	Rayleigh-Schrödinger perturbation theory
RHF	Restricted Hartree-Fock
RKS	Restricted Kohn-Sham
ROA	Raman Optical Activity
ROHF	Restricted open-shell Hartree-Fock
ROKS	Restricted open-shell Kohn-Sham
RPA	Random phase approximation
SCP	Self consistent perturbation theory
TDSCF	time-dependent self consistent field
TDHF	Time dependent Hartree-Fock
TDDFT	Time dependent density functional theory
TF	Tomas-Fermi
TFD	Tomas-Fermi-Dirac
TFW	Tomas-Fermi-Weizsacker
UHF	Unrestricted Hartree-Fock
UKS	Unrestricted Kohn-Sham
VROA	Vibrational Raman optical activity
VWN	Vosko-Wilk-Nusair

List of Figures

List of Tables

List of publications

1. "Noniterative density functional response approach: application to non-linear optical properties of *p*-nitroaniline and its methyl-substituted derivatives"
   K. B. Sophy, **Sapana V. Shedge**, and Sourav Pal
   ***J. Phys. Chem. A* 2008*, 112,* 11266–11272**

2. "Comparison of the auxiliary density perturbation theory and the non-iterative approximation to the coupled perturbed Kohn-Sham Method: case study of the polarizabilities of disubstituted azoarene molecules"
   Sapana V. Shedge, Javier Carmona-Espíndola, Sourav Pal and Andreas M. Köster
   ***J. Phys. Chem. A* 2010*, 114,* 2357–2364**

3. "Auxiliary density perturbation theory and non-iterative approximation to coupled-perturbed Kohn-Sham approach for dipole-quadrupole polarizability calculation"
   Sapana V. Shedge, Sourav Pal, Andreas M. Köster
   ***Chem. Phys. Lett.* 2011*, 510,* 185-190**

4. "Behaviour of density functional theory at stretched geometries of molecules"
   Sapana V. Shedge, Sayali P. Joshi, Sourav Pal
   ***Theor. Chem. Acc.* 2011*, 131,* 1094-1103**

5. "Theoretical study of frequency and temperature dependence of dipole-quadrupole polarizability of P_4 and adamantane"
   Sapana V. Shedge, Sourav Pal, Andreas M. Köster
   In preparation

Abstract

The main objective of this thesis is to develop non-iterative method for calculation of electric response properties such as polarizabilities, hyperpolarizabilities within density functional theory (DFT). The effect of a weak external perturbation on the electronic distribution of the molecule is reflected in its response properties. Dipole moment, polarizability and hyper-polarizability are the fundamental electric properties of molecule. These properties are widely studied due to the significance in identifying material with improved non-linear optical (NLO) properties [1].

For studying properties of large molecular systems, DFT is an obvious choice because of simplicity in applications. However, response properties using DFT have been calculated mainly using finite-field method. Recently, the non-iterative approach to response properties using DFT *i.e.* the non-iterative approximation to the coupled-perturbed Kohn-Sham (NIA-CPKS) [2-4] method has been developed with application to large molecules in mind. The presented work in this thesis focuses on the implementation of NIA-CPKS, for calculation of dipole-dipole polarizabilities and dipole-quadrupole polarizabililities.

CPKS is a standard method for calculation of the derivatives of the energy such as geometric derivatives, derivative with respect to magnetic field and electric field. Here in this thesis we focus mainly on energy derivative with respect to electric field, i.e. electric response properties. NIA-CPKS is the non-iterative approach developed within CPKS formalism. Here the derivative of the Kohn-Sham matrix is calculated numerically and used in CPKS equation for calculation of response density matrix. The electric polarizabilities can then be calculated as trace of response density with dipole or quadrupole moment integrals depending upon the kind of polarizability we want to calculate. This method has been implemented in deMon2k software which is based on KS-DFT [5]. We also present here the new implementation of NIA-CPKS in self consistent perturbation (SCP) formalism which is more efficient for calculation of polarizabiities [6]. The method has been validated by application to interesting class of systems and its comparison with higher level methods. We have also compared our method with another newly developed

analytical non-iterative method known as auxiliary density perturbation theory (ADPT)[7,8] implemented in deMon2k software. In this thesis, we present the application of our method for calculation of electric dipole-dipole polarizabilities, dipole-quadrupole polarizabilities. We have also studied here the frequency dependence and temperature dependence of dipole-qudrupole polarizabilities.

In one of the chapters we discussed the behaviour of DFT for electric response properties when the molecule is stretched along the bond axis [9]. The dipole-dipole and dipole-quadrupole polarizabilities calculated with different functional is presented. NIA-CPKS has been developed only for closed shell systems. In near future we aim to implement this method for application to open shell systems. The methodology for implementation of open shell NIA-CPKS is presented in this thesis. The geometric derivatives of the polarizabilities are important quantities in calculation of Vabrational Raman Optical Activity (VROA). Thus, we present here the methodology for implementation of geometric derivatives of the dipole-quadrupole polarizabilities within ADPT and NIA-CPKS.

The thesis is organized as follows:

Chapter 1: General overview and introduction to theoretical method.

In chapter one, we briefly review the theoretical methods available for electronic structure calculation. We discuss the wavefunction based methods, HF approximation and methods beyond Hatree-Fock approximation. This is followed by discussion about the early development of the density matrix theory and Kohn-Sham density functional theory (KS-DFT). Then we introduce here electric response properties and different methods available for calculation. We discuss about ADFT and basic structure of the deMon2k programme. We introduce the NIA-CPKS and ADPT method for calculation of polarizabilities.

Chapter 2: Calculation of static dipole-dipole polarizability from NIA-CPKS and its comparison with ADPT.

In chapter two, we present a theoretical study of the dipole-dipole polarizabilities of free and disubstituted azoarenes employing NIA-CPKS and its comparison with ADPT. Comparisons are made for disubstituted azoarenes, which shows push-pull mechanism. We study the effect of substitution of electron withdrawing and electron

donation group on dipole-dipole polarizabilities of azoarene molecules. We present the dipole-dipole polarizabilities of these molecules calculated with three different exchange-correlation functionals and two different auxiliary function sets. The computational advantages of both these methods are discussed here.

Chapter 3: Technical details of implementation NIA-CPKS version of SCP

Earlier implementation of NIA-CPKS was based on CPKS equation system. Here we present the technical details about new implantation of our approach in the framework of SCP method. This implementation is done for calculation of dipole-dipole and dipole-quadrupole polarizability. The advantages of implementation are discussed here. We briefly discuss the self consistent perturbation theory and ADPT implementation for calculation of perturbed density matrix. The chapter ends with the comparison of NIA-CPKS and ADPT.

Chapter 4: Calculation of dipole-quadrupole polarizabilities of tetrahedral molecules.

To validate the implementation of newer version of NIA-CPKS for calculation of dipole-quadrupole polarizabilities three tetrahedral molecules have been selected. The comparison between NIA-CPKS and ADPT results is presented for P_4, CH_4 and adamantane. We also report MP2 and CCSD results for comparison with our results to validate the methodology of our implementation. We study the basis set dependence of the dipole-quadrupole polarizability for selected set of molecules.

Chapter 5: *Ab initio* MD simulation of static and dynamic dipole-quadrupole polarizability.

The experimental values of dipole-quadrupole polarizabilities are measured at higher temperature and frequencies used for calculation. Therefore it is not always feasible to compare static polarizabilities obtained from theoretical methods with experimental results. In our earlier study we have observed the discrepancy between experimental and theoretical values of dipole-quadrupole polarizability of adamantane molecule. In this chapter we present the dipole-quadrupole polarizabilitie for different frequencies calculated with ADPT method. Molecular dynamic simulation will allow us to study the temperature dependence of these

polarizabilities and find the reason of discrepancy of our results from experimental values.

Chapter 6: Behaviour of DFT for electric response properties at distorted geometries of molecules.

We present here the rigorous calculation of electric response properties at distorted geometries of the molecules. We study here dipole-dipole polarizability and dipole-quadrupole polarizability for description of role of static and dynamic correlation for electric response properties. The calculations are performed with our new approach, non-iterative approximation to coupled-perturbed Kohn-Sham method (NIA-CPKS). These DFT results are compared with higher level *ab initio* such as CCSD and fully correlated full CI. We report here the dipole-dipole polarizability and dipole-quadrupole polarizability of HF, BH, H_2CO, CO and NO^+. We also present the effect of basis and functional on polarizability and dipole-quadrupole polarizability.

Chapter 7: Conclusions and future tasks

This chapter is based on final conclusion of the work presented in this thesis and discussion about the future work. The NIA-CPKS has been developed only for closed shell systems the extension of this approach for open shell system will facilitate in extending the scope of our method. Thus, the methodology of NIA-CPKS for UKS and ROKS is presented in this chapter. We also present the methodology to calculate dipole-dipole polarizability, dipole-quadrupole polarizability and electric–magnetic dipole polarizability derivatives with respect to nuclear coordinate's to simulation a VROA spectra.

References

1. Kanis, D. R.; Ratner, M. A.; Marks, T. J. *Chem. Rev*. **1994**, *94*, 195.
2. Sophy, K.B.; Pal, S. *J. Chem. Phys*. **2003** *118*, 10861.
3. Sophy, K.B.; Shedge, S.V.; Pal, S. *J. Phys. Chem. A* **2008,** *112*, 11266.
4. Shedge, S. V.; Carmona-Espíndola, J.; Pal, S.; Köster, A. M. *J. Phys. Chem. A*, **2010,** *114*, 2357.
5. Köster, A. M.; Calaminici, P.; Casida, M. E.; Flores, R.; Geudtner, G.; Goursot, A.; Heine, T.; Janetzko, F. M.; del Campo, J.; Patchkovskii, S.; Reveles, J. U.; Salahub, D. R.; Vela, A. *deMon2k, The deMon developers*; Cinvestav: Mexico City, Mexico, 2006. See http://www.demon-software.com
6. Shedge S. V.; Pal S.; Köster A. M. *Chem Phys Lett.* **2011**, *510*, 185.
7. Flores-Moreno, R.; Köster, A.M. *J. Chem. Phys.* **2008**, *128*, 134015.
8. Flores-Moreno, R. Ph.D. Thesis, Cinvestav, Mexico City, Mexico, 2006.
9. Shedge, S. V.; Joshi, S. P.; Pal, S. *Theor. Chem. Acc*. **2011 ,** *131*, 1094

CHAPTER 1

General overview and introduction to theoretical methods

1.1 Introduction

The electronic distribution of the molecule is affected by a weak electric perturbation and it can be analyzed with the study of electric response properties. Electric properties such as multipole moments, polarizabilities and hyperpolarizability are studied widely [1-3], due to their applicability in predicting long range atomic and molecular interactions [4]. These fundamental properties play an important role in designing new non-linear optical materials [5]. The higher polarizabilities such as dipole-quadrupole polarizabilities and dipole-octupole polarizabilities have been identified as dominant quantities in spectroscopic measurements such as interaction induced spectroscopy [6, 7] and surface-enhanced Raman scattering[8]. Thus a lot of interest lies in experimental and theoretical studies of electric properties of atoms and molecules. The experimental determinations of these multipole moments and polarizabilities are difficult and hence various theoretical methods have been developed for accurate calculation of these properties [9-16].

Density functional theory (DFT) [17-19] has been used extensively for calculating molecular response properties of a wide variety of atoms, molecules and

clusters. Many other approaches such as coupled-cluster (CC) and time-dependent self-consistent field (TDSCF) procedure [20, 21], the popular coupled-perturbed Hartree-Fock (CPHF) approach [22], and time-dependent Hartree-Fock (TDHF) based perturbation scheme[23] are available for property calculations. However, among these, DFT has been widely used. While the DFT approach is exact in principle, the popularity of the approach is mainly due to the simple working equations arising from the use of the electron density as the basic variable in the entire framework of the theory. Electron correlation effects and basis sets play important roles in the determination of response properties. DFT is well suited for large molecules and large basis sets and it takes care of electron correlation. However, it scales similarly to the Hartree-Fock theory in terms of computational demand when hybrid functionals are used. DFT calculations without such functionals can, with intelligent use of Fourier transforms or auxiliary basis sets, scale significantly better than Hartree-Fock (HF) method. The true practical applicability of DFT comes from the introduction of a fictitious non-interacting reference system as proposed by Kohn and Sham [24]. This circumvents the explicit construction of the unknown kinetic energy functional and guarantees the accuracy of the approach. Electric properties of molecules are studied to understand their response to an external weak perturbation. Typical examples are molecular dipole polarizabilities and hyperpolarizabilities. Several studies on molecules [25-35] and solids [36] have established that DFT is well suited for these property calculations. More recently, even temperature dependent polarizabilities were studied by first-principle DFT Born-Oppenheimer molecular dynamics (BOMD) simulations [37].

Most of these calculations have been done by using crude energy based numerical finite-field approach. These methods could be highly inaccurate for higher order energy derivatives such as polarizabilities and hyperpolarizabilities. However, the rigorous analytical results are available only for smaller molecules and smaller basis set. Therefore, there is a need to explore computationally feasible methods, which can handle large molecules with reasonable accuracy. The objective of this thesis is to develop a new method which simplifies the rigorous analytical method and gives reasonably accurate results of polarizabilities for large molecules with large basis. In this thesis, we present the non-iterative approach to response properties using DFT *i.e.* the non-iterative approximation to the coupled-perturbed Kohn-Sham (NIA-CPKS) [38-41]. The method has been developed with application

to large molecules in mind. Here we mainly focussed on implementation of NIA-CPKS for dipole-dipole polarizability and dipole-quadrupole polarizability in deMon2k software and its application to the interesting class of systems. To begin with, we introduce here the electric response properties, in section 1.1. We discuss various *ab initio* methods and evaluation of the response properties with these methods in section 1.2. In section 1.3 we present the detailed discussion about the density functional theory with special attention to Hohenberg-Kohn (HK) theorem, Kohn-Sham (KS) equation, and the different exchange-correlations functionals. In section 1.4 we discuss the calculation of response properties within DFT using CPKS formalism. We discuss here the non-iterative approach to solve the CPKS equation for calculation of dipole-dipole polarizability. The section 1.5, focuses mainly on the brief overview of auxiliary density functional theory (ADFT) and the auxiliary density perturbation theory (ADPT) developed within deMon2k. In section 1.6 we briefly review about the molecular dynamics (MD) and properties calculation within molecular dynamic simulation.

1.2 Introduction to electric response properties

Depending upon the type of perturbation the molecular properties can be categorised into various types. The perturbation can be due to external electric field, external magnetic field, nuclear magnetic moment or change in the nuclear geometry. In the presence of an arbitrary uniform electric field, the electron distribution of a molecule is distorted, thus it influences the wavefunction and leads to induced dipole moment, quadrupole moment etc. The Hamiltonian of such system depends upon the electric field perturbation. The perturbed Hamiltonian can be expressed as [42],

$$H(F) = H^0 - \mu_i F_i - \frac{1}{3}\theta_{ij} F_{ij} - \cdots \tag{1.1}$$

H^0 is the unperturbed Hamiltonian, μ_i and θ_{ij} are the dipole and quadrupole moment operators. F_i represents an electric field component and F_{ij} an electric field gradient, which denotes the non-homogeneous nature of the electric field. Energy and multipole moments also show explicit dependence on the electric field. According to Buckingham [43] and McLean and Yoshimine [44] the energy, dipole and

quadrupole moment of a molecule in terms of the static electric field can be written as,

$$E(F) = E^0 - \mu_i^0 F_i - \frac{1}{3}\Theta_{ij}^0 F_{ij} - \frac{1}{15}\Omega_{ijk}^0 F_{ijk} - \frac{1}{105}\Phi_{ijkl}^0 F_{ijkl} + \cdots$$
$$-\frac{1}{2}\alpha_{ij}F_iF_j - \frac{1}{3}A_{i,jk}F_iF_{jk} - \frac{1}{6}C_{ij,kl}F_{ij}F_{kl}$$
$$-\frac{1}{6}\beta_{ijk}F_iF_jF_k - \frac{1}{6}B_{ij,kl}F_iF_jF_{kl} + \cdots \quad (1.2)$$

$$\mu_i = \mu_i^0 + \alpha_{ij}F_j + \frac{1}{3}A_{i,jk}F_{jk} + \frac{1}{2}\beta_{ijk}F_jF_k + \frac{1}{3}B_{ij,kl}F_jF_{kl} + \cdots \quad (1.3)$$

$$\Theta_{ij} = \Theta_{ij}^0 + A_{k,ij}F_k + C_{ij,kl}F_{kl} + \frac{1}{2}B_{ij,kl}F_kF_l \quad (1.4)$$

Where E^0, μ^0, Θ^0, $\Omega^0$are the energy and permenant multiple moments of the free molecule, α_{ij} its dipole-dipole polarizability and β_{ijk} the corresponding (first) hyperpolarizability. $A_{k,ij}$ is the dipole-quadrupole polarizability and $B_{ij,kl}$ the dipole-dipole-quadrupole hyperpolarizability. The symmetry of the molecule reduces the number of components of above tensor quantities. For example a molecule belonging to T_d symmetry, there exist only one component of the octupole (Ω_{ijk}) and hexadecapole (Φ_{ijkl}) moment as well as of the dipole-dipole (α_{ij}) and dipole-quadrupole $(A_{k,ij})$ polarizability. In writing all the above expressions Einstein summation is used, with i and j spanning x, y and z directions.

It is clear from the energy expression that the dipole moment and polarizability of molecule are the first and second derivatives of ground state energy with respect to electric field perturbation at zero fields respectively. Similarly, dipole-quadrupole polarizability is the second derivative of energy with respect to electric field perturbation, F and field gradient, F' at their zero values.

$$\mu_i = -\left(\frac{\partial E}{\partial F_i}\right)_{F=0} \quad (1.5)$$

$$\alpha_{ij} = -\left(\frac{\partial^2 E}{\partial F_i \partial F_j}\right)_{F=0} \quad (1.6)$$

$$A_{i,jk} = -\left(\frac{\partial^2 E}{\partial F_i \partial F_{jk}}\right)_{F=0,F'=0} \quad (1.7)$$

The external electric field may either be time independent, which lead to static properties, or time dependent, leading to dynamic properties. Time-dependent fields are usually associated with electromagnetic radiation characterized by a frequency,

and static properties may be considered as the limiting case of dynamic properties when the frequency goes to zero.

According to Helmann-Feynman theorem [45,46], for the exact wavefunction and variational method the first derivative of energy with respect to electric field is equal to the expectation value of the derivative of the Hamiltonian. For electric properties, the first derivative of energy is equal to the expectation value of dipole moment operator. Further for a variational method, according to Wigner's (2n+1) rule [47], response up 3rd order can be calculated from the 1st order response of wave function or density.

1.3 Wavefunction based quantum chemical methods

The main objective of most quantum chemical approaches is to solve the time-independent, non-relativistic Schrödinger equation [48, 49]

$$\hat{H}\Psi_i\left(\vec{x}_1, \vec{x}_2, \ldots \vec{x}_N, \vec{R}_1, \vec{R}_2, \ldots \vec{R}_M\right) = E_i\Psi_i\left(\vec{x}_1, \vec{x}_2, \ldots \vec{x}_N, \vec{R}_1, \vec{R}_2, \ldots \vec{R}_M\right) \tag{1.8}$$

where $\hat{H}$ is the Hamiltonian operator for the total energy of the molecular system consisting of M nuclei and N electrons in the absence of magnetic or electric fields. It is composed of kinetic energy of constituent particles, potential energy due to attractive and repulsive interaction amongst the particles.

$$\hat{H} = -\frac{1}{2}\sum_{i=1}^{N}\nabla_i^2 - \frac{1}{2}\sum_{A=1}^{M}\frac{1}{M}\nabla_A^2 - \sum_{i=1}^{N}\sum_{A=1}^{M}\frac{Z_A}{|r_i - R_A|} + \sum_{i=1}^{N}\sum_{j>i}^{N}\frac{1}{|r_i - r_j|} + \sum_{A=1}^{M}\sum_{B>A}^{M}\frac{1}{|R_A - R_B|} \tag{1.9}$$

In the above equation, R_A and r_i are spatial coordinates of Ath nucleus and ith electron respectively. M_A is the ratio of the mass of nucleus A to the mass of an electron, and Z_A is the atomic number of nucleus A. The Laplacian operators ∇_i^2 and ∇_A^2 involve differentiation with respect to the coordinates of the ith electron and the Ath nucleus. The first term in Eq. (1.9) is the operator for the kinetic energy of the electrons; the second term is the operator for the kinetic energy of the nuclei; the third term

represents the coulomb attraction between electrons and nuclei; the fourth and fifth terms represent the repulsion between electrons and between nuclei, respectively. $\Psi_i(\vec{x}_1, \vec{x}_2, \ldots \vec{x}_N, \vec{R}_1, \vec{R}_2, \ldots \vec{R}_M)$ stands for the wave function of the ith state of the system, which depends on the 3N spatial coordinates $\{\vec{r}_i\}$, and the N spin coordinates1$\{\vec{s}_i\}$ of the electrons, which are collectively termed $\{\vec{x}_i\}$ and the 3M spatial coordinates of the nuclei, $\{\vec{R}_I\}$. The wave function contains all the information that can be possibly known about the system it describes. Ultimately, E_i is the numerical value of the energy of the state described by Ψ_i.

Solution of the eigenvalue problem Eq. (1.8) yields stationary state energies and the corresponding eigenfunctions. In absence of external perturbation, atoms and molecules are assumed to be in one of these states. It is however, very difficult to solve Eq. (1.8), even for small systems. Since, nuclei are much heavier than electrons, while considering electronic motions, they can virtually be assumed to be stationary. This is known as frozen-nuclei Born-Oppenheimer approximation (BOA) [50]. As a result of this approximation, the 1st term in Eq. (1.9), the kinetic energy of nuclei drops out and the inter-nuclear repulsion energy (third term in Eq. (1.9)) becomes constant. The constant added to an operator does not affect the eigenfunctions and simply adds to the eigenvalues. Thus the complete Hamiltonian given in equation (1.9) reduces to the so-called electronic Hamiltonian

$$\begin{aligned}\hat{H}_{elec} &= -\frac{1}{2}\sum_{i=1}^{N}\nabla_i^2 - \sum_{i=1}^{N}\sum_{A=1}^{M}\frac{Z_A}{|r_i - R_A|} + \sum_{i=1}^{N}\sum_{j>i}^{N}\frac{1}{|r_i - r_j|} + \sum_{A=1}^{M}\sum_{B>A}^{M}\frac{1}{|R_A - R_B|} \\ &= \hat{T} + \hat{V}_{Ne} + \hat{V}_{ee} \end{aligned} \quad (1.10)$$

The eigenvalues of the electronic Hamiltonian are the total electronic energies of the corresponding stationary states. The corresponding eigenfunctions are parametrically dependent on nuclear coordinates. The total energy E_{tot} is then the sum of E_{elec} and the constant nuclear repulsion term,

$$E_{tot} = E_{elec} + E_{nuc} \quad (1.11)$$

$$E_{nuc} = \sum_{A=1}^{M}\sum_{B>A}^{M}\frac{1}{|R_A - R_B|} \quad (1.12)$$

Addition of the inter-nuclear repulsion energy to the total electronic energy provides and effective potential energy surface (PES) $V_{eff}(R_1, R_2, \ldots R_M)$ of nuclear motion. The PES resulting from different electronic states is generally well separated and the interaction between two PES is negligible. Due to this, the nuclear motion is well separated from the electronic motion. Thus BOA turns to a very good approximation for electronic structure calculations as the problem of M + N entities reduces to N-electron problem with fixed nuclei. The concept of PES serves to bring back chemist's view of molecules, equilibrium structure, etc. in terms of energy.

However, even with BO approximation, it is difficult to solve a many electron problem. Except for few problems the Schrödinger equation cannot be solved exactly, so methods of approximation are needed in order to tackle these problems. The two basic methods of approximation are *variation* [51] and *perturbation* [48, 52, 53] theories. In variation theory, an initial guess is made as to the shape of the wavefunction, which is then optimized to approximate the true wavefunction for the problem. Thus variational principle gives the recipe for systematically approaching the wave function of the ground state Ψ_0, i. e., the state of lowest energy E_0. According to variational principle the energy computed as the expectation value of the Hamilton operator $\widehat{H}$ from any well behaved, guessed Ψ_{trial} will be an *upper bound* to the true energy of the ground state.

$$\frac{\langle \Psi_{trial}|H|\Psi_{trial}\rangle}{\langle \Psi_{trial}|\Psi_{trial}\rangle} = E[\Psi_{trial}] \geq E_0 \qquad (1.13)$$

The solution to Hatree-Fock and CI method is obtained variationally. In perturbation theory, the total Hamiltonian of the system is divided into two parts, a zeroth-order part, H_0which has known eigenfunctions and eigenvalues, and a perturbation, V. The wavefunctions from the part of the Schrödinger equation in which the solution is known are used as a starting point and then modified to approximate the true wavefunction for the Schrödinger equation of interest. Perturbation methods can be used in quantum mechanics for adding corrections to solutions that employ an independent-particle approximation, and the theoretical framework is then called *many body perturbation theory* (MBPT). The traditional coupled cluster method [54-58], is neither variational nor perturbative. This method has been established as the

state-of-the-art method for the description of many body systems in general and electronic structure theory in particular.

1.4 Hatree-Fock theory

HF is the central starting point for most *ab initio* quantum chemistry methods. The method assumes that the exact, *N*-body wave function of the system can be approximated by a single Slater determinant, an antisymmetrized product of one-electron wave functions (i.e., orbitals)[48,59,60].

$$\Phi_0(\vec{x}_1, \vec{x}_2 \ldots \vec{x}_N) = \left|\chi_i(x_1)\chi_j(x_2) \ldots . \chi_k(x_N)\right\rangle \tag{1.14}$$

By invoking the variational method, one can derive a set of *N*-coupled equations for the *N* spin orbitals. The method of Lagrange undetermined multipliers is used to minimize the energy with respect to the spin orbitals [48]. In the process, the spin-orbitals are varied under the constraint that the spin-orbitals form an orthonormal set. The variational minimization of energy with respect to choice of spin orbitals leads to Hartree-Fock equation. The Hartree-Fock equation is the eigen value equation

$$\hat{f}(\vec{x})\chi_a(\vec{x}) = \varepsilon_a\chi_a(\vec{x}) \tag{1.15}$$

Where

$$\hat{f}(\vec{x}) = \hat{T}_e + \hat{V}_{ne} + \upsilon_{HF}(\vec{x}) \tag{1.16}$$

$\hat{f}(\vec{x})$ is Fock operator, an effective one-electron Hamiltonian operator. It is sum of the kinetic energy operator $\hat{T}_e$, $\hat{V}_{ne}$, the nuclearelectronic interaction operator and $\upsilon_{HF}(\vec{x})$, the average potential experienced by an electrons due to motions of all other electrons.

$$\upsilon_{HF}(\vec{x}) = \sum_{j=1}^{N} J_j\,(\vec{x}) - \sum_{j=1}^{N} K_j(\vec{x}) \tag{1.17}$$

It includes the average Coulomb interaction defined by local operator $J_j(\vec{x})$ and a non-classical potential represented by a non-local operator $K_j(\vec{x})$ known as exchange potential. The exchange potential is consequence of the anti-symmetric nature of the wavefunction. The Fock operator being dependant on its eigenfunctions, the set of equations (1.15) - (1.17) are solved iteratively until some self consistency is achieved between successive equations. As a result a Slater

determinant corresponding to the best set of spin-orbitals and consequently the minimum energy or the ground state energy of the system is obtained.

For atoms, the HF equations can be exactly solved as integro-differential equations. For molecules, however, the explicit integration of the two-electron interaction terms is difficult as the orbitals involved are centred at different nuclei. Hence Roothan [61] introduced a finite set of Gaussian functions to define the spatial parts of atomic orbitals, which are then transformed to molecular orbital basis to achieve orthonormalization. For closed-shell systems, the spin-orbitals with opposite (spin-up and spin-down) spin functions are paired up and the problem can be simplified by using only spatial orbitals after spin-integration. This leads to Roothan-Hall equations and the method is known as restricted HF (RHF). The open-shell systems also have most of the electrons paired up and can be solved by restricted open-shell HF (ROHF) method. On the other hand, this simplification of electron pairing may not be considered and one may explicitly solve the HF equations using spin-orbitals. The method is called unrestricted HF (UHF) and leads to Pople-Nesbet equations. While an RHF or ROHF determinant is a pure eigenfunction of total spin operator, UHF determinant, in general, is not.

1.5 Electron correlation and post HF methods

The major simplification to the HF theory comes from independent particle picture by approximating wavefunction as a single Slatter determinant. HF theory only accounts for the average electron–electron interactions, and consequently neglects the correlation between electrons. Physically it corresponds to the motion of the electrons being correlated. The difference between exact energy and HF energy is called correlation energy as it arises due to partial ignorance of the electron-electron interactions. Though HF determinant recovers almost 99% of the total energy the remaining correlation energy is usually very important for describing chemical phenomena. Within the HF approximation the correlation between electrons with parallel spin is accounted by the electron exchange term. This type of correlation is called as Fermi correlation, which prevents two electrons of parallel spin being found at the same point in space. However, Coulomb correlation, the correlation between the electrons of apposite spin is neglected by the single determinant picture. The electron correlation can also be categorised as static and

dynamic correlation. The dynamic contribution is associated with the "instant" correlation between electrons, such as between those occupying the same spatial orbital. It is the correlation of the movement of electron. The static correlation is associated with electrons avoiding each other on a more "permanent" basis, such as those occupying different spatial orbitals. This is also called a near-degeneracy effect, as it becomes important for systems where different orbitals (configurations) have similar energies. Methods that include electron correlation require a multi-determinant wave function. Since HF is the best single determinant wave function for the ground state, it is generally used as starting guess for correlated methods. Multi-determinant methods are computationally much more involved than the HF model, but can generate results that systematically approach the exact solution of the Schrödinger equation. The correlation energy can be recovered by improving the approximations made in HF theory. This leads to various post HF theories which are collectively termed as many-body methods.

1.5.1 Configuration interaction

Configuration interaction (CI) wavefuction is expressed as a linear combination of ground and excited determinants. HF determinant is the ground state determinant and other determinants are defined as excitations with respect to HF occupancies [48, 62, 63]. Thus the configurations can be singly excited, doubly excited and so on, up to N-tuply excited with respect to HF configuration. The total wavefunction can thus be represented as

$$\Psi = \Phi_0 + \sum_{i\in occ}\sum_{a\in virt} C_i^a \Phi_i^a + \sum_{i,j\in occ}\sum_{a,b\in virt} C_{ij}^{ab}\Phi_{ij}^{ab} + \cdots \qquad (1.18)$$

Intermediate normalization has been used in the above expansion. The Φ_i^a indicates a singly excited determinant formed by excitation of electron from $i-th$ orbital (occupied) in HF determinant to the $a-th$ (virtual) orbital. Similarly, Φ_{ij}^{ab} indicates doubly excited determinant obtained by exciting the electrons from $i-th$ and $j-th$ orbitals to $a-th$ and $b-th$ orbitals respectively. When all possible excitations are considered in expansion the method is called as full CI. The corresponding coefficients are obtained using linear variation method. This leads to

eigenvalue problem for the Hamiltonian matrix. The matrix elements are calculated using Slater-Condon rules [48]. The lowest eigenvalue and the eigenvectors correspond to the ground state of the system and rest of them correspond to excited states of the system. The dimensions of the wavefunctions increase rapidly with the number of electrons as well as basis functions and practically, it becomes impossible to use FCI even for small molecules with moderate size basis sets. Thus truncation of the CI expansion solves the problem and one can get well-correlated wavefunctions and well-correlated energies as per the level of truncation. The expansion of the wavefunction formed by excluding all the configurations except HF and doubly excited configurations is known as CI doubles (CID). Truncation of CI expansion to doubles recovers most of the correlation energy. The molecular properties like dipole moments, polarizabilities, etc. are defined by one-electron operator. Hence the singly excited determinants can be included along with the doubly excited ones. The method is called CI singles and doubles (CISD) and describes the one-electron properties more accurately. Although singly excited determinants do not directly mix with HF, they interact through the doubly excited determinants and further improve the correlation energy. Accuracy can be improved by including the higher excited configurations leading to CISD and triples (CISDT), CISDT and quadruples (CISDTQ) and so on.

The truncation of CI expansion destroys the size-consistency and size-extensivity of the wavefunction. Size-consistency refers to additive separability of the energy during fragmentation, that is, if a molecule AB dissociates into its fragments A and B then energy of the system should follow the following relation

$$E_{AB} = E_A + E_B \tag{1.19}$$

Size-extensivity is related to scaling of the energy of the system with number of electrons. Due to non-interacting picture, HF energy properly scales with the number of electrons. Hence, size-extensivity is considered as a requirement of correlated methods. If total energy (and hence, the correlation energy) of a system approximately varies linearly with the number of electrons, the method is said to be size-extensive. The truncated CI has found to show the sub-linear dependence [48] of energy with the number of electrons, thus misinterpreting zero correlation energy per electron as the number of electrons tends to infinity.

1.5.2 Many body perturbation theory

The basic idea behind the perturbation theory is that the problem in hand is just slightly different than the problem that has been already solved either exactly or approximately [64-66]. In mathematical language this can be expressed by partitioning the Hamiltonian into two parts. First term is the reference term H_0 and second is the perturbation term, V, which is small compared to H_0. Thus the total Hamiltonian is written as

$$\widehat{H} = \widehat{H}_0 + \lambda V' \tag{1.20}$$

The reference term H_0 is the dominant part of the total Hamiltonian and its solution is known. H_0 is termed as zero[th] order Hamiltonian. The eigenfunctions $\{\Psi_i^0\}$ of $\widehat{H}_0$ form a complete se with the corresponding eigenvalues denoted by E_i^0. The second term, V, of equation 1.20 is unknown and it is viewed as a perturbation to the zero[th] order Hamiltonian. Perturbation method gives the systematic procedure for adding correction to solution that has been obtained from independent particle approximation. λ is the perturbation parameter which determine the strength of the perturbation. As the perturbation is increased from zero to a finite value, the energy and wave function must also change continuously, and they can be written as a Taylor expansion in powers of the perturbation parameter λ.

$$\Psi_i = \Psi_i^0 + \lambda\Psi_i^1 + \frac{\lambda^2}{2!}\Psi_i^2 + \frac{\lambda^3}{3!}\Psi_i^3 + \cdots$$

$$\mathrm{E}_i = \mathrm{E}_i^0 + \lambda\mathrm{E}_i^1 + \frac{\lambda^2}{2!}\mathrm{E}_i^2 + \frac{\lambda^3}{3!}\mathrm{E}_i^3 + \cdots \tag{1.21}$$

When $\lambda = 0$, $\mathrm{H} = \mathrm{H}_0$ and $\mathrm{E_i} = \mathrm{E_i^0}$ This is unperturbed or is zeroth order wavefunction and energy. at $\lambda = 1$ system is completely perturbed corresponding to the stationary states of the exact Hamiltonian. The $\Psi_\mathrm{i}^1, \Psi_\mathrm{i}^2$ .... and $\mathrm{E_i^1}, \mathrm{E_i^2}$ ..... are the first-order, second-order, etc., corrections. The parameter λ will eventually be set equal to 1, and the n[th]-order energy or wave function becomes a sum of all terms up to order n.

The MBPT is divided into various methods depending upon the way wavefunction at various orders is solved. The one developed by Brillouin and Wigner known as Brillouin-Wigner perturbation theory (BWPT) [66] and the other one developed by Rayleigh and Schrödinger known as Rayleigh-Schrödinger perturbation theory (RSPT) [64, 66, 67]. Both these approaches use Taylor series

expansion around the solutions of the zeroth order part. Also depending upon the partitioning of Hamiltonian there are two variants, namely Møller-Plessette (MP) and Epstein-Nesbet (EN) perturbation theories. In RSPT, the quantities in Eq. (1.21) are substituted in the Schrödinger equation. The terms with fixed power of V are then collected together and solved for energies and wavefunctions at various orders. In MP theory the zeroth-order wave function is an exact eigenfunction of the Fock operator, which thus serves as the unperturbed operator. The perturbation is the correlation potential. Thus MP-theory is a special application of RSPT. The MP based RSPT is now commonly used for correlated calculations of atoms and molecules. RSPT with MP partitioning leads to a size-extensive perturbation series. The acronyms MP2, MP4, MBPT(n), etc. have become very popular because of accuracy and relative simplicity of the method.

1.5.3 Coupled-cluster theory

The CC method is the most accurate quantum chemical method which can be applied for small to medium sized molecule [68-72]. The coupled-cluster (CC) methods include all corrections of a given type to infinite order. The ground state wavefunction of an N-electron system is obtained by action of an exponential wave-operator on a reference wavefunction, usually, the Hartree-Fock configuration.

$$|\Psi_0\rangle = e^T|\Phi_0\rangle \tag{1.22}$$

T is cluster operator and it is defined as the sum of one-electron excitation operator, two-electron excitation operator and so on up to N-electron excitation operators.

$$T = T_1 + T_2 + T_3 + \cdots T_{N_{elec}} \tag{1.23}$$

The T_i operator acting on an HF reference wave function Φ_0 generates all ith excited Slater determinants.

$$T_1\Phi_0 = \sum_{i}^{occ}\sum_{a}^{vir} t_i^a \Phi_i^a$$

$$T_2\Phi_0 = \sum_{i<j}^{occ}\sum_{a<b}^{vir} t_{ij}^{ab} \Phi_{ij}^{ab} \tag{1.24}$$

the expansion coefficients t is termed as amplitude corresponding to the cluster operators T. With the CC wave function in eq. (1.22) the Schrödinger equation becomes,

$$\hat{H}\, e^{T}|\Phi_0\rangle = E e^{T}\Phi_0 \qquad (1.25)$$

Above equation can be solved by variational [73-75] or non-variational approach. The standard formulation of coupled cluster theory is nonvariational. In traditional formulation of CC method the equations for energy and cluster amplitudes can be obtained by method of projection wherein the Schrödinger equation (1.25) is projected from left by HF configuration and excited configurations. The same set of equations can also be obtained by similarity transformation method.

If all cluster operators up to T_N are included in T; the method is known as full CC (FCC) and the CC wave function is equivalent to FCI. The exponential nature of the FCC wave operator makes it difficult to practice it even for the small molecules. The cluster operator must therefore be truncated at some excitation level. The lowest level of approximation is therefore, $T = T_2$, referred to as CCD. Using $T = T_1 + T_2$ gives the CCSD model, which is only slightly more demanding than CCD, and yields a more complete model. Both CCD and CCSD involve a computational effort that scales M_{basis}^{6} in the limit of a large basis set. The next higher level is CCSDT model. This scales to the order M_{basis}^{8}. CCSD is the most commonly used CC anasatz. Unlike CISD, CCSD (or in general, any truncated CC) continues to be size-consistent and size-extensive. This is because of the exponential nature of the wave operator, which includes higher excitations through the products of $T_1 and\, T_2$. Non-linearity of CC equation and non-variational nature are the only limitations of the method. Despite of truncation it gives highly accurate and systematically improving results during every iterative step. Provided the reference fragments correctly, the exponential nature of the wave operator guarantees the size-consistency of the overall wave function and energy. Thus CC is the most reliable method for calculation various chemical properties of molecule [76-78]. Ample of research have been done for further improvement of CC method and its development for calculation of various properties [79-83].

1.6 Density functional theory

A wavefunction for N electrons depends upon the 3N spatial coordinates of electrons and N spin coordinates. However, density $\rho(r)$ depends only upon 3 coordinates (x, y, z) and the spin. The basic idea of the density functional theory is to replace the complicated wavefunction by simpler density $\rho(r)$. The Thomas-Fermi (TF) model was in many aspects very successful and showed the basic steps to obtain the density functional for the total energy [84, 85]. In TF model the electrons are treated as independent particles forming a uniform electron gas and the electron-electron repulsion energy arises solely due to electrostatic interactions. In literature model has been used for calculations on atoms and molecules [86-88]. However, the accuracy of the model is limited. The TF method was found to give a very crude description of the electron density and the electrostatic potential. It was shown that the TF scheme is exact in the limit of infinite nuclear charge. The model has shown the infinite charge density at the nucleus. Also, the charge density does not decay exponentially away from the nucleus of the atom. The method does not account for binding of atoms to give molecules or solids. The model lacks the shell structure in the atom. All these and a few other defects have led to the modification of the model. Subsequently some modifications were applied to the TF model by Dirac, wherein, an exchange term was added to the TF equations [89]. This model was called the Thomas-Fermi-Dirac (TFD) model. Von Wiezsacker added a gradient term to the kinetic energy term of the TF model. This model came to be known as Thomas-Fermi-Weizsacker (TFW) model [90]. Despite the flaws in the TF model, it came to be known as the first approximation to the exact description of the ground state of any system in terms of the density; this turns out to be a density functional description, where, all properties of a system can be expressed in terms of the electron density.

The modern formulation of density functional theory originated with the fundamental theorems of Hohenberg and Kohn [91].

First Hohenberg-Kohn Theorem: The external potential $v(r)$ is determined, within a trivial additive constant, by the electron density, ρ(r).

In simple words, the electronic density provides the information of the number of electrons, by integration, and the position and type of nuclei, by cusps in the density

distribution. The Hamilton operator, can be built with this information and thus the energy can be obtained by solving the Schrödinger equation. Since the wave function depends on the nature of the Hamiltonian and this operator is determined by the electronic density. Thus all (ground state) properties of the system are determined by the electronic density. The ground state energy of the system is written as a functional of density $\rho(r)$.

$$E[\rho] = F_{HK}[\rho] + \int \rho(r)\, v(r) dr \tag{1.26}$$

$F_{HK}[\rho]$ is the HK universal functional of density $\rho(r)$ and it can be split into two contributions, the kinetic energy functional $T[\rho]$ and a functional that contains all remaining electron-electron interactions V_{ee}

$$F[\rho] = T[\rho] + V_{ee}[\rho] \tag{1.27}$$

$V_{ee}[\rho]$ contains the classical Coulomb interaction and the electronic quantum interaction, known as exchange-correlation energy. Thus the exact ground state energy of the system can be determined once the form of the $F_{HK}[\rho]$ is known. However, the exact form of the universal HK functional is unknown. Hence first HK theorem is thus only an existence theorem for the energy functional.

The second HK theorem provides the procedure to obtain the energy functional. It gives an energy variational principle to the energy functional.

Second HK theorem: For a trial density $\rho_t(r)$, such that $\int \rho_t(r) dr = N \; and \;\; \rho_t(r) \geq 0$

$$E_0 \leq E[\rho_t(r)] \tag{1.28}$$

Which says that the energy functional is always greater than or equal to the exact ground state energy, E_0. As stated above the determination of the form of the $F_{HK}[\rho]$ is the crucial part in construction of the energy functional for obtaining the exact ground state energy.

1.6.1 Kohn-Sham method

In 1965, Kohn and Sham [92] made a major step towards quantitative modelling of electronic structure, by introducing an elegant way for the evaluation of kinetic energy functional. They proposed the introduction of orbitals from a non-interacting reference system. For a non-interacting system the wave-function is just

the antisymmetric product of single particle solutions (known as orbitals), ψ_i. The exact expression for the kinetic energy of the non-interacting Kohn-Sham (KS) system is given as,

$$T_{KS}[\rho] = -\frac{1}{2}\sum_{i}^{occ}\langle\psi_i|\nabla^2|\psi_i\rangle \tag{1.29}$$

Occupied orbitals are labelled with $i\ or\ j$, and virtual orbitals are labelled with $a\ or\ b$. Letters $p\ or\ q$ will be used to label any molecular orbital, independent of its occupation. The electronic density which connects the fictitious non-interacting system with the real system is given by:

$$\rho(r) = \sum_{i}^{occ}|\psi_i(r)|^2 \tag{1.30}$$

In most approaches, $T_{KS}[\rho]$ is used as a first approximation to the kinetic energy of the real system. Using the explicit expression for the Coulomb interaction the energy functional is given by:

$$E[\rho] = T_{KS}[\rho] + \int v(r)\,\rho(r)dr + \frac{1}{2}\int\int\frac{\rho(r_1)\rho(r_2)}{|r_1 - r_2|}dr_1dr_2 + E_{xc}[\rho] \tag{1.31}$$

$E_{xc}[\rho]$ is the KS exchange-correlation energy functional. The orbitals for the noninteracting reference system are obtained by minimizing (1.31) imposing the restriction of orthonormality

$$\langle\psi_i|\psi_j\rangle = \delta_{ij} \tag{1.32}$$

The results obtained from the variation of (1.31) subject to orthonormality of orbitals are the single-particle Kohn-Sham equations. Their canonical form is given by:

$$\left(-\frac{1}{2}\nabla^2 + v(r) + \int\frac{\rho(r')}{|r - r'|}dr' + v_{xc}(r)\right)\psi_i(r) = \varepsilon_i\psi_i(r)\forall i \tag{1.33}$$

Here $v_{xc}[\rho]$ is the exchange-correlation potential. This is obtained as the functional derivative of the exchange-correlation energy:

$$v_{xc}(r) \equiv \frac{\delta E_{xc}[\rho]}{\delta\rho(r)} \tag{1.34}$$

KS method eliminates the unknown kinetic energy functional by introducing orbitals of a fictitious non-interacting reference system. However, the exchange-correlation

energy functional is still unknown. Various approximations are made to define the form of $E_{xc}[\rho]$. The quality of any DFT calculation using the KS method is determined mainly by the approximation used for the evaluation of $E_{xc}[\rho]$. The most common approximation is the local density approximation (LDA) in which the Dirac exchange [93] is combined with some approximation for the ideal electron gas correlation, like the one proposed by Vosko, Wilk and Nusair (VWN) [94]. More sophisticated approaches include the generalized gradient approximations (GGA) [95, 96] like BLYP [97-100] and PBE [101] or the hybrid functionals [102] like B3LYP. As the name suggests the $E_{xc}[\rho]$ is evaluated by an integral over a function that depends only on the density and its gradient at a given point in space.

Compared to the orbital-free DFT approaches the kinetic energy functional is evaluated more accurately in Kohn-Sham DFT. The other advantage for Kohn-Sham approach is that the technical knowledge can be inherited from *ab initio* methods. Kohn-Sham method is a very close analogue to the Hartree-Fock method and many ideas can be exported from each other. Programs like ADF [103, 104] or DMol [105] use numerical basis sets for the expansion of the Kohn-Sham orbitals. However, deMon2k programme [106], use the linear combination of Gaussian type orbitals (LCGTO) approximation with analytic Gaussian functions. In both cases the equations are recast in matrix form yielding Roothaan-Hall type equation systems [61a, 107].

The ordinary DFT is developed for calculation of ground stationary states, thus one cannot use it for calculation of optical properties or to treat excited states. Time dependent DFT has been developed for treatment of excited states within DFT framework. Time dependent density functional theory (TDDFT) is based on Runge-Gross theorem [108-114] which is the time dependent analogue of the first Hohenberg-Kohn theorem. The required variational principle is the Frenkel principle [115,116]. In addition, in time dependent Kohn-Sham theory it is assumed that a time dependent non-interacting reference system exists, which has density propagation equal to the real density $\rho(r,t)$[117].

1.6.2 Auxiliary density functional theory

In the LCGTO-DFT approach, the Kohn-Sham molecular orbitals are expanded into atomic orbitals. Here the molecular integrals are evaluated using

contracted (Cartesian) Gaussian type orbital (CGTO) functions. Using linear combination of GTOs the (KS-SCF) energy expression for close shell system is given as,

$$E_{SCF} = \sum_{\mu,\nu} P_{\mu\nu} H_{\mu\nu} + \frac{1}{2} \sum_{\mu,\nu} \sum_{\sigma,\tau} P_{\mu\nu} P_{\sigma\tau} \langle \mu\nu \| \sigma\tau \rangle + E_{xc}[\rho] \qquad (1.35)$$

where $\mu \; and \; \nu$ are the basis function and $P_{\mu\nu}$ is an element of the density matrix. $H_{\mu\nu}$ is matrix element of the core Hamiltonian. The core Hamiltonian contains kinetic energy and nuclear attraction integrals as well as one electron perturbation terms. The second term in eq. (1.35) represents the classical Coulomb repulsion between the electrons and involves four-centre electron-electron repulsion integrals. Here the two-electron Coulomb operator is denoted by the ‖ symbol. The last term represents the exchange-correlation energy. In deMon2k [106] auxiliary functions are used to fit the charge density. The approximate density $\tilde{\rho}(r)$ is expanded into primitive Hermite Gaussians $\bar{k}(r)$ centred on atoms [118,119] as,

$$\tilde{\rho}(r) = \sum_{\bar{k}} x_{\bar{k}} \, \bar{k}(r) \qquad (1.36)$$

Here the primitive Hermite Gaussian auxiliary functions are denoted by a bar. The above auxiliary density is used for the variational fitting of the Coulomb potential [120,121]. As a result, the N^4 scaling of Coulomb integrals is avoided. In ADFT the approximated density is also used for the calculation of the exchange-correlation energy [122]. The ADFT energy expression is given as,

$$E_{SCF} = \sum_{\mu,\nu} P_{\mu\nu} H_{\mu\nu} + \sum_{\mu,\nu} \sum_{\bar{k}} P_{\mu\nu} \langle \mu\nu \parallel \bar{k} \rangle x_{\bar{k}} - \frac{1}{2} \sum_{\bar{k},\bar{l}} x_{\bar{k}} x_{\bar{l}} \langle \bar{k} \parallel \bar{l} \rangle + E_{xc} \qquad (1.37)$$

The fitting coefficients $x_{\bar{k}}$ are obtained by the variational minimization of the difference between the Kohn-Sham and auxiliary density in a Coulombic metric according to Dunlap [108]. Different to the original work from Dunlap *et al.* no charge conservation constraint is employed [123]. As a result the following inhomogeneous equation system [124] for the determination of the fitting coefficients collected in the vector ***x*** is obtained:

$$\mathbf{G}\,\boldsymbol{x} = \boldsymbol{J} \qquad (1.38)$$

Here **G** and ***J*** denote the Coulomb matrix and vector. They are defined as:

$$G_{\bar{k}\bar{l}} = \langle \bar{k} \| \bar{l} \rangle \tag{1.39}$$

$$J_{\bar{k}} = \sum_{\mu,\nu} P_{\mu\nu} \langle \mu\nu \| \bar{k} \rangle \tag{1.40}$$

The formal solution to this equation is given by[69],

$$x_{\bar{k}} = \sum_{\bar{l}} G^{-1}_{\bar{k}\bar{l}} J_{\bar{l}} = \sum_{\bar{l}} \sum_{\mu,\nu} \langle \bar{k} \| \bar{l} \rangle^{-1} \langle \bar{l} \| \mu\nu \rangle P_{\mu\nu} \tag{1.41}$$

For the calculation of the exchange-correlation contribution in ADFT it is convenient to introduce a second set of fitting coefficients. These so-called exchange-correlation fitting coefficients are given by [125]:

$$z_{\bar{k}} \equiv \sum_{\bar{l}} \langle \bar{k} \| \bar{l} \rangle^{-1} \langle \bar{l} | v_{xc}[\tilde{\rho}] \rangle \tag{1.42}$$

It should be noted that the calculation of the exchange-correlation fitting coefficients involves a numerical integration and that these coefficients are usually spin polarized. The ADFT Kohn-Sham matrix elements are then given as,

$$K_{\mu\nu} = H_{\mu\nu} + \sum_{\bar{k}} \langle \mu\nu \| \bar{k} \rangle (x_{\bar{k}} + z_{\bar{k}}) \tag{1.43}$$

As can be seen from the above equation the ADFT Kohn-Sham matrix elements depend only on the Coulomb and exchange-correlation coefficients. Thus only the approximated density is numerically calculated on a grid. Because this density is linearly scaled by construction, the necessary grid work is considerably reduced. In fact, calculation of the Kohn-Sham potential is in ADFT identical to orbital free DFT approaches with the auxiliary density as basic variable. This has also significant importance for the calculation of higher energy derivatives which we will see in the next section.

1.7 Electric response properties: methods of calculation

In section 1.1 we discussed the electric response properties using derivative formula. These properties can be calculated either numerically or analytically. A

straight forward method is to solve Schrödinger equation for the system of interest at various field values and obtain the numerical derivatives of energy by finite difference method. This approach is known as finite-field approach and requires very accurate evaluation of wavefunction and energy, although, no computational developments are required. But the method involves numerical instabilities. In analytical method, explicit expressions for wavefunction derivatives are solved and used to obtain molecular properties. There are three main methods available for calculation of response properties, namely, derivative techniques, perturbation theory based on the energy and perturbation theory based on expectation values of properties, often called response or propagator methods. For variationally optimized wave functions (HF or multi configuration SCF) the $2n + 1$ rule is applied which says that the knowledge of the n^{th} derivative or response of the wave function is sufficient for calculating a property to order $2n + 1$[47]. For non-variational wave functions the n^{th}-order wave function response is required for calculating the n^{th}-order property. However, this can be avoided by a technique first illustrated by Handy and Schaefer for CISD geometry derivatives, often referred to as the *Z-vector* method [126]. This method has been later generalized for other types of wave functions and derivatives by formulating it in terms of a Lagrange function [127]. As per Hallman-Feyman theorem, though the calculation of first order response is avoided for variationally optimized wavefunction, it is necessary for second (and higher) derivatives. Therefore, for calculation of polarizabilities (second order property) we need wavefunction response of first order. Generally the CPHF method is used to compute analytical gradients from single-determinant (HF) reference for calculation of polarizabilities and hyperpolarizabilities. The CPHF equations need to be solved iteratively due to implicit dependence of coupled equations on first order response. The propagator or response method known as random phase approximation (RPA) [128] is identical to CPHF or TDHF [129,130] for static case in given basis. When the coupled perturbed approach is implemented in DFT it is known as coupled perturbed Kohn-Sham method (CPKS). Recently, two non iterative methods have been presented for calculation of first order response of density. The first method we discuss here is known as non-iterative approximation to coupled perturbed Kohn-Sham (NIA-CPKS) method [38, 39, 131-133]. NIA-CPKS is the simplification to the iterative CPKS formalism. This is numerical-analytical

method. There is another non-iterative method proposed by Roberto *et al.* [124, 134] is an alternative to the CPKS approach for calculation of electric response properties. This method is known as auxiliary density perturbation theory (ADPT).

1.7.1 Non-iterative approximation to coupled perturbed Kohn-Sham (NIA-CPKS)

CPKS is the conventional approach used for calculation of static response of the electric field perturbation [135-142]. The derivative of KS equation with respect to field gives the CPKS equation.

$$\mathbf{K}^{(\lambda)}\,\mathbf{c} + \mathbf{K}\,\mathbf{c}^{(\lambda)} = \mathbf{S}^{(\lambda)}\,\mathbf{c}\;\boldsymbol{\varepsilon} + \mathbf{S}\,\mathbf{c}^{(\lambda)}\,\boldsymbol{\varepsilon} + \mathbf{S}\,\mathbf{c}\,\boldsymbol{\varepsilon}^{(\lambda)} \qquad (1.44)$$

In case of electric perturbation, the derivative of KS-operator matrix, $\mathbf{K}^{(\boldsymbol{\lambda})}$, consists of the two-electron and the response term. The $\mathbf{K}^{(\boldsymbol{\lambda})}$ has an explicit dependence on perturbed coefficients $\mathbf{c}^{(\boldsymbol{\lambda})}$ and as a result the CPKS equation need to be solved iteratively for self consistency. The two electron term in $\mathbf{K}^{(\boldsymbol{\lambda})}$ constitutes complicated functional derivative of Coulomb as well as the exchange-correlation term with respect to the electric field perturbation, which is algebraically complicated and time consuming step in the completely analytic CPKS method. The NIA-CPKS approach gives single step solution to CPKS equations [38,131]. This approach is a combination of numerical and analytical procedures to obtain the electric response in terms of perturbed density matrix. Here the complicated iterative scheme to solve CPKS is avoided. This makes the method practical to use for large molecules and large basis sets. This approach can be used for closed shell case only. Within NIA-CPKS, the elements of the derivative KS matrix are computed as the difference between the elements of KS matrices calculated at suitably chosen electric field values around zero.

$$K_{\mu\nu}^{(\lambda)} = \frac{K_{\mu\nu}(+\Delta F_\lambda) - K_{\mu\nu}(-\Delta F_\lambda)}{2\,\Delta F} \qquad (1.45)$$

Here $K_{\mu\nu}^{(\lambda)}$ is an element of the perturbed KS matrix in the atomic orbital basis. The values $+\Delta F_\lambda$ and $-\Delta F_\lambda$ in the parentheses denote the symmetrically chosen field value and ΔF is the magnitude of the electric field. Using this perturbed KS matrix the derivative of molecular orbital coefficients $\mathbf{c}^{(\lambda)}$ in terms of the atomic orbital

basis is obtained analytically by solving the CPKS equation in a single step. The coefficient derivative leads to the first order perturbed density matrix with the elements:

$$P_{\mu\nu}^{(\lambda)} = 2\sum_{i}^{occ} c_{\mu i}^{(\lambda)} c_{\nu i} + c_{\mu i} c_{\nu i}^{(\lambda)} \tag{1.46}$$

The NIA-CPKS for calculating dipole-polarizability has been implemented in 1.7 version of deMon2k programme. The method has been validated and tested for various exchange-correlation functionals and basis set by application to some interesting class of systems. [39,132,133].

1.7.2 Auxiliary density perturbation theory

ADPT is derived from self-consistent perturbation (SCP) theory [134, 142-147] in the framework of ADFT [124]. For calculation of linear response of KS matrix requires the knowledge of linear response of density matrix is required. For closed shell systems this matrix can be obtained from SCP theory as follows:

$$P_{\mu\nu}^{(\lambda)} = \frac{\partial P_{\mu\nu}}{\partial \lambda} = 2\sum_{i}^{occ}\sum_{a}^{uno} \frac{\mathcal{K}_{ia}^{(\lambda)} - \varepsilon_i S_{ia}^{(\lambda)}}{\varepsilon_i - \varepsilon_a}\left(c_{\mu i}c_{\nu a} + c_{\mu a}c_{\nu i}\right) - \frac{1}{2}\sum_{\sigma,\tau} P_{\mu\sigma} S_{\sigma\tau}^{(\lambda)} P_{\tau\nu} \tag{1.47}$$

The overlap matrix derivatives in equation (1.47) vanish in the case of perturbation independent basis and auxiliary functions discussed here, and the expression for the perturbed density matrix elements simplifies to,

$$P_{\mu\nu}^{(\lambda)} = 2\sum_{i}^{occ}\sum_{a}^{uno} \frac{\mathcal{K}_{ia}^{(\lambda)}}{\varepsilon_i - \varepsilon_a}\left(c_{\mu i}c_{\nu a} + c_{\mu a}c_{\nu i}\right) \tag{1.48}$$

Here λ is the perturbation parameter which represents an electric field component in this case and ε_i and ε_a are orbital energies of the ith occupied and ath unoccupied orbitals. The superscript notation refers always to partial derivatives, *i.e.* does not affect molecular orbital coefficients in molecular integral transformations. The perturbed KS matrix $\mathcal{K}_{ia}^{(\lambda)}$is given in the molecular orbital representation as,

$$\mathcal{K}_{ia}^{(\lambda)} = \sum_{\mu,\nu} c_{\mu i} c_{\nu i} K_{\mu\nu}^{(\lambda)} \tag{1.49}$$

with:

$$K_{\mu\nu}^{(\lambda)} = H_{\mu\nu}^{(\lambda)} + \sum_{\bar{k}} \langle \mu\nu \parallel \bar{k} \rangle \left(x_{\bar{k}}^{(\lambda)} + z_{\bar{k}}^{(\lambda)} \right) \tag{1.50}$$

The perturbed exchange-correlation coefficients are given by:

$$z_{\bar{k}}^{(\lambda)} = \sum_{\bar{l}} \langle \bar{k} \parallel \bar{l} \rangle^{-1} \langle \bar{l} | v_{xc}^{(\lambda)}[\tilde{\rho}] \rangle \tag{1.51}$$

Since $v_{xc}^{(\lambda)}[\tilde{\rho}]$ is a functional of the approximated density it follows:

$$\begin{aligned} \langle \bar{l} | v_{xc}^{(\lambda)}[\tilde{\rho}] \rangle &= \iint \bar{l}(r) \frac{\delta v_{xc}[\tilde{\rho}]}{\delta \tilde{\rho}(r')} \frac{\partial \tilde{\rho}(r')}{\partial \lambda} dr dr' \\ &= \sum_{\bar{m}} \langle \bar{l} | f_{xc}[\tilde{\rho}] | \bar{m} \rangle x_{\bar{m}}^{(\lambda)} \end{aligned} \tag{1.52}$$

Compared to the standard kernel of LCGTOs, the scaling of the ADPT kernel integrals is reduced by 2 orders of magnitude. The exchange-correlation kernel $f_{xc}[\tilde{\rho}]$ is defined as the second derivative of the exchange-correlation energy:

$$f_{xc}[\tilde{\rho}(r), \tilde{\rho}(r')] \equiv \frac{\delta^2 E_{xc}[\tilde{\rho}]}{\delta \tilde{\rho}(r)\, \delta \tilde{\rho}(r')} \tag{1.53}$$

For pure density functionals, the arguments of the approximated densities are collapsed. Thus we obtain [148]:

$$f_{xc}[\tilde{\rho}(r), \tilde{\rho}(r')] \equiv \frac{\delta^2 E_{xc}[\tilde{\rho}]}{\delta \tilde{\rho}(r)\, \delta \tilde{\rho}(r')}\, \delta(r - r') = \frac{\delta^2 E_{xc}[\tilde{\rho}]}{\delta \tilde{\rho}(r)^2} = \frac{\delta v_{xc}[\tilde{\rho}]}{\delta \tilde{\rho}(r)} \tag{1.54}$$

The numerical calculation of the kernel matrix elements in ADFT is described in ref [40] . With the explicit form for the perturbed exchange-correlation fitting coefficients we can rewrite the perturbed Kohn-Sham matrix as:

$$K_{\mu\nu}^{(\lambda)} = H_{\mu\nu}^{(\lambda)} + \sum_{\bar{k}} \langle \mu\nu \parallel \bar{k} \rangle\, x_{\bar{k}}^{(\lambda)} + \sum_{\bar{k},\bar{l}} \langle \mu\nu \parallel \bar{k} \rangle F_{\bar{k}\bar{l}} x_{\bar{l}}^{(\lambda)} \tag{1.55}$$

Where,

$$F_{\bar{k},\bar{l}} = \sum_{\bar{m}} \langle \bar{k} \| \bar{m} \rangle^{-1} \langle \bar{m} | f_{xc}[\tilde{\rho}] | \bar{l} \rangle \tag{1.56}$$

Inserting equation (1.55) via equation (1.49) into equation (1.48) yields an explicit expression for the perturbed density matrix in terms of the perturbed fitting

coefficients. On the other hand, the derivation of the fitting equation (1.38) itself, assuming perturbation independent basis and auxiliary functions yields:

$$\sum_{\mu,\nu} P_{\mu\nu}^{(\lambda)} \langle \mu\nu \parallel \bar{m} \rangle = \sum_{\bar{k}} x_{\bar{k}}^{(\lambda)} \langle \bar{k} \| \bar{m} \rangle \tag{1.57}$$

By combining equation (1.48), (1.49), (1.48) and (1.50) we then find:

$$\sum_{\mu,\nu} P_{\mu\nu}^{(\lambda)} \langle \mu\nu \parallel \bar{m} \rangle = 4 \sum_{i}^{occ} \sum_{a}^{uno} \frac{\langle \bar{m} \| ia \rangle H_{ia}^{(\lambda)}}{\varepsilon_i - \varepsilon_a} + 4 \sum_{i}^{occ} \sum_{a}^{uno} \sum_{\bar{k}} \frac{\langle \bar{m} \| ia \rangle \langle ia \| \bar{k} \rangle}{\varepsilon_i - \varepsilon_a} x_{\bar{k}}^{(\lambda)} +$$

$$4 \sum_{i}^{occ} \sum_{a}^{uno} \sum_{\bar{k}} \frac{\langle \bar{m} \| ia \rangle \langle ia \| \bar{k} \rangle}{\varepsilon_i - \varepsilon_a} F_{\bar{k},\bar{l}}$$

$$= \sum_{\bar{k}} \langle \bar{m} \| \bar{k} \rangle \, x_{\bar{k}}^{(\lambda)} \tag{1.58}$$

Thus the perturbed density can be eliminated and the response equation can be formulated solely in terms of the perturbed fitting coefficients. As a result the dimension of the corresponding equation system is dramatically reduced, namely to the number of auxiliary functions, and a direct, non-iterative, solution becomes feasible. Further notation can be simplified by introducing the perturbation independent Coulomb and exchange-correlation coupling matrices **A** and **B**. Their elements are given by:

$$A_{\bar{k}\bar{l}} = \sum_{i}^{occ} \sum_{a}^{uno} \frac{\langle \bar{k} \parallel ia \rangle \langle ia \parallel \bar{l} \rangle}{\varepsilon_i - \varepsilon_a} \tag{1.59}$$

$$B_{\bar{k},\bar{l}} = \sum_{i}^{occ} \sum_{a}^{uno} \sum_{\bar{m},\bar{n}} \frac{\langle \bar{k} \parallel ia \rangle \langle ia \parallel \bar{m} \rangle}{\varepsilon_i - \varepsilon_a} \langle \bar{m} \| \bar{n} \rangle^{-1} \langle \bar{n} | f_{xc}[\tilde{\rho}] | \bar{l} \rangle = \sum_{\bar{m}} A_{\bar{k}\bar{m}} F_{\bar{m}\bar{l}} \tag{1.60}$$

Similarly, we define the elements of the perturbation vector as:

$$b_{\bar{k}}^{(\lambda)} = \sum_{i}^{occ} \sum_{a}^{uno} \frac{\langle \bar{k} \parallel ia \rangle H_{ia}^{(\lambda)}}{\varepsilon_i - \varepsilon_a} \tag{1.61}$$

Inserting these quantities into equation (1.58) yields:

$$(\mathbf{G} - 4\,\mathbf{A} - 4\,\mathbf{B})\ \boldsymbol{x}^{(\lambda)} = 4\,\boldsymbol{b}^{(\lambda)} \tag{1.62}$$

Note that the term in parentheses is perturbation independent and, thus need to be calculated only one time. We then find for the perturbed fitting coefficients [124]:

$$\boldsymbol{x}^{(\lambda)} = 4\,(\mathbf{G} - 4\,\mathbf{A} - 4\,\mathbf{B})^{-1}\,\boldsymbol{b}^{(\lambda)} \tag{1.63}$$

In the case of polarizability calculations three different perturbation vectors need to be calculated, each for one field component. Once a perturbed fitting coefficient vector is obtained it is inserted into equation (1.55) in order to obtain the corresponding perturbed Kohn-Sham matrix. With the perturbed Kohn-Sham matrix the perturbed density matrix is calculated via the SCP equation (1.48). Therefore, the final ADPT result is identical to the corresponding CPKS solution. The difference is the elimination of the perturbed density matrix from the response equation system in ADPT. As already discussed this is accompanied by a significant reduction of the dimensionality of this equation system and, thus permits direct, non-iterative, solutions. From the perturbed density matrix the polarizability tensor elements are calculated as:

$$\alpha_{\lambda\eta} = \sum_{\mu,\nu} \mathrm{P}_{\mu\nu}^{(\lambda)} \langle \mu \mid \mathrm{r}_{\eta}\, \nu \rangle \tag{1.64}$$

where λ denotes the Cartesian component of the electric field and η of the dipole moment integral.

1.8 Molecular dynamics methods

Molecular properties are very sensitive to the environment and the temperature. The effects of a finite temperature can be incorporated by means of the statistical mechanics methods. The representative samplings of the system are generated at finite temperature known as simulation. There are two major techniques for generating an ensemble namely Monte Carlo (MC) and molecular dynamics (MD). However, time-dependent phenomenon can be studied with molecular dynamic simulations. The method generates a series of time-correlated points in phase space (a trajectory) by propagating a starting set of coordinates and velocities according to Newton's second equation by a series of finite time steps.

1.8.1Classical molecular dynamics

The basic principle of classical molecular dynamic is that the nuclear motion in a molecular system is treated by the classical equations of motion. The forces on atoms are derived from classical potential such as Lennard–Jones, Buckhingham, etc. These classical potentials do not describe the electronic motion and hence, classical MD becomes computationally much cheap. Here the successive configurations of the system are generated by integrating the Newton's equation of motion. Thus the time correlation of positions and velocities of the atoms in the system can be explained. Hence, MD is a deterministic approach, in which the state of the system at any future time can be predicted from its current state [149].

The trajectory is obtained by solving the differential equations involved in the Newton's second law. Given a set of atoms of masses M_I at position R_I one can write

$$F_I = M_I \ddot{\boldsymbol{R}}_I \tag{1.65}$$

Where F_I is the force on atom I, which is related to the potential $U(\boldsymbol{R}_I)$as

$$F_I = -\frac{\partial U(\boldsymbol{R}_I)}{\partial \boldsymbol{R}_I} \tag{1.66}$$

Velocity-Verlet algorithm is the most commonly used time integration algorithm in molecular dynamics methods to solve the above equations [149]. The basic idea is to write two third-order Taylor expansions for the position $R_I(t)$, one forward and one backward in time. Adding these two equations gives a recipe for predicting the position a time step Δt later from the current and previous positions, and the current acceleration.

Accelaration can be calculated from force or equivalently, the potential. Velocities are needed to calculate kinetic energy, it can be calculated as

$$\boldsymbol{V}_I(t) = \frac{\boldsymbol{R}_I(t+\Delta t) - \boldsymbol{R}_I(t-\Delta t)}{2\Delta t} \tag{1.67}$$

The velocities, forces and instantaneous values of all properties obtained after every ∇t step is stored. This time ordered information can be used to calculate time correlation function, and thus can be used to calculate the transport properties such as diffusion coefficient, viscosity coefficient, etc. The temperature dependent properties can also be calculated from the equipartition law.

$$\frac{3}{2}NK_BT = \left\langle \sum_{i=1,N} \frac{1}{2} m_i v_i^2 \right\rangle \tag{1.68}$$

In classical MD it is difficult to account for the local atomic properties such as, chemical bonding, including the chemical reactions which form and break bonds in a quantum mechanical fashion. On the other hand, quantum dynamics of the nuclear motion of a large molecular system becomes highly computationally expensive. These difficulties can be accomplished by the use of *ab initio* MD (AIMD).

1.8.2 *Ab Initio* molecular dynamics

In AIMD, the motion of the individual atoms is simulated using forces which are calculated quantum mechanically [150, 151]. The nuclei are much heavier than the electrons, thus should be moved classically using the Newton's equation of motion under the electronic potential derived from quantum mechanical approach. In 1985, in a seminal paper, Car and Parrinello initiated the field of AIMD by combining the conventional MD technique with the DFT and were termed to be CPMD [152]. Thus the study of formation and breaking of chemical bonds became possible, in contrast to the conventional MD. A number of other techniques have been developed which are based on minimization of the electronic orbitals to their ground state at each time step. These techniques were referred to as BOMD [153].

Born-Oppenheimer molecular dynamics

It is the most commonly applied approach to AIMD. The BOMD simulation solving the static electronic structure problem is solved in each molecular dynamics step, given the set of fixed nuclear positions at that instance of time [153]. Where the time-independent Shrödinger equation is solved and simultaneously nuclei are propagating through classical molecular dynamics. The electronic problem is solved using DFT for obtaining the ground state eigenvalue. For an interacting system of electrons with classical nuclei fixed at positions$\{R^N\}$, the total ground state energy can be found by minimizing the KS energy functional with respect to basis subject the orthonormality contrain. The corresponding Lagrangian for BOMD is given as

$$\mathcal{L}_{BO}\left(R^N, \dot{R}_N\right) = \sum_{I=1}^{N} \frac{1}{2} M_I \dot{R}_I^2 - min_{\{\phi_i\}} E^{KS}[\{\phi_i\}, R^N] \tag{1.69}$$

Equations of motion are given as

$$M_I \ddot{R}_I = -\nabla_I \left[min_{\{\phi_i\}} E^{KS}[\{\phi_i\}, R^N] \right] \quad (1.70)$$

The equation of motion ensures that the minimization of the electronic energy is done at each MD step.

1.9 Motivation and objectives of the thesis

In last few years electric response properties have been studied in great details for various systems due to its wide application in predicting various chemical phenomena. Along with its fundamental importance in understanding molecular interaction, it is understood that the spectroscopic measurements are dominated by polarizabilities. Dipole-quadrupole polarizabilities and their derivatives with Cartesian coordinates are important quatities in vibrational Raman optical activities (VROA). Also the nonlinear optical properties (NLO) such as hyperpolarizabilities are influential tools for designing newer and efficient NLO materials. The experimental methods are complicated and time consuming, thus the theoretical methods have played important role in calculating these properties with reasonable accuracy. Various theoretical methods have been developed for calculation of electric response properties. However, the available analytical methods cannot be applied to the metal clusters, bigger organic molecules along with large basis sets. The numerical methods can serve the purpose but one has to compromise with the accuracy. This has motivated us to develop a new numerical-analytical method for calculation of electric response properties.

The conventional CPKS approach of response calculation method is computationally expensive due to its iterative nature. The functional derivative of the exchange-correlation energy is the foremost bottle neck for building derivative Kohn-Sham matrix. Thus our formalism provides the major simplification to the CPKS approach. The calculation of perturbed KS matrix with finite-field method leads to single step solution to CPKS, thus the name NIA-CPKS. The method has been developed for studying electric properties of large molecules and basis sets with reasonable accuracy. In chapter 2, we present the rigorous calculation of dipole-dipole polarizabilities of some push-pull systems with good basis set and its comparison with ADPT method. In this thesis we present the newer implementation of NIA-CPKS in SCP formalism within deMon2k. Technical details of the

implementation are presented in chapter 3. There are fewer studies available for accurate and efficient calculation of dipole-quadrupole polarizbilities. The implementation of NIA-CPKS is further extended for calculation of dipole-quadrupole polarizabilities and applied for some interesting tetrahedral systems. The detailed discussion on dipole-quadrupole polarizabilities can be found in chapter 4. In literature it has been seen that the temperature and frequency effects are important for dipole-quadrupole polarizabilities. Chapter 5 focuses on the study of dynamic dipole-quadrupole polarizabilities at elevated temperature. The calculations are performed using ADPT method along MD trajectories. In chapter 6, we present the detail discussion on behaviour of dipole-dipole polarizabilities and dipole-quadrupole polarizabilities at stretched geometries. The major conclusions drawn from the present study and the future scope of the method are discussed in chapter7.

References:

1. Sekino, H.; Bartlett, R. J. *J. Chem. Phys*. **1986**, 84, *2726*.
2. Kondo, A. E.; Piecuch, P. J. Paldus *J. Chem. Phys.* **1996**, 104, 8566.
3. Ghosh, K. B.; Piecuch, P.; Pal, S.; Adamowicz L. J. *Chem. Phys.* **1996**, *104*, 6582.
4. Buckingham, A. D. in: B. Pullman (Ed.), Intermolecular Interactions:From Diatomics to Biopolymers, Wiley,New York, **1978**, p.1.
5. Hanna, D. C.; Yuratich, M. A.; Cotter, D. Non-linear Optics of Free Atoms and Molecules, Springer, Berlin, 1979.
6. Cohen, R.; Birnbaum, G. *J. Chem. Phys*. **1977**, *66*, 2443.
7. Collision and Interaction Induced Spectroscopy, edited by G. C. Tabisz and Neuman M. N. (Kluwer, Dordrecht, 1995)
8. Moskovits, M. *J. Raman Spectrosc.* **2005**, *36*, 485.
9. Sekino, H.; Bartlett, R.J. *J. Chem. Phys.* **1986**, *84***,** 2726.
10. Sekino, H.; Bartlett, R. *J. Chem. Phys.* **1991**, *94***,** 3665.
11. Karna, S. P.; Dupuis, M. *J. Comput. Chem.* **1991**, *12* , 487.
12. Rice, J. E.; Amos, R. D. Colwell, S. M.; Handy, N. C. ; Sanz, J. *J. Chem. Phys.* **1990**, *3*, 8828.
13. Stott, M. J.; Zaremba, E. *Phys. Rev. A* **1980**, *21*, 12.
14. Mahan, G. D. *Phys. Rev. A* **1980**, *22*, 1780 .
15. Deb B. M.; Ghosh, S. K. *J. Chem. Phys.* **1982**, *77*, 342.
16. Ghosh S. K.; Deb B. M. *Chem. Phys.* **1982**, *71* , 295.
17. Hohenberg, P.; Kohn, W. *Phys. Rev.* **1964,** *136*, B864.
18. Coleman, A. J. The Force Concept in Chemistry BM Deb: New York: Van Nostrand Reinhold, 1981; pp 418.
19. Dreisler, R. M.; Gross, E. K. U. Density Functional Theory; Springer: Berlin, 1990.
20. Sekino, H.; Bartlett, R. J. *J. Chem. Phys.* **1986,** *84*, 2726.
21. Sekino, H.; Bartlett, R. J. *J. Chem. Phys.* **1991**, *94*, 3665.
22. Karna, S. P.; Dupuis, M. *J. Comput. Chem.* **1991**, *12*, 487.
23. Rice, J. E.; Amos, R. D.; Colwell, S. M.; Handy, N. C.; Sanz, J. *J. Chem. Phys.* **1990**, *93*, 8828.
24. Kohn, W.; Sham, L. J. *Phys. Rev.* **1965**, *140*, A1133.

25. Chong. D.P. *J. Chin. Chem. Soc.* **1992**, *39*.
26. Chong. D.P. *Chem. Phys. Lett.* **199**4, *217*, 539.
27. Duffy, P.; Chong, D. P.; Casida, M. E.; Salahub, D. R. *Phys. Rev. A* **1994**, *50*, 4707.
28. Guan, J.; Casida, M. E.; Köster, A. M.; Salahub, D. R. *Phys. Rev. B* **1995**, *52*, 2184.
29. Guan, J.; Duffy, P.; Carter, J. T.; Chong, D. P.; Casida, K. C.; Casida, M. E.; Wrinn, M. *J.Chem. Phys.* **1993**, *98*, 4753.
30. Jasien, P. G.; Fitzgerald, G. *J. Chem. Phys.* **1990**, *93*, 2554.
31. Lee, A. M.; Colwell, S. M. *J. Chem. Phys.* **1994**, *101*, 9704.
32. Sim, F.; Salahub, D. R.; Chin, S. *Int. J. Quantum Chem.* **1992**, *43*, 463.
33. Dixon, D.A.; Matsuzawa, N. *J. Phys. Chem.* **1994**, *98*, 3967.
34. Matsuzawa, N.; Dixon, D.A. *J. Phys. Chem.* **1994**, *98*, 2545.
35. Calaminici, P.; Jug, K.; Köster, A.M.; Ingamells, V.E.; Papadopoulos, M.G. *J. Chem. Phys.* **2000**, *112*, 6301.
36. Mahan, G. D.; Subbaswamy, K. R. Local Density Theory of Polarizability; Plenum Press: New York, 1990.
37. Gamboa, G.U.; Calaminici, P.; Geudtner, G.; Köster, A.M. *J. Phys. Chem. A* **2008**, *112*, 11969.
38. Sophy K.B.; Pal S. *J. Chem. Phys.* **2003**, *118*, 10861.
39. Sophy K.B.; Shedge S.V.; Pal S, *J. Phys. Chem. A* **2008**, *112*, 11266.
40. Shedge S.V.; Carmona-Espíndola J.; Pal S.; Köster A.M. *J. Phys. Chem. A* **2010**, *114*, 2357.
41. Shedge S.V.; Pal S.; Köster A.M. *Chem. Phys. Lett.* **2011**, *510*, 185.
42. Buckingham, A. D. *Adv. Chem. Phys.* **1967**, *12*, 107.
43. Buckingham, A. D. in: Hirsschfelder J. O. (Ed.), Advances in Chemical Physics, Interscience, New York, 1967, p. 107.
44. McLean, A. D.; Yoshimine, M. *J. Chem. Phys.* **1967**, *47*, 1927.
45. Hellmann, H. *Einführung in die Quantenchemie*, Deuticke, Leipzig, p. 285 (1937).
46. Feynman, R. P. *Phys. Rev.* **1939**, *56*, 340.
47. Wigner, E. *Math. Natur. Anz*. (Budapest) **1935**, *53*, 477.
48. Szabo, A.; Ostlund N. S.; *Modern Quantum Chemistry*, (McGraw-Hill, New York, (1989)

49. Levine, I. N.; *Quantum Chemistry*, (IV Edition, Prentice Hall, New Delhi, 1995)
50. Born M.; Oppenheimer, J. R. *Ann. Phys.* **1927**, *84*, 457.
51. Epstein, S. T. The Variation Principle in Quantum Mechanics, (Academic, New York, 1974).
52. Fernández, F. M. Introductio to Perturbation Theory in Quantum Mechanics (CRC Press, Florida, 2000).
53. Møller C.; Plesset, M. S. *Phys. Rev.* **1934**, *46*, 618.
54. (a) Cizek, J. *Adv. Chem. Phys.* **1969**, *14*, 35 ; (b) Cizek, J. *J. Chem. Phys.* **1966**, *45*, 4256; (c) Cizek J.; Paldus, J. *Int. J. Quantum Chem.* **1971,** *5*, 359.
55. (a) Bartlett, R. J. *Annu. Rev. Phys. Chem.* **1981**, *32*, 359; (b) Bartlett, R. J. *J. Chem. Phys.* **1989**, *93*, 1697; (c) Bartlett, R. J. ; Musial, M. *Rev. Mod. Phys.* **2007**, *79*, 291.
56. Paldus, J. in Computational Methods in Molecular Physics, Edited by Wilson S.and F. Diercksen, G. H. (NATO AS1 Ser., B: Phys., p. 19. Plenum, New York and London, 1992).
57. Cederbaum, L. S.; Alon O. E.; Streltsov, A. I. *Phys. Rev. A.* **2006**, *73*, 043609.
58. Farnell, D. J. J.; Zinke, R.; Schulenburg J.; Richter, J. *J. Phys. C* **2009**, *21*, 406002; Dean, D. J.; Gour, J. R.; Hagen, G.; Hjorth-Jensen, M.; Kowalski, K.; Papenbrock, T.; Piecuch, P.; Wloch, M. *Nucl. Phys. A* **2005**, *752*, 299.
59. (a) Hartree, D. R.; *Proc. Cambridge Phil. Soc.* **1928,** *24*, 89. (b) Fock, V. *Z. Physik* **1930** *61*, 126.
60. Slater, J. C. *Phys. Rev.* **1930,** *35*, 210.
61. (a) Roothan, C. C. J. *Rev. Mod. Phys.* **1951**, *23*, 69. (b) ibid. **1960**, *32*, 179.
62. Shavitt, I. in *Methods in Electronic Structure Theory*, edited by Schaefer H. F. III, (Plenum, New York, 1977), p189.
63. Karwowski, J. in *Methods in Computational Molecular Physics*, NATO ASI Series B: Physics, Vol. 293, edited by Wilson S. and Dierksen, G. H. F. (Plenum, New York, 1992), p65.
64. Raimes, S. *Many-Electron Theory*, (North-Holland, Amsterdam, 1972)
65. Manne, R. *Int. J. Quant. Chem.* **1977**, *S11*, 175.
66. Lindgren, I.; Morrison, J. *Atomic Many-Body Theory*, (Springer-Verlag, Berlin, (1982)
67. Urban, M.; Hubač, I.; Kellö, V.; Noga, J. *J. Chem. Phys.* **1980**, *72*, 3378.

68. Bartlett, R. J. *Annu. Rev. Phys. Chem.* **1981**, *32*, 359.
69. (a) Cizek, J. *J. Chem. Phys.* **1966**, *45*, 4256. (b) ibid. *Adv. Quant. Chem.* **1969**, *14* , 35. (c) Bartlett, R. J. *J. Chem. Phys.* **1989**, *93*, 1697. (d) ibid. in .Modern Electronic Structure Theory, Part II., *Advanced Series in Physical Chemistry* - Vol. 2, edited by D. R. Yarkony, (World Scientific, Singapore, 1995), p1047.
70. (a) Noga, J.; Bartlett, R.J. *J. Chem. Phys.* **1987**, *86*, 7041. (b) Trucks, G. W.; Noga, J.; R. Bartlett, J. *Chem. Phys. Lett.* **1988**,*145*, 548.
71. (a) Černušać, I.; Noga, J.; Diercksen, G.H.F.; Sadlej, A.J. *Chem. Phys.* **1988**, *125*, 548. (b) Noga, J.; Pluta, T. *Chem. Phys. Lett.* **1997**, *264*, 101.
72. (a) Noga, J.; Kucharski, S.A.; Bartlett, R.J. *J. Chem. Phys.* **1989**, *80*, 3399. (b) Watts, J.D.; Cernusak, I.; Noga, J.; Bartlett, R.J.; Bauschlicher Jr., C.W.; Lee, T.J.; Rendell, A.P. ; Taylor, P.R. *J. Chem. Phys.* **1990**, *93*, 8875. (c) Piecuch, P.; Kucharski, S.A. ; Kowalski, K. *Chem. Phys. Lett.* **2001**, *344*, 176.
73. Pal, S.; Mukherjee, D. *Pramana* **1982**, *18*, 261.
74. Pal, S.; Prasad, M. D.; Mukherjee, D. *Theor. Chim. Acta.* **1983**, *62*, 523.
75. (a) Bartlett, R. J.; Noga, J. *Chem. Phys. Lett.* **1988**, *150*, 29. (b) Bartlett, R. J.; Kucharski, S. A.; Noga, J. *Chem. Phys. Lett.* **1989**, *155*, 133.
76. Manohar, P. U.; Vaval, N.; Pal, S. *Chem. Phys. Lett.* **2004**, *387*, 442.
77. Vaval, N.; Manohar, P.; Pal, S.*Collect. Czech. Chem. Commun.* **2005**, *70*, 851.
78. Manohar, P. U.; Vaval, N.; Pal, S.*J. Mol. Struct. THEOCHEM* **2006**, 768, 91.
79. Banik, S.; Pal, S.; Durga Prasad, M. *J. Chem. Phys.* **2008**, *129*, 134111.
80. Banik, S.; Pal, S.; Durga Prasad, M. *J. Chem. Theor. Comput.* **2010**, 6, 3198.
81. (a)Pal, S. *Phys. Rev. A* **1989**, *39* (39. (b) ibid. *Int. J. Quantum. Chem.* 41 (1992) 443.
82. (a)Ajitha, D.; Vaval, N.; Pal, S. *J. Chem. Phys.* **1999**, *110*, 2316. (b) Ajitha, D.; Pal, S.; *Chem. Phys. Lett.* **1999**, *309*, 457. (c) ibid. *J. Chem. Phys.* **2001**, *114* , 3380.
83. (a) Shamasundar, K. R.; Pal, S. *Int. J. Mol. Sci.* **2002**, *3*, 710.
    (b) Shamasundar, K. R.; Asokan, S.; Pal, S. *J. Chem. Phys.* **2004**, *120*, 6381.
84. Thomas, L. H. *Proc. Cambridge Philos. Soc.* **1927**, *23*, 542.
85. Fermi, E.; *Z. Phys.* **1928**, *48*, 73.
86. Alonso, J. A.; Girifalco, L. A. *J. Phys. Chem. Solids* **1977**, *38*, 869.
87. Jacob, B.; Gross, E. K. U.; Dreizler, R. M. *J. Phys. B* **1978**, *11*, 22.
88. Gross, E. K. U.; Dreizler, R. M. *Phys. Rev. A* **1979**, *20*, 1798.

89. Dirac, P. A. M. *Proc. Cambridge Philos. Soc.* **1930**, *26*, 376.
90. von Weizsacker, C. F. *Z. Phys.* **1935**, *96*, 431.
91. Hohenberg, P.; Kohn, W. *Phys. Rev.* **1964**, *136*, 864.
92. Kohn W.; Sham, J. *Phys. Rev.* **1965**, *137*, A1697.
93. Dirac, P. A. M. *Proc. Camb. Phil. Soc.* **1930**, *26*, 376.
94. Vosko, S. H.; Wilk, L.; Nusair, M. *Can. J. Phys.* **1980**, *58*, 1200.
95. Langreth, D. C.; Mehl, M. J. *Phys. Rev. B* **1983**, *28*, 1809.
96. Perdew, J. P.; Yue, W. *Phys. Rev. B* **1986**, *33*, 8800.
97. Becke, A. D. *Phys. Rev. A* **198**8, *38*, 3098.
98. Colle, R.; Salvetti, D. *Theor. Chim. Acta* **1975**, *37*, 329.
99. Colle, R.; Salvetti, D. *J. Chem. Phys.* **1983**, *79*, 1404.
100. C. Lee, W. Yang, and R. G. Parr, Phys. Rev. B 37, 785 (1988).
101. Perdew, J. P.; Burke, K.; Ernzerhof, M. *Phys. Rev. Lett.* **1996**, *77*, 3865.
102. Becke, A. D. *J. Chem. Phys.* **1993**, *98*, 5648.
103. Baerends, E. J.; Ellies, D. E.; Ros, P. *Chem. Phys.* **1973**, *2*, 41.
104. te Velde, G.; Baerends, E. J. *J. Comput. Phys.* **1992**, *99*, 84.
105. Delley, B. *J. Chem. Phys.* **1990**, *92*, 508.
106. Köster, A. M.; Calaminici, P.; Casida, M. E.; Flores, R.; Geudtner, G.; Goursot, A.; Heine, T.; Janetzko, F. M.; del Campo, J.; Patchkovskii, S.; Reveles, J. U.; Salahub, D. R.; Vela, A. *deMon2k, The deMon developers*; Cinvestav: Mexico City, Mexico, 2006. See http://www.demon-software.com
107. Hall, G. G. *Proc. Roy. Soc. Ser. A* **1951**, *205*, 541.
108. Ipatov, A.; Fouqueau, A.; Perez del Valle, C.; Cordova, F.; Casida, M. E.; Köster, A. M.; Vela, A.; Jamorski, C. J. *J. Mol. Struct. (THEOCHEM)* 2006, *179*, 762.
109. Runge, E.; Gross, Phys. E. K. U. *Rev. Lett.* **1984**, *52*, 997.
110. Casida, M. E. In Recent Advances in Density Functional Methods, edited by Chong, D. P. (World Scientific, Singapore, 1995), Vol. I, p. 155.
111. Casida, M. E. in Recent Developments and Application of Modern Density FunctionalTheory, edited by J. M. Seminario (Elsevier, Amsterdam, 1996), p. 391.
112. van Gisbergen, S. J. A.; Snijders, J. G.; Baerends, E. J. J. *Chem. Phys.* **1998**, *109*,10644.
113. Heinze, H. H.; Della-Sala, F.; Görling, A. *J. Chem. Phys.* **2002**, *116*, 9624.

114. Dreuw A.; Head-Gordon, M. *Chem. Rev.* **2005**, *105*, 4009.
115. Frenkel, J. Wave Mechanics, Advanced General Theory (Oxford University Press, London, 1934), p. 436.
116. Moccia, R. *Int. J. Quantum Chem.* **1973**, *7*, 779.
117. Boettger, J. C.; Trickey, S. B. *Phys. Rev. B* **1996**, *53*, 3007.
118. Köster, A. M. *J. Chem. Phys.* **2003**, *118*, 9943.
119. Dunlap, B. I.; Connolly, J. W. D.; Sabin, J. R. *J. Chem. Phys.* **1979**, *71*, 4993.
120. Mintmire, J. W.; Sabin, J. R.; Trickey, S. B. *Phys. Re*V. *B* **1982**,*26*, 1743.
121. Köster, A. M.; Reveles, J. U.; del Campo, J. M. *J. Chem. Phys.* **2004**, *121*, 3417.
122. Dunlap, B. I.; Connolly, J. W. D.; Sabin, J. R. *J. Chem. Phys.* **1979**, *71*, 4993.
123. Köster, A. M.; Calaminici, P.; Go´mez, Z.; Reveles, U. J. A Celebration of the Contributions of Robert G. Parr. In *Reviews of Modern Quantum Chemistry*; Sen, K., Ed.; World Scientific: Singapore, 2002.
124. Flores-Moreno, R.; Köster, A. M. *J. Chem. Phys.* **2008**, *128*, 134105.
125. van Leeuwen, R.; *Phys. Rev. Lett.* **1999**, *82*, 3863.
126. Handy, N. C.; Schaefer, H. F. III, *J. Chem. Phys.*, **1984**, *81*, 5031
127. Helgaker, T.; Jørgensen, P. *Theor. Chim. Acta.*, **1989**, *75*, 11.
128. Thouless, D. J. Quantum Mechanics of Many Body Systems, Academic, New York (1961).
129. Linderberg,J.; Öhrn, Y. Propagators in Quantum chemistry, Academic Press, London (1974). 127
130. Dalgarno, A.; Victor, G. A. *Proc. R. Soc. London Ser. A*, **1966,** *291*, 291.
131. Sophy, K. B. Ph.D. Thesis, University of Pune, Pune, India, 2007.
132. Sophy, K. B.; Calaminici, P.; Pal, S. *J. Chem.Theory Comput.* **2007**, *3*, 716.
133. Sophy, K. B.; Pal, S. *THEOCHEM* **2004**, *676*, 89.
134. Flores-Moreno, R. Ph.D. Thesis, Cinvestav, Mexico City, Mexico, 2006.
135. Gerratt, J.; Mills, I. M. *J. Chem. Phys.* **1968**, *49*, 1719.
136. Pople, J. A.; Krishnan, R.; Schlegel, H. B.; Binkley, J. S. *Int. J. Quantum Chem.Symp.* **1979**, *13*, 225.
137. Fournier, R. *J. Chem. Phys.* **1990**, *92*, 5422.
138. Karna, S. P.; Dupuis, M. *J. Comput. Chem.* **1991**, *12*, 487.
139. Komornicki, A.; Fitzgerald, G. *J. Chem. Phys.* **1993**, *98*, 1398.

140. Colwell, S. M.; Murray, C. W.; Handy, N. C.; Amos, R. D. *Chem. Phys. Lett.* **1993**, *210*, 261.
141. Lee, A. M.; Colwell, S. M. *J. Chem. Phys.* **1994**, *101*, 9704.
142. Yamaguchi, Y.; Osamura, Y.; Goddard, J. D.; Schaefer III, H. F. A New Dimension to Quantum Chemistry: Analytic Dericative Methods in *Ab Initio* Molecular Electronic Structure Theory (Oxford University Press, New York, 1994).
143. Diercksen, G.; McWeeny, R. *J. Chem. Phys.* **1966**, *44*, 3554.
144. Dodds, J. L.; McWeeny, R.; Raynes, W. T.; Riley, J. P. *Mol. Phys.* **1977**, *33*, 611.
145. Dodds, J. L.; McWeeny, R.; Sadlej, A. J. *Mol. Phys.* **1977**, *34*, 1779.
146. McWeeny, R. *Phy. Rev.* **1962**, *126*, 1028.
147. McWeeny, R. in: Sekino, H. (Ed.), Methods of Molecular Quantum Mechanics, Academic Press, London, 2001
148. Gelfand, I. M.; Fomin, S. V. *Calculus of Variations*; Prentice Hall: Englewood Cliffs, NJ, 1963.
149. Allen, M. P.; Tildesley, D. J. *Computer Simulation of Liquids.* Claredon Press, Oxford (1987).
150. Payne, M. C.; Teter, M. P.; Allan, D. C.; Arias, T. A.; Joannopoulos, J. D. *Rev. Mod. Phys.* **1992**, *64*, 1045.
151. Tuckerman, M. E.; Ungar, P. J.; von Rosenvinge, T.; Klein. M. L. *J. Phys. Chem.* **1996**, *100*, 12878.
152. Car, R.; Parrinello, M. *Phys. Rev. Lett.* **1985**, *55*, 2471.
153. Marx, D.; Hütter, J. *Ab Initio Molecular Dynamics: Theory and Implementation* published in Modern Methods and Algorithms of Quantum Chemistry, Edited by J. Grotendorst, NIC series **3** (2000).

CHAPTER 2

Calculation of static dipole-dipole polarizability using NIA-CPKS and its comparison with ADPT

Abstract:

In this chapter we present a theoretical study of the polarizabilities of free and disubstituted azoarenes employing ADPT and NIA-CPKS method. Both methods are non-iterative, but use different approaches to obtain the perturbed density matrix. NIA-CPKS is different from the conventional CPKS approach in that the perturbed Kohn-Sham matrix is obtained numerically, thereby yielding a single-step solution to CPKS. ADPT is an alternative approach to the analytical CPKS method in the framework of ADFT. It is shown that the polarizabilities obtained using these two methods are in good agreement with each other. The comparisons are made for disubstituted azoarenes, which give support to the push-pull mechanism. Both methods reproduce the same trend for polarizabilities due to the substitution pattern of the azoarene moiety. Our results are consistent with the standard organic chemistry 'activating/deactivating' sequence. We present the polarizabilities of the above molecules calculated with three different exchange-correlation functionals and two different auxiliary function sets. The computational advantages of both methods are discussed, too.

2.1 Introduction

Recently, a lot of work has been devoted for calculation of electric response properties of various orders. Thus various techniques have been developed for calculation of these properties. The response of a molecule to an electric field perturbation in terms of the electron density is given by the derivative of the density with respect to the electric field components. These derivatives or density responses can be obtained self consistently for variational energy expressions. The variational equations transcribed in a basis set involve the derivatives of the KS matrix and can be shown to be equivalent to CPKS equations. The response property can also be calculated using linear response time-dependent density functional theory (LR-TDDFT) [1-7]. The precise relationship between these two approaches is discussed in the literature [8, 9]. There is no difference, however, between the LR-TDDFT and CPKS approach for static response properties with fixed basis set, which is the case here. The CPKS method has proven very useful for response property calculations [10, 11]. In the KS formalism the analytic derivative approach requires the solution of the CPKS equations in order to obtain the first order response of the molecular electron density. The CPKS equations involve the evaluation of the functional derivative of the exchange-correlation potential for the construction of the KS matrix derivative. Since the KS matrix derivatives depend on the perturbed density, the CPKS equations need to be solved in an iterative manner. This involves the transformation of molecular integrals from the original atomic orbital basis to the molecular orbital basis. As a result, the straightforward evaluation of second order response equations in DFT scales formally as N^5, where N denotes the number of basis functions in the system. Thus for large molecules this approach is not feasible. This situation has motivated us to put forth new formalisms in which the CPKS equation can be solved in a single step. One of them is the so-called NIA-CPKS method [12-16]. Here the derivative of the KS matrix is obtained by a finite-field approximation and it is used in the CPKS equation to calculate the perturbed density matrix for polarizability calculations. It is a numerical-analytical method because only the derivative of the KS matrix is obtained numerically. The standard finite-field method [17] already implemented in deMon2k is different from the NIA-CPKS in that the energy derivatives are obtained numerically. The other non-iterative approach is ADPT [18] where the perturbed density matrix is obtained non-

iteratively by solving an inhomogeneous equation system with the dimension of the number of auxiliary functions used to expand the approximated density. ADPT is derived from SCP theory [19-24] in the framework of the ADFT method [18, 25]. Both methods are implemented in deMon2k [26] which permit a direct comparison.

The main aim of the comparison presented in this chapter is to validate the reliability of approximated density approaches for perturbation calculations, in particular the calculation of dipole-dipole polarizabilities, for electronically more complicated systems. Because of their technological importance [27-37] we have selected azoarenes for this study. They are classical push-pull systems with large polarizabilities and hyperpolarizabilities [38-41]. For comparison LDA as well as GGA are employed. Thus for the first time ADPT GGA polarizabilities are reported.

2.2 Theory and computational details

As we discussed in chapter 1 the dipole-dipole polarizability is the second derivative of energy with respect to electric field at zero field value. Theoretically the response of the electric field perturbation can be obtained in terms of perturbed density matrix. A trace of the product of the response density matrix and dipole moment integrals give all the components of dipole-dipole polarizability. For our calculation the perturbed density matrix is calculated using NIA-CPKS method. It can also be calculated with ADPT. The detail discussion about the NIA-CPKS and ADPT implementation has been already presented in Chapter1. The average polarizabilities are calculated as normalized trace of the corresponding tensor:

$$\bar{\alpha} = \frac{1}{3}\left(\alpha_{xx} + \alpha_{yy} + \alpha_{zz}\right) \qquad (2.1)$$

For our comparative study of azoarene polarizabilities free azoarene and nine of its para-disubstituted derivatives are studied. The six different substituents, NH_2, OH, CHO, CN, OCH_3, and NO_2 include electron donating as well as withdrawing groups. An electron donating group on one side and an electron withdrawing group on the other side make azoarene a push-pull system. In order to facilitate comparison with the calculations of Hinchliffe *et al.* [41] the molecular structures were optimized at the B3LYP/6-311++G (2d, 1p) level of theory with GAMESS. The polarizability

values reported in table 2.1 were calculated using both NIA-CPKS and ADPT employing the PBE functional [42] and GEN-A2* auxiliary function sets [43]. In order to study the functional dependency of NIA-CPKS and ADPT polarizabilities we also employed the local VWN [44] and gradient corrected BLYP [45, 46] functional. The AUXIS and BASIS options specified in the tables refer to the type of density used for the calculation of the exchange-correlation energy and potential. They are calculated either from the auxiliary functions (AUXIS) or the basis functions (BASIS). Thus the AUXIS option refers to ADFT and ADPT calculations. Independent of the used density the exchange-correlation energies and potentials are numerically integrated on an adaptive grid [47] with an accuracy of 10^{-6} a.u. per matrix element. Analytic ADPT polarizabilites are calculated only with the AUXIS option, whereas NIA-CPKS polarizabilities are calculated for both options. In both cases the Coulomb energy is calculated by the variational fitting procedure proposed by Dunlap, Connolly and Sabin [48]. For the density fitting GEN-A2 and GEN-A2* auxiliary function sets are employed. Spherical orbitals were used instead of Cartesian orbitals, as they possess no linear dependencies. We have used 6-311++G (2d, 2p) basis set throughout the calculations of polarizabilities.

For polarizability calculations employing finite difference methods the SCF convergence criterion was tightened to 10^{-10} a.u. in all cases. In order to allow direct comparison the same convergence criterion was used in the ADPT calculations reported in table 2.1. The ADPT polarizabilities in table 2.3 were obtained with the default SCF convergence criterion of deMon2k (10^{-6} a.u.). For the finite-field perturbation (FFP) calculations the procedure of Kurtz *et al.* [17] as implemented in deMon2k was applied [49]. As field strength the deMon2k default value of 0.032 a.u. was used. For the calculation of the perturbed Kohn-Sham matrix in the NIA-CPKS framework, field strength of 0.001 a.u. was employed.

2.3 Results and discussion

In figure 2.1 the structure of the parent azoarene molecule is depicted. In the disubstituted derivatives the substituents X and Y (NH_2, OH, CHO, CN, OCH_3, and NO_2) replace the hydrogen atoms at the 15^{th} and 20^{th} position. All disubstituted molecules have trans geometry about the azo linkage and they are nearly planar [50-

52]. At this point it is worth to mention that azoarenes crystallize in non-centrosymmetric space groups which ensure the nonlinear activity of the crystals [53]. The polarizabilities calculated using ADPT, NIA-CPKS and FFP methods with PBE and GEN-A2* are presented in table 2.1 for sake of comparison. As this table shows all employed perturbation approaches within deMon2k yield essentially the same results at this level of theory. In particular, the variation between AUXIS and BASIS results, *i.e.* perturbation calculation with the approximated and the exact Kohn-Sham density, are in the same range as between analytic and finite-field approaches. This demonstrates the reliability of the analytic, non-iterative, ADPT approach. The qualitative order of the azoarene polarizabilities is in all approaches the same.

In table 2.1 we also compare our results with the B3LYP values reported by Hinchliffe *et al*. [39]. In general the B3LYP polarizabilities are smaller than ours. We attribute this mainly to the different functionals used and the basis set which is optimized for Hartree-Fock based methods. We would like to emphasize that we used this basis set to facilitate comparison with other computational approaches. In fact DFT optimized basis sets augmented with field induced polarization functions are much better suited for the calculation of GGA polarizabilities. However, this is not the topic of this report and we refer the interested reader to the corresponding literature [54-56]. By and large the qualitative trends of the PBE and B3LYP polarizabilities are similar. In detail we have observed that the smallest enhancement of polarizability from the parent azoarene molecule is due to the pair OH/CN which is consistent with the observation of Hinchliffe *et al*. [39]. The largest enhancement is observed for OCH_3/NO_2 and NH_2/NO_2 substitution. But among these two pairs Hinchliffe *et al.* [39] observed largest enhancement in NH_2/NO_2 where as in our calculations we found that OCH_3/NO_2 shows largest increment. However the difference between the increment due to OCH_3/NO_2 and NH_2/NO_2 is not very large, as observed from table 2.1. For other substituent, only minor discrepancies are observed. Unfortunately, experimental values are not available for the here discussed systems.

In table 2.2 NIA-CPKS polarizabilities of the studied azoarenes are listed. These calculations were performed with the VWN, BLYP and PBE functional in

combination with the GEN-A2 and GEN-A2* auxiliary function set. As this table shows the NIA-CPKS polarizabilities vary little with respect to the different functionals and auxiliary function sets. The polarizabilities are slightly enlarged if the larger GEN-A2* auxiliary function set is used. With respect to the functional we note that VWN and BLYP polarizabilities are usually very similar despite the different approximations they represent. On the other hand, PBE polarizabilities are usually a little bit smaller. The qualitative ordering of the azoarene polarizabilities in table 2.2 is for all methods the same. The only exception is the inversion of the NH_2/NO_2 and OCH_3/NO_2 substituted azoarene polarizabilities at the BLYP/GEN-A2* level of theory.

In table 2.3 ADPT polarizabilities of the studied azoarenes are listed. The employed methodologies are the same as in table 2.2. By and large, similar trends as for the NIA-CPKS polarizabilities are observed. Again the only exceptions in the ordering of table 2.1 are inversions in the order of the NH_2/NO_2 and OCH_3/NO_2 disubstituted azoarenes. These inversions are observed for all functionals with the GEN-A2 auxiliary function set in the ADPT calculations. Compared to the NIA-CPKS results the differences between the ADPT polarizabilities calculated with the GEN-A2 and GEN-A2* auxiliary function sets are larger. This is due to the fact that in ADPT calculations the approximated density is also used for the calculation of the exchange-correlation potential. Obviously, higher angular momentum auxiliary functions are needed for the description of the response to the external field. This is also underlined by the ADPT/GEN-A2* polarizabilities which are for all employed functionals in excellent agreement with their NIA-CPKS/GEN-A2* counterparts. At this point it is also worth to mention that the ADPT polarizabilities in table 2.3 are obtained with the standard SCF threshold of deMon2k, *i.e.* no tightening of the SCF procedure was employed. The comparison of the ADPT/PBE/GEN-A2* polarizabilities from table 2.1 and 2.3 reveals that the SCF tightening is insignificant for the analytic ADPT polarizabilities. Of course, this is in sharp contrast to the numerical methods.

2.4 Conclusions

In this chapter we presented the polarizabilities of free and disubstituted azoarenes calculated with the non-iterative ADPT and NIA-CPKS method. In this context ADPT GGA polarizabilities are reported for the first time. The results obtained are compared to standard finite-field perturbation polarizabilities. We have shown that all three methods give consistent result within a chosen methodology, *i.e.* a given functional and given basis and auxiliary function sets. In particular, the qualitative ordering of the polarizabilities of the studied azoarenes is very similar with all methodologies. The observed increments in polarizabilities by substituting the 15^{th} and 20^{th} hydrogen atom of free azoarene with activating and deactivating groups are in accordance with the standard organic chemistry 'activating/deactivating' sequence. Thus push-pull mechanisms are correctly reproduced at all studied levels of theory. These results underline the reliability of the ADPT approach in which the perturbation calculation is performed only with the auxiliary density. The direct comparison of ADPT and NIA-CPKS polarizabilities show that the difference between perturbation calculations with the approximated and exact KS density is in the same range as the difference between analytic and finite-field results. Therefore, the errors associated with the ADPT approach are within the intrinsic accuracy of KS perturbation theory.

Already for medium sized molecules, like the here studied azoarenes, the difference in the ADPT polarizabilities obtained with the GEN-A2 and GEN-A2* auxiliary function sets are rather small. This fuels the hope that reliable polarizability trends for systems in the nanometer regime are predictable with the ADPT/GEN-A2 level of theory. Our studies also show that NIA-CPKS maybe an interesting alternative to the ADPT approach for the calculation of static polarizabilities for very large systems. If GEN-A2* auxiliary function sets are used the ADPT polarizabilities are in quantitative agreement with the corresponding polarizabilities obtained from the exact perturbed KS density. This strongly motivates the extension of the ADPT approach to other perturbation parameters.

The comparison with the results from Hinchliffe *et al.* indicates that the incorporation of exact exchange, as in the B3LYP hybrid functional, changes

significantly the polarizability values. For the here studied systems a decrease is observed. We believe that range-separated hybrid functionals would be even more appropriate for the properties being treated here [8]. This represents an interesting avenue to further improve DFT polarizabilities and, thus is a strong motivation for us to incorporate exact exchange in the ADPT and NIA-CPKS formulation without scarifying the computational advantages of these methods. Work in this direction is under way in our laboratories. Fukui functions are other response properties that can be calculated using both NIA-CPKS and ADPT. There are already ADPT calculations of this response property [57] and NIA-CPKS can also be further extended.

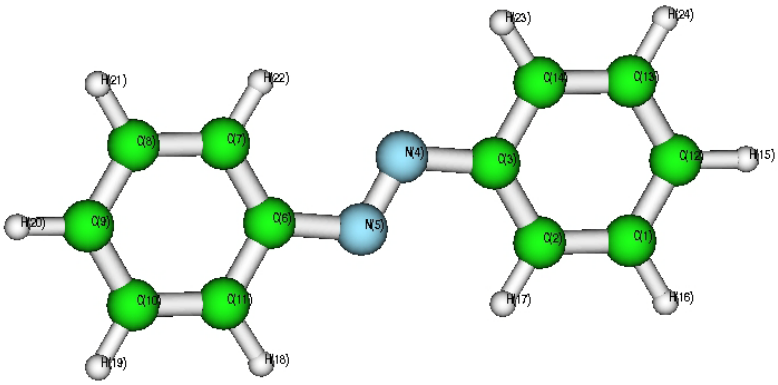

Figure 2.1. B3LYP/6-311G (2d, 1p) optimized geometry of parent azoarene molecule.

Table 2.1: Static polarizabilities [a.u.] of azoarene and disubstituted azoarene molecules calculated with the PBE functional and GEN-A2* auxiliary function set using ADPT, NIA-CPKS and finite field perturbation (FFP) method.

	AUXIS			BASIS		
X,Y	ADPT	NIA-CPKS	FFP	NIA-CPKS	FFP	Ref. 39
H, H	192.42	192.53	192.91	193.18	193.22	183.82
OH,CN	242.53	242.26	242.84	242.59	242.53	227.98
OH, CHO	243.39	243.28	243.90	243.92	244.05	228.07
OH, NO_2	249.41	249.74	249.91	248.49	249.25	230.35
NH_2, CN	261.73	261.70	262.22	261.82	261.84	247.79
NH_2, CHO	263.70	263.50	264.40	264.42	264.20	246.26
OCH_3, CHO	265.27	265.27	265.84	266.22	266.14	247.03
OCH_3, CN	266.75	266.95	267.26	267.06	267.03	246.88
NH_2, NO_2	271.89	272.23	272.52	271.34	271.70	256.50
OCH_3, NO_2	272.39	272.56	272.95	272.66	272.29	249.86

Table 2.2: NIA-CPKS polarizabilities [a.u.] of azoarene and disubstituted azoarene molecules calculated with the VWN, BLYP and PBE functional using GEN-A2 and GEN-A2* auxiliary function sets.

	GEN-A2			GEN-A2*		
X,Y	VWN	BLYP	PBE	VWN	BLYP	PBE
H, H	192.68	193.42	192.04	193.8	194.52	193.18
OH, CN	242.81	242.81	241.81	243.53	243.56	242.59
OH, CHO	244.08	243.76	242.87	245.15	244.92	243.92
OH, NO_2	249.87	249.90	248.28	250.15	250.16	248.49
NH_2, CN	262.57	262.24	261.15	263.04	262.87	261.82
NH_2, CHO	265.28	264.41	263.29	266.11	265.50	264.42
OCH_3, CHO	266.50	265.36	264.61	267.90	266.91	266.22
OCH_3, CN	267.54	266.87	265.93	268.59	267.86	267.06
NH_2, NO_2	272.90	272.44	270.85	273.30	273.56	271.34
OCH_3, NO_2	273.35	272.66	271.03	273.65	273.30	272.66

Table 2.3: ADPT polarizabilities [a.u.] of azoarene and disubstituted azoarene molecules calculated with the VWN, BLYP and PBE functionl using GEN-A2 and GEN-A2* auxiliary function sets.

	GEN-A2			GEN-A2*		
X,Y	VWN	BLYP	PBE	VWN	BLYP	PBE
H, H	195.51	194.36	192.14	193.50	194.28	192.40
OH,CN	245.37	244.36	242.21	243.55	244.14	242.36
OH, CHO	247.27	247.27	243.70	244.88	244.27	243.39
OH, NO_2	252.50	254.14	248.96	250.92	251.85	249.41
NH_2, CN	265.96	266.58	262.41	263.31	263.45	261.73
NH_2, CHO	269.17	266.69	264.96	265.54	266.16	263.71
OCH_3, CHO	270.06	267.85	265.51	267.26	267.25	265.28
OCH_3, CN	270.41	268.20	266.42	268.36	268.15	266.75
NH_2, NO_2	277.07	275.88	272.42	273.76	274.19	271.89
OCH_3-NO_2	276.49	273.57	271.70	274.34	274.88	272.38

References

1. Casida, M. E. Recent Developments and Applications of Modern Density Functional Theory; Seminario, M. J., Ed.; Elsevier: Amsterdam, 1996.
2. Casida, M. E.; Jamorski, C.; Bohr, F.; Guan, J. *ACS Symposium Series* **1996**, *628*, 145.
3. Casida, M. E.; Wesolowski, T. A. *Int. J. Quantum Chem.* **2004**, *96*, 577.
4. Görling, A. *Int. J. Quantum Chem.* 1998, *69*, 265.
5. Görling, A.; Heinze, H. H.; Ruzankin, S. P.; Staufer, M.; Rösch, N. *J. Chem. Phys.* **1999**, *110*, 2785.
6. Ipatov, A.; Fouqueau, A.; del Valle, C. P.; Cordova, F.; Casida, M. E.; Köster, A. M.; Vela, A.; Jamorski, C. J. *J. Mol. Struct.: THEOCHEM* **2006**, *762*, 179.
7. Jamorski, C.; Casida, M. E.; Salahub, D. R. *J. Chem. Phys.* **1996**, *104*, 5134.
8. Casida, M. E. *J. Mol. Struct. THEOCHEM* **2009**, 3, 914
9. Casida, M. E. TDDFT for Excited States, in Computational Methods in Catalysis and Materials Science, part of the IDECAT Course book series, Philippe Sautet and Rutger A. van Santen Ed.,Willey-VCH: Weinheim, Germany, 2008, pp.33.
10. Kamiya, M.; Sekino, H.; Tsuneda, T.; Hirao, K. *J. Chem. Phys.* **2005**, *122*, 234111.
11. Banerjee, A.; Harbola, M. K. *Pramana-J. Phys.* **1997**, *49*, 455.
12. Sophy, K. B. PhD Thesis, University of Pune, India, 2007.
13. Sophy, K. B.; Calaminici, P.; Pal, S. *J. Chem.Theory and Comp.* **2007**, *3*, 716.
14. Sophy, K. B.; Pal, S. *J. Chem. Phys.* **2003**, *118*, 10861.
15. Sophy, K. B.; Pal, S. *J. Mol. Struct. THEOCHEM* **2004**, *676*, 89.
16. Sophy, K. B.; Shedge, S. V.; Pal, S. *J. Phys. Chem. A* **2008**, *112*, 11266.
17. Kurtz, H. A.; Stewart, J. J. P.; Dieter, K. M. *J. Comp. Chem.* **1990**, *11*, 82.
18. Flores-Moreno, R.; Köster, A., M. . *J. Chem. Phys.* **2008**, *128*, 134105.
19. Diercksen, G.; McWeeny, R. *J. Chem. Phys.* **1966**, *44*, 3554.
20. Dodds, J. L.; McWeeny, R.; Raynes, W. T.; Riley, J. P. *Mol. Phys.* **1977**, *33*, 611.
21. Dodds, J. L.; McWeeny, R.; Sadlej, A. J. *Mol. Phys.* **1977**, *34*, 1779.

22. McWeeny, R. *Physical Review* **1962**, *126*, 1028.
23. McWeeny, R. Methods of Molecular Quantum Mechanics; Sekino, H., Ed.; Academic Press: London, 2001.
24. McWeeny, R.; Diercksen, G. *J. Chem. Phys.* **1968**, *49*, 4852.
25. Flores-Moreno, R. Analytical derivatives in LCGTO-DFT Pseudo-Potential Methods with Auxiliary Functions, CINVESTAV 2006.
26. Köster, A. M.; Calaminici, P.; Casida, M. E.; Flores, R.; Geudtner, G.; Goursot, A.; Heine, T.; Janetzko, F.; M. del Campo, J.; Patchkovskii, S.; Reveles, J. U.; Salahub,D. R.; Vela, A. deMon2k, *The deMon developers*, Cinvestav, Mexico-City, **2006**.
27. Ågren, H.; Vahtras, O.; Koch, H.; Helgaker, T.; Jørgensen, P. *J. Chem. Phys.* **1993**, *98*, 6417.
28. Bishop, D. M. *Adv. Chem. Phys.* **1998**, *104*, 1.
29. Bulat, F. A.; Toro-Labbé, A.; Champagne, B.; Kirtman, B.; Yang, W. *J. Chem. Phys.* **2005**, *123*, 14319.
30. Champagne, B.; Perpete, E. A.; Jacquemin, D.; van Gisbergen, S. J. A.; Baerends, E. J.; Soubra-Ghaoui, C.; Robins, K. A.; Kirtman, B. *J. Phys. Chem. A* **2000**, *104*, 4755.
31. Daniel, C.; Dupuis, M. *Chem. Phys. Lett.* **1990**, *171*, 209.
32. Davis, D.; Sreekumar, K.; Sajeev, Y.; Pal, S. *J. Phys. Chem. B* **2005**, *109*, 14093.
33. Kanis, D. R.; Ratner, M. A.; Marks, T. J. *Chem. Rev.* **1994**, *94*, 195.
34. Mikkelsen, K. V.; Luo, Y.; Ågren, H.; Jorgensen, P. *J. Chem. Phys.* **1995**, *102*, 9362.
35. Morley, J. O. *J. Phys. Chem.* **2002**, *98*, 11818.
36. Quinet, O.; Champagne, B.; Kirtman, B. *J. Mol. Struct.: THEOCHEM* **2003**, *633*,199
37. Sim, F.; Chin, S.; Dupuis, M.; Rice, J. E. *J. Phys. Chem.* **1993**, *97*, 1158.
38. Albert, I. D. L.; Morley, J. O.; Pugh, D. *J. Phys. Chem.* **1995**, *99*, 8024.
39. Hinchliffe , A.; Nikolaidi, B.; Machado, H. J. S. *Int. J. Mol. Sci.* **2004**, *5*, 224.
40. Jug, K.; Chiodo, S.; Janetzko, F. *Chem. Phys.***2003,** *287*, 161.
41. Varanasi, P. R.; Jen, A. K. Y.; Chandrasekhar, J.; Namboothiri, I. N. N.; Rathna, A. *J. Am. Chem. Soc.* **1996**, *118*, 12443.
42. Perdew, J. P.; Burke, K.; Ernzerhof, M. *Phys. Rev. Lett.* **1996**, *77*, 3865.

43. Calaminici, P.; Janetzko, F.; Köster, A. M.; Mejia-Olvera, R.; Zuniga-Gutierrez, B. *J. Chem. Phys.* **2007**, *126*, 044108.
44. Vosko, S.H.; Wilk, L.; Nusair, M. Can. *J. Phys.* **1980**, *58*, 1200.
45. Becke, A.D. Phys. Rev. A **1988**, *38*, 3098.
46. Lee, C.; Yang, W.; Parr, R.G. *Phys. Rev. B* **1988**, *37*, 785.
47. Köster, A. M.; Flores-Moreno, R.; Reveles, J. U. *J. Chem. Phys.* **2004**, *121*, 681.
48. Dunlap, B.I.; Connolly, J.W.D.; Sabin, J.R. *J. Chem. Phys.* **1979**, *71*, 4993.
49. Calaminici, P.; Jug, K.; Köster, A.M. *J. Chem. Phys.* **1998**, *109*, 7756.
50. Brown, C. J. *Acta Cryst.* **1966**, *21*,146.
51. Huang, X.; Kuhn, G. H.; Nesterov, V. N.; Averkiev, B. B.; Penn, B.; Antipin, M. Y.; Timofeeva, T. V. *Acta. Cryst.* **2002**, *C58*, o624.
52. Liu, X.-G.; Feng, Y.-Q.; Meng, X.-Q.; Liang, Z.-P.; Yang, G. *Acta. Cryst.* **2005**, *E61*, o1694.
53. Adams, H.; Allen, R. W. K.; Chin, J.; O'Sullivan, B.; Styring, P.; Sutton, L. R. *Acta.Cryst.* **2004**, *E60*, o289.
54. D.P.Chong. *Chem. Phys. Lett.* **199**4, *217*, 539.
55. Calaminici, P. Chem. *Phys. Lett.* **2003**, *374*, 650.
56. Calaminici, P.; Köster, A.M.; Vela,A.; Jug, K. *J. Chem. Phys.* **2000**, *113*, 2199.
57. Flores-Moreno R.; Melin J., Ortiz J. V.; Merino G. J. Chem. Phys. **2008**, 129, 224105

CHAPTER 3

Technical details of implementation: NIA-CPKS version of self consistent perturbation theory

Abstract:

In this chapter we present the newer implementation of NIA-CPKS in SCP formalism. Here we introduce SCP in short which is followed by elaborate discussion of our recent methodology. The advantages of implementing NIA-CPKS in perturbation branch of ADPT which has been derived from SCP have been listed here. The comparison between NIA-CPKS and ADPT has been presented at the end of the chapter.

3.1 Introduction

Theoretically the perturbation due to external electric field can be obtained in the form of perturbed density matrix. In the KS formalism the first order response of the molecular electron density can be calculated analytic by solving CPKS equations [1-8]. The CPKS equations involve the evaluation of the functional derivative of the exchange-correlation potential for the construction of the KS matrix derivative. The straightforward evaluation of second order response equations in DFT scales formally as N^5. This makes the evaluation of second derivatives in KS methods as expensive as in standard SCF methods. The dependence of the KS matrix on perturbed coefficients makes the CPKS procedure iterative. Thus there is a need of efficient method for evaluation electric response efficiently with more computational ease. NIA-CPKS approach gives single step solution to CPKS equation [9-15]. Implementation and methodology of NIA-CPKS have been discussed in chapter1 and chapter 2. The foremost implementation of NIA-CPKS was done in 1.7 version of deMon2k. With the further development of the software the NIA-CPKS has been implemented in newer versions and now the method has been implemented in master version of the deMon2k. The other non-iterative approach we discussed in chapter1 is ADPT [16, 17] where the perturbed density matrix is obtained non-iteratively by solving a system of inhomogeneous equation with the dimension of the number of auxiliary functions used to expand the approximated density. ADPT is derived from SCP theory [17-22] in the framework of the ADFT method [16, 17]. The implementation of both these methods in same software has facilitated a direct comparison of results.

This has further motivated us to implement NIA-CPKS in framework of SCP theory [15]. In this chapter we present the newer implementation of NIA-CPKS approach in SCP formalism. The short introduction to the SCP method has been presented in next section which follows the technical details of our new implantation. We also present here some discussion on comparison of NIA-CPKS with ADPT.

3.2 Self-consistent perturbation method

For the evaluation of response properties the calculation of the perturbed density matrix is obligatory. As we discussed in first chapter this matrix can be obtained from the CPKS equations. However, an alternative and more direct

approach for the calculation of the perturbed density matrix is SCP theory [18-22] proposed by McWeeny and co-workers. In this approach, unlike CPKS, the explicit response of the molecular orbitals is not needed. Instead the linear response of the density matrix is calculated iteratively [21]. Thus it avoids the intermediate calculation of perturbed orbitals and give the substantial computational advantage over CPKS. In SCP theory the first order perturbed density matrix in non-orthonormal set is given as,

$$P_{\mu\nu}^{(\lambda)} = \frac{\partial P_{\mu\nu}}{\partial \lambda} = 2\sum_{i}^{occ}\sum_{a}^{uno} \frac{\mathcal{K}_{ia}^{(\lambda)} - \varepsilon_i S_{ia}^{(\lambda)}}{\varepsilon_i - \varepsilon_a}\left(c_{\mu i}c_{\nu a} + c_{\mu a}c_{\nu i}\right) - \frac{1}{2}\sum_{\sigma,\tau} P_{\mu\sigma}S_{\sigma\tau}^{(\lambda)}P_{\tau\nu} \quad (3.1)$$

The expressions have been derived with the use of subspace projector matrices to treat separately the occupied-occupied, virtual-virtual and occupied-virtual blocks. The Löwdin orthogonalised atomic orbitals have been used to simplify the derivation [23, 24]. For thorough derivation one can refer to ref [17, 22]. The energy formulae have also been generated for calculation of perturbed density for perturbation dependent basis set for calculation of perturbation of varies orders and various forms [19]. In this work for calculation of electric response properties we focus on perturbation independent basis set. Thus for perturbation independent basis set the expression simplifies to

$$P_{\mu\nu}^{(\lambda)} = 2\sum_{i}^{occ}\sum_{a}^{uno} \frac{\mathcal{K}_{ia}^{(\lambda)}}{\varepsilon_i - \varepsilon_a}\left(c_{\mu i}c_{\nu a} + c_{\mu a}c_{\nu i}\right) \quad (3.2)$$

The perturbed density matrix is thus determined solely in terms of quantities defined in the non-orthogonal basis, without any need for intermediate transformations. The construction of the linear response of the Kohn-Sham and density matrices resembles the SCF procedure thus the iterative solution of (3.2) is often referred to as McWeeny's SCP theory. Since the response density matrix is the quantity of interest the McWeeny's formulation appear to be more adequate for DFT methods.

3.3 Implementation of NIA-CPKS in SCP formalism

In chapter 1, we discussed our former implementation of NIA-CPKS in 1.7 version of deMon2k [25]. Within NIA-CPKS approach the perturbed KS matrix is

calculated numerically by finite-difference at suitably chosen electric field, it can be represented as,

$$K_{\mu\nu}^{(\lambda)} = \frac{K_{\mu\nu}(+\Delta F_\lambda) - K_{\mu\nu}(-\Delta F_\lambda)}{2\Delta F} \tag{3.3}$$

Substituting this perturbed KS matrix into Eq. (3.2) yields the perturbed density matrix. This represents our new implementation of NIA-CPKS in master version of deMon2k. Our earlier NIA-CPKS implementation was using the CPKS equations for obtaining perturbed molecular orbital coefficients and, thereby, the perturbed density matrix. Our new implementation can be seen as a NIA-CPKS version of self-consistent perturbation theory. Because ADPT is also based on SCP this simplifies considerably the implementation effort in our perturbation branch of deMon2k. Once the perturbed density matrix is calculated, dipole-dipole polarizability and dipole-quadrupole polarizability tensor elements are obtained from,

$$\alpha_{\lambda\eta} = \sum_{\mu,\nu} \mathrm{P}_{\mu\nu}^{(\lambda)} \langle \mu \mid \mathrm{r}_\eta \, \nu \rangle \tag{3.4}$$

$$A_{\lambda,\eta\zeta} = \sum_{\mu,\nu} P_{\mu\nu}^{(\lambda)} \langle \mu | r_{\eta\zeta} \nu \rangle \tag{3.5}$$

Here λ denotes the Cartesian component of the electric field and $\eta\zeta$ that of the quadrupole moment integrals. ADPT and NIA-CPKS approaches are implemented in deMon2k. For detailed discussion about the implementation of ADPT and older implantation of NIA-CPKS approach for dipole-polarizability, we refer to [16, 17, 9-14].

3.4 Comparison between NIA-CPKS and ADPT

In this section we summarise the points of comparison between two non-iterative approaches viz. ADPT and NIA-CPKS. As we discussed in earlier chapters both approaches are developed to reduce computation efforts and calculate reasonably accurate electric properties of large systems. Though both the approaches are non-iterative the methodology to calculate electric response is very different from one another. ADPT is completely analytical method, however NIA-CPKS is

numerical analytical. Within NIA-CPKS, programming of the algebraically complicated functional derivatives of the exchange-correlation term in the KS operator matrix has been cleverly avoided. This gives the direct solution to CPKS equations. In ADPT the perturbed KS matrix is calculated analytically using perturbed fitting coefficients as described in chapter 1. In this approach the direct calculation of perturbed density matrix is avoided by solving inhomogeneous equation systems which gives non-iterative solution.

The exchange-correlation part of the KS-operator matrix can be evaluated using, either the auxiliary basis or the orbital basis, for fitting the density. Since the derivative KS operator matrix is constructed numerically within NIA-CPKS; both alternatives for obtaining the density are available for the response property calculation. This is not possible in ADPT formalism, here fitting is performed with auxiliary basis only. In earlier implementation of NIA-CPKS, perturbed coefficients were calculated explicitly and thereby perturbed density matrix was calculated. This was the marked difference between NIA-CPKS and ADPT. The newer implementation facilitates direct calculation of response density matrix by reducing computational efforts.

References:

1. Gerratt, J.; Mills, I. M. *J. Chem. Phys.* **1968**, *49*, 1719.
2. Pople, J. A.; Krishnan, R.; Schlegel, H. B.; Binkley, J. S. *Int. J. Quantum Chem.Symp.* **1979**, *13*, 225.
3. Fournier, R. *J. Chem. Phys.* **1990**, *92*, 5422.
4. Karna, S. P.; Dupuis, M. *J. Comput. Chem.* **1991**, *12*, 487.
5. Komornicki, A.; Fitzgerald, G. *J. Chem. Phys.* **1993**, *98*, 1398.
6. Colwell, S. M.; Murray, C. W.; Handy, N. C.; Amos, R. D. *Chem. Phys. Lett.* **1993**, *210*, 261.
7. Lee, A. M.; Colwell, S. M. *J. Chem. Phys.* **1994**, *101*, 9704.
8. Yamaguchi, Y.; Osamura, Y.; Goddard, J. D.; Schaefer III, H. F. A New Dimension to Quantum Chemistry: Analytic Dericative Methods in *Ab Initio* Molecular Electronic Structure Theory (Oxford University Press, New York, 1994).
9. Sophy K.B.; Pal S. *J. Chem. Phys.* **2003**, *118*, 10861.
10. Sophy, K. B. Ph.D. Thesis, University of Pune, Pune, India, 2007.
11. Sophy, K. B.; Calaminici, P.; Pal, S. *J. Chem.Theory Comput.* **2007**, *3*, 716.
12. Sophy, K. B.; Pal, S. *THEOCHEM* **2004**, *676*, 89.
13. Sophy K.B.; Shedge S.V.; Pal S, *J. Phys. Chem. A* **2008**, *112*, 11266.
14. Shedge S.V.; Carmona-Espíndola J.; Pal S.; Köster A.M. *J. Phys. Chem. A* **2010**, *114*, 2357.
15. Shedge S.V.; Pal S.; Köster A.M. *Chem. Phys. Lett.* **2011, *510,* 185.**
16. Flores-Moreno, R.; Köster, A. M. *J. Chem. Phys.* **2008**, *128*, 134105.
17. Flores-Moreno, R. Ph.D. Thesis, Cinvestav, Mexico City, Mexico, 2006.
18. Diercksen, G.; McWeeny, R. *J. Chem. Phys.* **1966**, *44*, 3554.
19. Dodds, J. L.; McWeeny, R.; Raynes, W. T.; Riley, J. P. *Mol. Phys.* **1977**, *33*, 611.
20. Dodds, J. L.; McWeeny, R.; Sadlej, A. J. *Mol. Phys.* **1977**, *34*, 1779.
21. McWeeny, R. *Phy. Rev.* **1962**, *126*, 1028.
22. McWeeny, R. in: Sekino, H. (Ed.), Methods of Molecular Quantum Mechanics, Academic Press, London, 2001
23. Löwdin, P. O. *J. Chem. Phys.* **1950**, *18*, 365.

24. Szabo, A.; Ostlund, N. S. Modern Quantum Chemistry (Dover Publications Inc., Mineola, 1996), p. 142.
25. Köster, A. M.; Calaminici, P.; Casida, M. E.; Flores, R.; Geudtner, G.; Goursot, A.; Heine, T.; Janetzko, F. M.; del Campo, J.; Patchkovskii, S.; Reveles, J. U.; Salahub, D. R.; Vela, A. *deMon2k, The deMon developers*; Cinvestav: Mexico City, Mexico, 2006. See http://www.demon-software.com

CHAPTER 4

Calculation of dipole-quadrupole polarizabilities of tetrahedral molecules

Abstract:

In this chapter, the newer implementation NIA-CPKS has been validated for the calculation of dipole-quadrupole polarizabilities. The NIA-CPKS results are compared with the dipole-quadrupole polarizabilities calculated using ADPT. The calculations are performed on three tetrahedral molecules viz., CH_4, P_4 and adamantane ($C_{10}H_{16}$). The assessment with higher level methods such as MP2 and CCSD results proved the reliability of the methodology used for NIA-CPKS and ADPT.

4.1 Introduction

The higher order polarizabilities such as, dipole-quadrupole polarizabilities (A) and dipole-octupole polarizabilities (E) have gained attention in recent years [1, 2]. These polarizabilities are important for the description of surface-enhanced Raman scattering and interaction induced light scattering spectra. A, E and the derivatives of dipole-quadrupole polarizability with respect to Cartesian coordinates and vibrational normal coordinates $(\partial A/\partial Q)$ are determined experimentally using collision induced light scattering and high resolution infrared absorption spectroscopies [3]. Maroulis and Hohm have collaboratively studied dipole-quadrupole polarizability of some interesting tetrahedral molecules such as OsO_4 [4], $Ge(CH_3)_4$ [5], P_4 [6], group IV tetrachlorides [7]. They also performed a careful comparison between theory and experiment. However, their theoretical calculations are based on the finite-field approach in the framework of many body perturbations (MP) and CC methods [8, 9]. An analytic approach was first presented by Amos to evaluate static (A) values. This scheme is based on the CPHF method [10]. Quinet *et. al.* have recently developed a procedure based on the time dependent HF scheme for evaluating both frequency dependent electric dipole-quadrupole polarizability and first order derivative of dipole-quadrupole polarizability. The quantity $(\partial A/\partial Q)$ [11] is directly relevant to the determination of VROA intensities. VROA spectroscopy is receiving increasing attention due to its broad range of applications including the characterization of conformational dynamics in proteins [12].

For studying large molecular systems, DFT is an obvious choice because of simplicity in applications. However, response properties using DFT have been calculated mainly at the finite-field method. Recently, the non-iterative approaches to response properties using DFT *i.e.* ADPT [13] and NIA-CPKS [14-18] method have been developed with application to large molecules in mind. These methods are implemented in deMon2k software [19]. The details of implementation can be found in chapter 1 and chapter 3 of this thesis. Both the methods have been tested for calculation of dipole-dipole polarizabilities and validated by comparison with higher level methods. This has further motivated us to extend these two non-iterative approaches to dipole-quadrupole polarizability calculation. In this chapter for calculation of dipole-quadrupole polarizabilities we used the newly implemented NIA-CPKS version of SCP [20]. This chapter mainly focuses on validation of NIA-

CPKS and ADPT approach for calculation of dipole-quadrupole polarizability. CCSD, (FF) MP2 and experimental results are reported here for the purpose of comparison with our method. Calculations are performed on P_4, CH_4 and adamantane($C_{10}H_{16}$) molecules of tetrahedral symmetry.

4.2 Theory and computational details

Energy and multipole moments show explicit dependence on the electric field. According to Buckingham [21] and McLean and Yoshimine [22] the energy, dipole and quadrupole moment of a molecule in terms of the static electric field can be written as,

$$\begin{aligned} E(F) = E^0 - \mu_i^0 F_i - \frac{1}{3}\Theta_{ij}^0 F_{ij} - \frac{1}{15}\Omega_{ijk}^0 F_{ijk} - \frac{1}{105}\Phi_{ijkl}^0 F_{ijkl} + \cdots \\ -\frac{1}{2}\alpha_{ij}F_iF_j - \frac{1}{3}A_{i,jk}F_iF_{jk} - \frac{1}{6}C_{ij,kl}F_{ij}F_{kl} \\ -\frac{1}{6}\beta_{ijk}F_iF_jF_k - \frac{1}{6}B_{ij,kl}F_iF_jF_{kl} + \cdots \end{aligned} \tag{4.1}$$

Where E^0, μ^0, Θ^0, $\Omega^0$are the energy and permenant multiple moments of the free molecule, α_{ij} its dipole polarizability and β_{ijk} the corresponding (first) hyperpolarizability. $A_{k,ij}$ is the dipole-quadrupole polarizability and $B_{ij,kl}$ the dipole-dipole-quadrupole hyperpolarizability. For a molecule belonging to T_d symmetry, there exists only one component of the octupole (Ω_{ijk}) and hexadecapole (Φ_{ijkl}) moment as well as of the dipole (α_{ij}) and dipole-quadrupole $(A_{k,ij})$ polarizability. In this chapter, we investigate the dipole-quadrupole polarizabilities of T_d structures for which the only non-vanishing component is $A_{x,yz}$.

In general, all possible components of the dipole-quadrupole polarizability $A_{k,ij}$ can be obtained as a trace of the product of the response density matrix and quadrupole integrals.

$$A_{k,ij} = Tr\left(P_k^{(\lambda)} \cdot \Theta_{ij}\right) \tag{4.2}$$

Where $P_k^{(\lambda)}$ is the density matrix derivative with respect to the external electric field in x, y and z direction. Θ_{ij} represents quadrupole moment integrals. As we discussed in chapter3 density matrix derivatives are either obtained by ADPT or NIA-CPKS.

Choice of proper basis set and geometry is crucial for electric property determination. We have used large basis sets along with adequate diffuse and polarization functions for dipole-quadrupole polarizability calculation. P_4, CH_4 and adamantane molecules of tetrahedral symmetry are considered here in our study. All calculations are performed in the (symmetry adapted) standard orientation of these molecules. Fig 4.1 represents the structure of these three molecules. Geometry and basis sets for the above mentioned molecules are as follows:

P_4: P_4 molecule has a cage like structure. We have used the most recent experimental P-P bond length, 2.1958Å [23]. Four different basis sets, P0 [6s5p2d], P1 [6s5p3d], P2 [6s5p3d1f], P3 [6s5p4d2f] were constructed on a (14s9p)[5s4p] [24] substrate. The detailed construction of the basis set is given in ref [6].

CH_4: In standard orientation geometry, C is at origin and the four C-H bonds lie along the directions defined by the origin and the points (1,1,1),(1,-1,-1), (-1,1,-1) and (-1,-1,1). The equilibrium geometrical parameters are used for calculations, C-H bond length is set to be 1.08587 Å [25]. We have used four basis sets M1 [6s4p2d1f/4s2p1d], M2 [6s4p3d1f/4s2p1d], M3 [6s4p4d1f/4s2p1d], M4 [6s4p4d2f/4s2p1d] for dipole-quadrupole polarizability calculation. All four basis sets are constructed on (9sp/4s)/[4s2p/2s]. Details of the construction of basis sets are given in ref [7]. All basis sets used are already been proven to be of good quality for dipole-quadrupole polarizability calculations.

Adamantane ($C_{10}H_{16}$): Adamantane molecule also has a cage structure like P_4. C-C and C-H bond lengths used were 1.54024 Å and 1.1124 Å, respectively. These molecular parameters were obtained experimentally from electron diffraction measurements [26]. Here we have used smallest, M1 and largest, M2 basis set which was constructed for methane molecule. To study the stability of different functional local, VWN [27], and generalized gradient approximated, PBE [28], functional were used. For density fitting the GEN-A2 and GEN-A2* [29] auxiliary function sets were employed.

4.3 Results and discussions

We discuss here the results of our calculations for the systems described above. For the validation of our methods, we also report finite-field (FF) MP2 and (FF) CCSD values of dipole-quadrupole polarizabilities. (FF) MP2 and (FF) CCSD

$A_{x,yz}$ values were calculated by taking a finite difference of quadrupole moments obtained from respective (full) MP2 and CCSD calculations at two different field values viz. 0.001 and -0.001 a.u. Within the NIA-CPKS approach, we have used the same field value for the construction of KS matrix derivatives. Two options, AUXIS and BASIS, mentioned in the tables, refer to the type of density used for the calculation of the exchange-correlation energy and potential. They can be calculated from either the auxiliary functions (AUXIS) or the basis functions (BASIS). Thus the AUXIS and BASIS options refer to ADPT and RI-DFT calculations. By construction analytical ADPT dipole-quadrupole polarizabilities can only be calculated with the AUXIS option, whereas NIA-CPKS dipole-quadrupole polarizabilities were calculated for both options. All reported values are in atomic units.

In table 4.1, dipole-quadrupole polarizabilities of P_4 for four different basis sets are listed. As this table shows, $A_{x,yz}$, calculated using PBE/GEN-A2* functional, is larger than those from VWN/GENA2* functional and the trend is the same for all four basis sets. Whereas, reverse trend is observed in case of GEN-A2 PBE values are lower than those of VWN. We observed that $A_{x,yz}$ is usually increasing with the addition of polarization functions. This trend is independent from the used functional and methodology from the P0 to the P2 basis set. However, from P2 to P3 exceptions are observed. In case of ADPT, dipole-quadrupole polarizabilities calculated with GEN-A2 are consistently larger than calculated with GEN-A2* for all basis sets and both functionals. NIA-CPKS also follows the same trend except for P_4 basis with PBE functional, GEN-A2* values are greater than GEN-A2. Quadrupole polarizabilities calculated with BASIS option within NIA-CPKS are lower than those calculated from GEN-A2 and GEN-A2* except for P0 and P3 basis with VWN functional. ADPT and NIA-CPKS are in good agreement with each other for dipole-quadrupole polarizability. In particular, ADPT/GEN-A2* results are in excellent agreement with NIA-CPKS BASIS results. This underlines the quality of the ADPT approach. The same was observed in our previous study of dipole-dupole polarizabilities [30]. $A_{x,yz}$ calculated with (FF) MP2, are within the range of our DFT values. CCSD values are larger than MP2. Our DFT results are in better agreement with CCSD results than MP2. Both CCSD and MP2 values are close to NIA-CPKS/VWN/BASIS and ADPT/VWN/GEN-A2* quadrupole

polarizabilities. The reported $A_{x,yz}$ values by Maroulis *et al.* using (FF) MP2 for the P0, P1 and P2 basis are 83.6, 85.4 and 85.1, respectively [6]. Their values are different from our (FF) MP2 values. This is because our calculations were done with a P-P bond length of 2.1958 Å, which is the most recently reported experimental bond length and their calculations were performed using an older experimental bond length (2.2228 Å). The other reason for this disagreement is that the number of basis functions is different even though the basis set is the same. Because we chose a Cartesian orbital representation in deMon2k, 6d and 10f functions are used in the calculation which results in a larger number of basis functions compared to those used by Maroulis *et al.* Moreover, our calculations are based on full MP2 level of theory whereas Maroulis *et al.* have frozen the 20 inner most MOs in their MP2 calculation. The experimental *A* obtained from depolarized collision induced light scattering a measurement [31] is 77±26 $e^2a_0^2E_H^{-1}$. Our theoretical $A_{x,yz}$ using the GEN-A2* auxiliary function set and the VWN functional is closer to this reported experimental value.

Table 4.2 represents the dipole-quadrupole polarizability of CH_4 molecule. The electric properties of methane molecule are well studied with theory and experiments. Maroulis has designed the basis sets which work well for calculation of response electric properties [8]. We have used the four of these basis sets for calculation. These four basis sets are named as M1 [6s4p2d1f/4s2p1d], M2 [6s4p3d1f/4s2p1d], M3 [6s4p4d1f/4s2p1d], M4 [6s4p4d2f/4s2p1d]. The basis set is built upon (9s5p/4s)/[4s2p/2s] substrate for carbon and hydrogen respectively. Suitable polarization and diffuse functions are added on the substrate, further details of the basis set are given in corresponding paper [8]. Calculated results are compared with finite-field MP2 and CCSD. Going from M1 to M4 MP2 and CCSD results of dipole quadrupole polarizability are reducing. Whereas, NIACPKS/BASIS shows that M3 gives maximum $A_{x,yz}$ and M2 gives minimum value for both the functional. Such trend is not observed for GEN-A2 and GEN-A2* for both ADPT and NIACPKS. For BASIS option PBE functional shows higher dipole-quadrupole polarizability, however, reverse trend is observed in case of NIA-CPKS/GEN-A2*. NIA-CPKS/GEN-A2 and ADPT are not showing any such trend. Both the methods have given larger GEN-A2* dipole-quadrupole polarizabilities than GEN-A2. BASIS results lie between GEN-A2 and GEN-A2* for NIA-CPKS. BASIS results

are close to CCSD values. Again ADPT and NIA-CPKS are in good agreement with each other and with the CCSD and MP2. The experimentally derived dipole-quadrupole polarizability is 11.3 $e^2a_0^2E_H^{-1}$[32]. Our theoretical results are close to the experimental result too. This again proves the reliability of both our methods.

The table 4.3 lists the dipole-quadrupole polarizability for adamantane molecule. Adamantine is comparatively larger molecule than the P_4 and CH_4. M1 to M4 basis sets are seen to be working excellent for methane molecule thus we have selected the smallest M1 and largest M4 basis for calculation of dipole-quadrupole polarizabilities of adamantane. The purpose of choosing this particular molecule and basis set was to check the applicability of our methods for large basis set. M1 and M4 have 656 and 876 basis functions which are highest among the basis sets used in this work. It can be seen from the table 4.3 that both methods are working well for the selected basis set. For VWN functional $A_{x,yz}$ is increasing with increase in number of basis functions. NIA-CPKS/BASIS follows the similar trend for both the functional, whereas reverse trend is seen for both the methods when PBE functional is used with GEN-A2 and GEN-A2* auxiliary functions. Dipole-quadrupole polarizabilities calculated with GEN-A2 auxiliary functions are higher than that of GEN-A2* for both the methods and basis sets. Within NIA-CPKS BASIS results lie between GEN-A2 and GEN-A2*. The difference between the NIA-CPKS/GEN-A2 and ADPT/GEN-A2 is comparatively greater than the NIA-CPKS-GEN-A2* and ADPT-GEN-A2*. NIA-CPKS/GEN-A2* and ADPT/GEN-A2* dipole-auadrupole polarizabilities are in good agreement with each other. This highlights that both our methods works excellent and can be used for large basis sets and large molecules. The experimentally derived dipole-quadrupole polarizability is 102±7.7 $e^2a_0^2E_H^{-1}$ [33]. All theoretical results are in disagreement with experimental observations. Our results for larger basis are quite similar to the results reported by Maroulis *et al.* [33] and the TDHF values reported by Quinet *et al.* [11] at smaller basis set which indicate that the large discrepancy between experiment and theory in adamantane is not a basis set problem. This shows that a fault in the electronic structure description is unlikely. Therefore, further studies are necessary.

4.4 Conclusion and scope of the work

In this chapter, we have presented the results of dipole-quadrupole polarizabilities calculated with two non-iterative approaches viz. ADPT and NIA-CPKS. These methods are implemented in deMon2k and illustrated for the tetrahedral molecules P_4, CH_4 and adamantane ($C_{10}H_{16}$). The results obtained are compared with (FF) MP2, CCSD and experimental dipole-quadrupole polarizabilities. We have shown that both methods provide consistent results within a chosen methodology, *i.e.* given functionals, basis sets and AUXIS or BASIS option. Qualitatively the ordering of the dipole-quadrupole polarizabilities of all three molecules is same for all methodologies. CCSD and (FF) MP2 have shown good agreement with dipole-quarupole polarizabilities calculated from ADPT and NIA-CPKS for the P_4 and CH_4 molecules. The results of our methods are also consistent with other theoretical studies reported in the literature. It has been observed that GEN-A2* auxiliary function sets are needed for quantitative accurate results, at least for small systems. These results highlight the stability of the ADPT and NIA-CPKS approach. In this study we have focused on the validation of our non-iterative methods for static dipole-quadrupole polarizability calculations. To the best of our knowledge this is the first time that non-iterative methods are used for dipole-quadrupole polarizability calculations within DFT. These methods will facilitate the study of large molecular systems such as clusters and bio-molecules without compromising accuracy. The observed discrepancy between experimental and theoretical dipole-quadrupole polarizabilities for adamantane raises many questions, in particular on the temperature and frequency dependency of these values. So far only estimates are available in the literature. The methodology to obtain dynamic electric response is already developed within ADPT [34]. Thus it can be used for studying the dynamic dipole-quadrupole polarizabilities. The temperature effects can be added by first principle BOMD simulations. This was already successfully applied to dipole-polarizabilities [35] and can be extended to dipole-quadrupole polarizabilities.

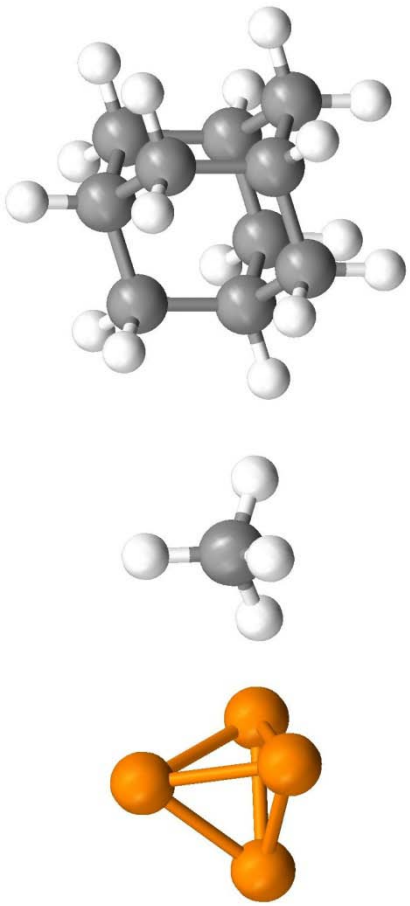

Fig 4.1 Tetrahedral geometries of P_4, CH_4 and adamantane($C_{10}H_{16}$)

Table 4.1: Static dipole-quadrupole polarizability ($A_{x,yz}$) of P_4 [a.u.].

Basis	Basis Functi-ons	Functional	NIA-CPKS			ADPT		CCSD	MP2
			BASIS	GEN-A2*	GEN-A2	GEN-A2*	GEN-A2		
P0[1]	132	PBE	83.3726	83.9818	84.7874	83.5986	85.4600	82.7363	81.7878
		VWN	81.5881	81.2707	86.0756	81.1477	86.2040		
P1[2]	156	PBE	85.1419	86.3161	86.3950	85.8753	87.3610	83.0694	82.3996
		VWN	84.1123	84.5174	88.6108	83.9323	89.0184		
P2[3]	196	PBE	86.2429	87.5432	87.7090	87.2405	88.3394	83.6203	82.6886
		VWN	85.5854	85.5836	90.2155	85.1816	90.8808		
P3[4]	260	PBE	86.1470	87.2131	87.0288	87.0432	88.1526	84.0828	83.1699
		VWN	85.7363	85.6880	89.9586	84.7702	90.4400		

[1][6s5p2d]
[2][6s5p3d]
[3][6s5p3d1f]
[4][6s5p3d2f]

Table 4.2: Static dipole-quadrupole polarizabilities ($A_{x,yz}$) of CH_4 [a.u.].

Basis	Basis Functi-ons	Functional	NIA-CPKS			ADPT		CCSD	MP2
			BASIS	GEN-A2*	GEN-A2	GEN-A2*	GEN-A2		
M1[1]	88	PBE	9.086	9.5317	8.6818	9.6044	8.5383	9.1882	9.2257
		VWN	8.9051	9.543	8.664	9.537	8.5619		
M2[2]	94	PBE	9.0761	9.5012	8.6517	9.6011	8.5054	9.1726	9.1833
		VWN	8.9002	9.5256	8.6534	9.5245	8.4605		
M3[3]	100	PBE	9.1047	9.4825	8.6819	9.6042	8.5067	9.1793	9.1915
		VWN	8.9256	9.5299	8.6499	9.5297	8.43		
M4[4]	110	PBE	9.0932	9.5062	8.713	9.6147	8.5265	9.1109	9.1246
		VWN	8.9106	9.5145	8.6603	9.5008	8.6722		

[1][6s4p2d1f/4s2p1d]
[2][6s4p3d1f/4s2p1d]
[3][6s4p4d1f/4s2p1d]
[4][6s4p4d2f/4s2p1d]

Table 4.3: Static dipole-quadrupole polarizabilities ($A_{x,yz}$) of adamantane [a.u.].

Basis	Basis Functions	Functional	NIA-CPKS		ADPT		
			BASIS	GEN-A2*	GEN-A2	GEN-A2*	GEN-A2
M1	656	PBE	10.5451	9.3205	15.8529	9.4776	13.1082
		VWN	11.4226	10.5766	15.9183	10.8307	12.6258
M4	876	PBE	10.6512	8.9593	15.7236	8.8324	11.5483
		VWN	11.6553	10.9805	16.1264	11.3859	13.0564

References

1. Maroulis, G.; Pouchan, C. *J. Chem. Phy. B*, **2003**, *107*, 10683.
2. Karamamanis, P.; Maroulis, G. *J. Chem. Phys.* **2006**, *124*, 071101.
3. Tabisz, G. C.; Neuman, M. N. (Eds.), Collision and Interaction Induced Spectroscopy, Kluwer, Dordrecht, 1995.
4. Hohm U.; Maroulis, G. *J. Chem. Phys*. **2004**, *121*, 10411.
5. Maroulis, G.; Hohm, U. *Phys. Rev. A*, **2007**, *76*, 032504.
6. Hohm, U.; Loose, A.; Maroulis, G.; Xenides, D. *Phys. Rev. A*, **2000**, *61*, 053202.
7. Hohm, U.; Maroulis, G. *J. Chem. Phys.* **2006**, *124*, 124312.
8. Maroulis, G. *Chem. Phys. Lett.* **1994**, *226*, 420.
9. Maroulis, G. *Chem. Phys. Lett.* **1999,** *312*, 255.
10. Amos, R. D. *Chem. Phys. Lett.* **1982**, *87*, 23.
11. Quinet, O.; Liégeois, V.; Chanpagne, B. *J. Chem. Theory Comput.* **2005**, *1*, 444.
12. McColl, I. H.; Blanch, E. W. ; Gill, A. C.; Rhie, A. G. O. ; Ritchie, M. A. ; Hecht, L.; Nielsen, K.; Barron, L. D. *J. Am. Chem. Soc.* **2003**, *125*, 10019.
13. Flores-Moreno, R.; Köster, A. M. *J. Chem. Phys.* **2008**, *128*, 134015.
14. Sophy, K. B.; Pal, S. *J. Chem. Phys.* **2003**, *118*, 10861.
15. Sophy, K. B.; Pal, S. *THEOCHEM* **2004**, *676*, 89.
16. Sophy, K. B.; Calaminici, P.; Pal, S. *J. Chem.Theory Comput.* **2007**, *3*, 716.
17. Sophy, K. B.; Shedge, S. V.; Pal, S. *J. Phys. Chem. A*, **2008**, *112*, 11266.
18. Shedge S.V.; Carmona-Espíndola J.; Pal S.; Köster A.M. *J. Phys. Chem. A* **2010**, *114*, 2357.
19. Shedge S.V.; Pal S.; Köster A.M. *Chem. Phys. Lett.* **2011,** *510,* 185.
20. Köster, A. M.; Calaminici, P.; Casida, M. E.; Flores, R.; Geudtner, G.; Goursot, A.; Heine, T.; Janetzko, F. M.; del Campo, J.; Patchkovskii, S.; Reveles, J. U.; Salahub, D. R.; Vela, A. *deMon2k, The deMon developers*; Cinvestav: Mexico City, Mexico, 2006. See http://www.demon-software.com
21. Buckingham, A. D. in: J. O. Hirsschfelder (Ed.), Advances in Chemical Physics, Interscience, New York, 1967, p. 107.
22. McLean, A. D.; Yoshimine, M. *J. Chem. Phys.* **1967**, *47*, 1927.

23. Boudon, V.; Mkdami, E. B.; Burger, H.; Pierre, G. *Chem. Phys. Lett.* **1999**, *305*, 21.
24. Schäfer, A.; Huber, C.; Ahlrichs, R. *J. Chem. Phys.*, **1994**, *100*, 5829.
25. Gray, D. L.; Robiette, A. G. *Mol. Phys.* **1979**, *37*, 1901.
26. Hargittai, I.; Hedberg, K. W. *J. Chem. Soc. Chem. Commun.* **1971**, p.1499.
27. Vosko, S. H.; Wilk, L.; Nusair, M. *Can. J. Phys.* **1980**, *58*, 1200.
28. Perdew, J. P.; Burke, K.; Ernzerhof, M. *Phys. Rev. Lett.* **1996**, *77*, 3865,.
29. Calaminici, P.; Janetzko, F.; Köster, A. M.; Mejia-Olvera, R. ; Zuniga-Gutierrez, B. *J.Chem. Phys.* **2007**, *126*, 044108.
30. Shedge, S. V.; Carmona-Espíndola, J.; Pal, S.; Köster, A. M. *J. Phys. Chem. A*, **2010**, *114*, 2357.
31. Hohm, U. *Chem. Phys. Lett.* **1999**, *31*, 117.
32. Buck, U.; Schleusener, J.; Mallik, D. J.; Secrest, D. *J. Chem. Phys.* **1981**, *74*, 1707.
33. Maroulis, G.; Xenides, D.; Hohm, U.; Loose, A. *J. Chem. Phys.* **2001**, *115*, 7957.
34. Carmona-Espíndola, J.; Flores-Moreno, R.; Köster, A. M. *J. Chem. Phys.* **2010**, *133*, 84102.
35. Gamboa, G. U.; Calaminici, P.; Geudtner, G.; Köster, A. M. *J. Phys. Chem. A*, **2008**, *112*, 1196.

CHAPTER 5

Ab initio MD simulation of static and dynamic dipole-quadrupole polarizability

Abstract:

The frequency and temperature dependence of dipole-quadrupole polarizability of tetrahedral P_4 and adamantane molecules have been studied using first-principle all-electron density functional theory calculation. The recently developed time-dependent auxiliary density functional theory has been extended for the calculation of dynamic dipole-quadrupole polarizabilities. Temperature effects are incorporated by BOMD simulations recorded up to 100 ps. The dynamic dipole-quadrupole polarizabilities are calculated along these trajectories. The analysis of these results shows that frequency and temperature effects can be significant for the accurate calculation of dipole-quadrupole polarizability. In particular, we identified that the adamantane dipole-quadrupole polarizability increase significantly with temperature whereas the P_4 dipole-quadrupole polarizability varies only marginally with temperature. Our analysis indicates that the strong temperature dependence of the adamantane dipole-quadrupole polarizability is the main reason for the observed discrepancy between experiment and theory.

5.1 Introduction

Plenty of experimental and theoretical studies are available on electric properties of atoms and molecules. Most of the work has focused on multipole moments, dipole-polarizabilities and first hyperpolarizabilities [1-3]. The experimental determinations of these multipole moments and polarizabilities are difficult and hence various theoretical methods have been developed for accurate calculation of these properties [4-11]. Electric properties are very sensitive to the basis set and electron correlation effects. These effects have been addressed well for the multipole moments and dipole-dipole polarizabilities [12-14]. However, few attempts have been made for accurate estimation of higher moment polarizabilities, such as dipole-quadrupole (A) and dipole-octupole polarizabilities (E). These polarizabilities dominate some of the spectroscopic measurements such as interaction induced spectroscopy [15, 16] and surface-enhanced Raman scattering [17]. Hence accurate values of dipole-quadrupole polarizabilities are necessary for precise determination of intermolecular interactions [18]. There are few combined experimental and theoretical studies in the literature for the determination of static dipole-quadrupole polarizabilities of molecules of tetrahedral (T_d) symmetry [19-21]. In most cases, the theoretical calculations have given fairly good estimates of these polarizabilities. However, some of the tetrahedral molecules have shown substantial mismatch between the theoretical and experimental results [21-23]. These polarizabilities were calculated with finite-field method and absence of frequency effects could be one reason for the observed discrepancy.

Quinet *et al.* have proposed the analytical TDHF method for the calculation of frequency-dependence of dipole-quadrupole polarizability and its derivatives with respect to atomic Cartesian coordinates [24]. Despite the inclusion of frequency effects, they have observed large discrepancy between theoretical and experimental dipole-quadrupole polarizability for adamantane in T_d symmetry. In chapter 4, we have analysed the effect of basis sets on the dipole-quadrupole polarizabilty of P_4, CH_4 and adamantane using either ADPT or NIA-CPKS method [25]. While ADPT is completely analytical, NIA-CPKS is a mixed numerical analytical approach. Both methods are implemented in deMon2k [26]. The details of implementation and validation of these two methods for dipole-dipole polarizability and dipole-quadrupole polarizabilities are presented in our previous papers [25, 27-29]. Similar

to former theoretical results for adamantane, our ADPT and NIA-CPKS also severely underestimate the experimental results [25]. As per our earlier observations, the basis set size effect is negligible and it is not responsible for the observed mismatch between the experimental and theoretical dipole-quadrupole polarizability of adamantane. Since the experiment involves elevated temperatures the observed discrepancy raises the question on the influence of finite-temperatures on dipole-quadrupole polarizabilities. To the best of our knowledge a systematic study of temperature-dependence of dipole-quadrupole polarizability has so far never been presented.

In this chapter, we present a detailed study of frequency and temperature dependence of the dipole-quadrupole polarizabilities of P_4 and adamantane. We have selected P_4 as a reference system because its calculated dipole-quadrupole polarizability matches well with the depolarized collision induced light scattering measurement at 800 K. The time-dependent ADPT variant has been used to calculate the dynamic dipole-quadrupole polarizabilities [30]. The temperature effects are studied with first-principle BOMD simulations in the framework of ADFT [31]. This methodology has been already successfully used for the calculation of the temperature dependence of dipole-dipole polarizabilities with deMon2k [32]. Here, we present the extension of ADPT method for the calculation of dynamic dipole-quadrupole polarizabilities and study the effect of temperature on it using BOMD simulations. Our results are compared with experimental and other theoretical values.

5.2 Theory

The theoretical definitions of electric moment and polarizability tensors of atoms and molecules have been provided by Buckingham [33] and McLean and Yoshimine[34]. Detailed discussion has been already presented in Chapter 1. Computationally, all components of the dipole-quadrupole polarizability tensor, $A_{k,ij}$, can be obtained as a trace of the product of the response density matrix and quadrupole integrals.

$$A_{k,ij} = Tr\left(P^{(k)} \cdot \Theta_{ij}\right) \tag{5.1}$$

Here $P^{(k)}$ denotes the density matrix derivative with respect to the external electric field in x, y or z direction. Θ_{ij} represents a quadrupole moment integral

matrix. The density matrix derivatives are obtained by ADPT. The working equations for the calculation of static and dynamic response properties within ADPT are presented in ref 27 and 30.

When the molecule is strictly in T_d symmetry, the only non-vanishing component of the dipole-quadrupole polarizability is $A_{x,yz}$. However, in BOMD simulations the dipole-quadrupole polarizability components are not rotationally invariant. Thus it is necessary to use the concept of rotational invariance for analysing the properties in terms of quantities that are independent of the coordinate systems. This can be achieved by decomposition of tensors of different ranks into irreducible parts with respect to the continuous group of rotations. Jerphagnon *et al*. [35, 36], Chemla *et al.* [37], and Sirotin [38] have introduced irreducible tensors for non-linear optics. Here we have followed the same formalism for the calculation of our dipole-quadrupole polarizability tensors in BOMD simulations. Cartesian tensors of rank n, $T(n)$ have 3^n components, an irreducible rank-n tensor is labelled in addition by its weight J [39-41].

We have considered the case of symmetric 3rd rank tensors here. For the most general non-centrosymmetric system, a third rank tensor has 27 components [42]. The irreducible tensors of weight 0, 1, 2, 3 corresponding to 3rd rank tensor are called pseudo-scalar, vector, pseudo-deviator and septor. The pseudo-scalar vanishes for symmetric 3rd rank tensors and, therefore, this component is absent in our calculations.

There are 3 vectors for 3rd rank tensor defined as,

$$V_i^1 = \sum_j T_{ijj}\,, V_j^2 = \sum_k T_{kjk}\; and\;\; V_k^3 = \sum_i T_{iik} \tag{5.2}$$

The three vectors are traces and, thus, irreducible under the rotational group. They can be recast in an embedded form as third-rank tensor:

$$T_{ijk}^{(1,1)} = \frac{1}{10}\left(4V_i^1\delta_{jk} - \delta_{ik}V_j^1 - \delta_{ij}V_k^1\right) \tag{5.3}$$

$$T_{ijk}^{(1,2)} = \frac{1}{10}\left(-V_i^2\delta_{jk} + 4\,\delta_{ik}V_j^2 - \delta_{ij}V_k^2\right) \tag{5.4}$$

$$T_{ijk}^{(1,3)} = \frac{1}{10}\left(-V_i^3\delta_{jk} - \delta_{ik}V_j^3 + 4\delta_{ij}V_k^3\right) \tag{5.5}$$

In our calculations we have defined the square root of the square sum of all these 3 embedded tensors as dipolar. The two pseudo-deviators are obtained by forming rank-2 pseudo-tensors by contraction with ϵ (totally anti-symmetric third-rank tensor known as Levi-Civitta).

$$D_{ij}^{1} = -\frac{1}{2}\sum_{i,m}(\epsilon_{ilm}\,T_{mlj} + \epsilon_{jlm}T_{mlj}) - \frac{1}{3}T^{(0)}\delta_{ij} \tag{5.6}$$

$$D_{ij}^{2} = -\frac{1}{2}\sum_{i,m}(\epsilon_{mlj}\,T_{ilm} + \epsilon_{mli}T_{jlm}) - \frac{1}{3}T^{(0)}\delta_{ij} \tag{5.7}$$

Their embedded form in the rank-3 tensor space is given as,

$$T_{ijk}^{(2,1)} = \frac{1}{3}\sum_{l}\left(2\epsilon_{ijl}D_{lk}^{1} + D_{il}^{1}\epsilon_{ijk}\right) \tag{5.8}$$

$$T_{ijk}^{(2,2)} = \frac{1}{3}\sum_{l}\left(\epsilon_{ijl}D_{lk}^{2} + 2D_{il}^{2}\epsilon_{ijk}\right) \tag{5.9}$$

We have recorded the square root of the square sum of these 2 tensors and defined this quantity as deviator. The septor is the natural form of the of a third-rank tensor. It can be obtained as,

$$S_{ijk} = \frac{1}{6}\left(T_{ijk} + T_{jki} + T_{kij} + T_{jik} + T_{ikj} + T_{kji}\right) \tag{5.10}$$

We have recorded the square root of the square sum of this tensor and named it septor. For the analysis of dipole-quadrupole polarizabilities along MD trajectories, we have recorded the above defined dipolar, deviator and septor components for each selected step along the trajectory. We have also recorded the dipole-quadrupole polarizability as square root of the square sum of all tensor components. Finally, at the end of the simulation, we have calculated average of all these components along the BOMD trajectories.

5.3 Computational details

In last chapter we have justified the appropriate methodology for reliable calculations of static dipole-quadruple polarizabilities using deMon2k software [25]. The generalized gradient approximated PBE [43] functional along with GEN-A2* [44] auxiliary functions gave good results of dipole-quadrupole polarizabilities.

Thus, we have followed the same methodology throughout this work. We have studied frequency dispersion for P_4 and adamantane. Both molecules are of cage like structure and possess T_d symmetry. The 0 K frequency dependent calculations are performed using the experimental geometry of P_4 and adamantane. The geometric parameters for both the molecules are reported in our earlier work [25]. We have used P0 [6s5p2d] [45] basis set for P_4 molecule, for both 0 K and higher temperature dipole-quadrupole polarizability calculations. All results are reported in atomic units. The frequencies (in a.u.) used for frequency dependent dipole-quadrupole polarizability of P_4 are 0.071981, 0.083831, 0.088558, 0.103158, 0.1200 and 0.1301389. Some of these frequencies were used by Maroulis *et al.* [46] for studying the frequency dispersion of dipole-dipole polarizabilities of P_4. For adamantane, we have used the comparatively smaller basis set, DV0 [3s2p/2s][47]. The frequency-dependent polarizabilities are reported for frequency range of 0.02 a.u. to 0.1 a.u by an interval of 0.02 a.u. These results are compared with dynamic dipole-quadrupole polarizabilities reported by Quinet *et al*. [24]

The finite temperature BOMD trajectories were calculated with the VWN/DZVP/A2 level of theory employing ADFT. For the P_4 molecule, 7 trajectories were recorded in a temperature range from 600-1200 K with an interval of 100 K. Each trajectory has a length of 100 ps and was recorded with a time step of 1fs. For adamantane we have recorded 10 trajectories in a temperature range between 300 and 750 K with an interval of 50 K. Again we used a trajectory length of 100 ps with time steps of 0.5 fs. The temperature in the canonical BOMD simulations was controlled by a Nosé-Hoover chain thermostat [48, 49]. The dipole-quadrupole polarizabilities were calculated along the recorded trajectories every 100 fs. for both molecules. Due to the computational demand of dipole-quadrupole polarizabilities along the BOMD trajectories, we have chosen smaller basis sets for these calculations. The computational levels of dipole-quadrupole polarizability calculations along BOMD trajectories for P_4 and adamantane were PBE/P0 [6s5p2d]/GEN-A2* and PBE/DV0/GEN-A2*, respectively.

5.4 Results and discussion

When the molecule remains strictly in T_d symmetry, the only non-zero component of dipole-quadrupole polarizability is septor component and the other

components vanish. For our 0K calculations, we assume T_d symmetry of the molecule, thus the only average septor component survives and becomes equal to the average dipole-quadrupole polarizabilities. In fig. 5.1, the average septor components of P_4 molecule calculated at 0K and at 1000 K are plotted against corresponding frequencies. As per our knowledge, the effect of frequencies on dipole-quadrupole polarizabilities of P_4 has not been studied earlier either theoretically or experimentally. The rotationally invariant septor component of dipole-quadrupole polarizability involves $A_{x,yz}$ tensor elements and therefore these components can be compared with septor component at 0K. These calculations are performed using ADPT in combination with BOMD. MD trajectories are calculated at experimental temperature of 1000K. It can be seen from fig. 5.1 that the average septor components at 1000K are increasing smoothly with frequency. The static septor component at 0K is lower than the corresponding 1000K component nearly by 7a.u. However, the difference between 0K and 1000K septor component is increasing with increase of frequencies. For the experimental frequency, 0.0885584 a.u., 0K septor component is lower than 1000K component by ~9 a.u. For the highest frequency used in these calculations the difference between 0K and 1000K component is 18 a.u. The experimental A obtained from depolarized collision induced light scattering measurement is 77±26 a. u. Theoretical value of average septor component of $A_{x,yz}$ at 0K is 227.09 a.u and the septor component at 1000K is 235.859 a.u. The theoretical value of the average polarizability at 1000K is 236.211 a u. The experimental value of A can be converted into average polarizability for comparison with our theoretical result. Considering the experimental error bars our theoretical value of average polarizability matches well with experimental average polarizability component, 188.61±64 a.u.

The frequency dispersion results of dipole-quadrupole polarizabilities of adamantane molecules are presented in fig 5.2. Our results calculated with ADPT are compared with the results of Quinet *et al.*[24] Their calculations were performed at TDHF/DV0[3s2p/2s] level of theory. We have used the same basis set for our calculations so that both the methods can be compared for calculation of dynamic dipole-quadrupole polarizabilities. These are 0K polarizabilities therefore here we have plotted $A_{x,yz}$ component of dipole-quadrupole polarizability against the corresponding frequencies. A fig. 5.2 shows that the Dipole-quadrupole

polarizabilities are increasing with the frequencies. The static component of $A_{x,yz}$ is 9.453175a.u. and at the highest frequency of 0.1 a.u. the component value becomes 9.9368976a.u. Thus the increment of ~0.5 a.u. is observed which shows that the frequency does not affect the dipole-quadrupole polarizabilities of adamantane molecule to large extent. The comparison between curves of ADPT and TDHF polarizabilities shows that qualitatively both methods behave identical. However, higher increments are observed for the ADPT polarizabilities. The static dipole-quadrupole polarizability of ADPT and TDHF differ nearly by 0.3 a. u. Both the methods are in excellent agreement with each other at 0.08 and 0.1 a.u. of frequency. DFT polarizabilities are lower than TDHF at frequency 0.08 a.u. and reverse is observed at 0.1a.u. The experimentally reported dipole-quadrupole polarizability component of adamantane is 102±7.8 a.u. Theoretical value of $A_{x,yz}$ calculated from various studies is one order of magnitude smaller than the experimental measurement. Thus our results clarify that the dispersion does not explain the huge difference observed between the experimental and theoretical value for adamantane. All the experimental polarizabilities are measured at higher temperatures, thus for direct comparison between the experimental and theoretical values the finite temperature effect has to be accounted in theoretical calculations. By using ADPT in combination with canonical BOMD temperature dependent static and dynamic polarizabilities can be calculated.

We report here the effect of temperature on dynamic dipole-quadrupole polarizabilites of P_4 and adamantane. In table 5.1 and table 5.2, we report the rotationally invariant components of dynamic dipole-quadrupole polarizability of P_4 and adamantane respectively. The averages of deviator, dipolar and septor components along with average polarizability and standard deviation of polarizability are tabulated in the table. P_4 results are calculated for temperature ranging from 600K to 1200K by an interval of 100K. Adamantane results are reported for 300K to 750K with an increment of 50K. It can be seen from the table 5.1, that the dipolar and deviator components are increasing with increase of temperature. However, septor and average dipole-quadrupole polarizabilities are increasing up to 1100K and at 1200K it is giving slightly lower value than reported component at 1100K. Similarly, in case of adamantane all these components are increasing with temperature. However, compared to P_4 higher increment is observed

for adamantane molecule. Difference between septor and average polarizability is less. Average dipole-quadrupole polarizability includes the effect of all the tensor components of at corresponding temperature. Average polarizability is increasing nearly by 18 a.u. when the temperature increases from 300 to 750, however, in case of P_4 the value of this component is increasing by nearly 4 a.u. from 600-1200K. For the molecule of T_d symmetry the dipolar component must be zero. The table 5.1 shows that the dipolar contribution for P_4 is ~3.4% of its average polarizabilities at 600K as the temperature increases to 1200K it becomes ~5%. Hence, the assumption of T_d symmetry for P_4 molecule at higher temperature works well. As a result the experimental dipole-quadrupole polarizability of P_4 molecules matches well with the theoretical value. On the other hand for adamantane molecule the dipolar component is nearly 40% of its average polarizability at 300K. Compared to P_4 the dipolar contribution for adamantane is increasing faster with the temperature, it becomes 50% of its average polarizability at 750 K. Thus for adamantane the temperature effects are much more important than for P_4. Our analysis shows that adamantane at elevated temperatures cannot be considered in T_d symmetry. This might be the main source of error in the analysis of the experimental data. For comparison with our results calculated by ADPT, we convert this experimental value of $A_{x,yz}$ to average dipole-quadrupole polarizability and it gives value as 249±19.106 a.u. The theoretical value of the average polarizability and the average septor component calculated at experimental temperature (605 K) and frequency 0.0885584 a.u. are 43.239 a.u. and 51.131 a.u. respectively. The experimental value is very much different from our theoretical result. The inclusion of frequency and temperature effects do not raise theoretical polarizabilities to match the experimental results. Thus the interpretation of the experiment assuming only the $A_{x,yz}$ active component is not realistic for elevated temperatures.

5.5 Conclusions

In conclusion we have shown that the time dependent ADPT can be used for calculation of dynamic dipole-quadrupole polarizabilities. Using time dependent ADPT in combination with BOMD the simultaneous effect of temperature and frequency on dipole-quadrupole polarizability can be studied. Thus our

implementation facilitates the direct comparison between experimental and theoretical polarizabilities at given temperature and frequencies. The methodology has been validated by calculation over the P_4 and adamantane molecule. It has been seen that the average dipole-quadrupole polarizabilities of P_4 increases with increase of frequency. Similarly, the frequency dispersion at experimental temperature has also shown the same trend. The inclusion of frequency and temperature has not affected the polarizabilities values of P_4 to large extent. Hence, the dipole-quadrupole polarizabilities of P_4 are not significantly affected by frequency and temperature. The theoretical measurements are well within the experimental upper bound. The dispersion study of adamantane molecule has shown the similar trend as that of P_4 molecules. The comparison of time dependent ADPT with TDHF for calculation dipole-quadrupole polarizabilities has shown the reliability of our approach. The dispersion results of ADPT and TDHF have shown the same qualitative behaviour. Even though, dipole-quadrupole polarizabilities of adamantane increase with the frequency, they do not increase to the extent to match the experimental results. Study of dispersion does not fully explain the reason of large discrepancy between experimental and theoretical values for adamantane molecule. The calculation of dynamic dipole-quadrupole polarizability at experimental frequency and the range of temperature have shown the interesting results for P_4 and adamantane molecule. For analysing dipole-quadrupole polarizabilities along the BOMD simulation we have reported here the rotationally invariant tensors of third rank tensor for symmetric case. The analysis of these tensor components have shown that the answer for discrepancy lies in the symmetry distortion of the molecule at higher temperature. The difference between average polarizability and septor component tells about the symmetry distortion. The P_4 molecule remains more or less in T_d symmetry at elevated temperature thus the assumption of T_d symmetry for experimental evaluation of polarizabilities works well. However, the adamantane molecule no longer remains in Td symmetry at higher temperature. Thus, this might be the main source of error in the analysis of the experimental data. Our study clearly reveals the reasons for observed discrepancy of experimental and theoretical observations for adamantane molecule. On the other hand our calculations have demonstrated the potential of our methodology for calculation of dynamic dipole-quadrupole polarizabilities at higher temperatures. The ADPT implementation can be further extended for calculation of geometric

derivative of dipole-quadrupole polarizabilities. Both these quantities are directly involved in determination of vibrational Raman optical activity (VROA) [24, 50].

Fig.5.1: Frequency dependence of dipole-quadrupole polarizability (0K values converted to match the rotational invariant septor component) calculated at 0K and 1000K (experimental temperature). Computational level of theory: ADPT/PBE/P0[6s5p2d]/GEN-A2*.

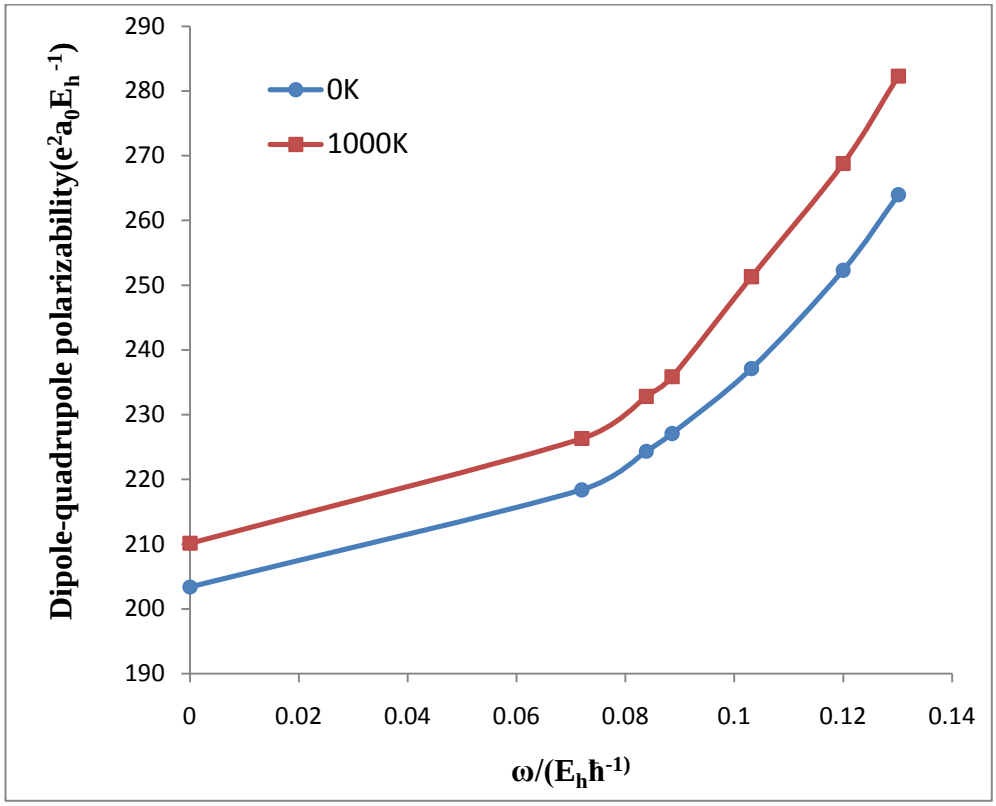

Fig.5.2: Frequency dependence of dipole-quadrupole polarizability (0K values converted to match the rotational invariant septor component) calculated at 0K and compared with results reported by Quinet *et al.*[24] Computational level of theory: ADPT/PBE/DV0/GEN-A2*.

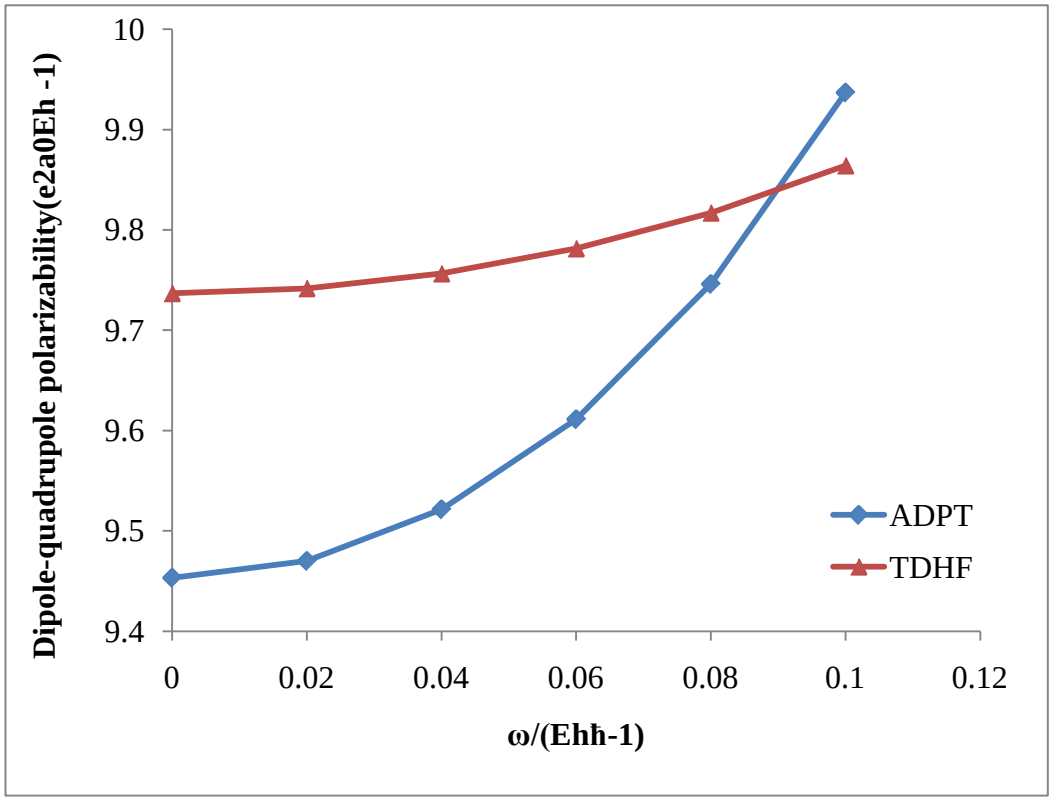

Table 5.1 P4: The rotational invariant components of dipole-quadrupole polarizability calculated along BOMD trajectories for various temperatures and experimental frequency of 0.0885584 a.u. (514.5 nm). Polariabilities are calculated at ADPT/PBE/P0 [6s5p2d]/GEN-A2* level of theory.

T(K)	Average Dipolar	Average Deviator	Average Septor	Average Polarizability	Standard Deviation Polarizability
600	7.935	1.088	233.161	233.339	11.186
700	8.764	1.139	234.459	234.674	12.847
800	9.945	1.203	234.733	235.009	13.392
900	10.040	1.276	235.685	235.962	13.758
1000	11.354	1.324	235.859	236.211	14.442
1100	12.151	1.502	236.727	237.150	16.393
1200	12.217	1.657	236.558	236.970	15.987

Table 5.2 Adamantane(C10H16): The rotational invariant components of dipole-quadrupole polarizability calculated along BOMD trajectories for various temperatures and experimental frequency of 0.0885584 a.u. (514.5 nm). Polariabilities are calculated at ADPT/PBE/P0 [6s5p2d]/GEN-A2* level of theory.

T(K)	Average Dipolar	Average Deviator	Average Septor	Average Polarizability	Standard Deviation Polarizability
300	15.865	5.176	36.345	40.622	8.730
350	17.711	5.649	36.903	42.045	9.020
400	19.687	5.917	37.070	43.233	9.720
450	20.625	6.277	38.991	45.426	9.894
500	21.082	6.645	41.040	47.539	10.743
550	22.902	7.107	41.322	48.775	10.995
600	24.238	7.733	45.847	53.510	11.974
650	25.500	7.735	45.353	53.761	12.121
700	27.121	7.978	45.699	55.069	12.915
750	29.462	8.363	48.219	58.463	13.725

References

1. Boggard M. P.; Orr, B. J. in Molecular Structure and Properties, edited by A.D.Buckingham (Butterworths, London, 1975), Vol. 2, p. 149.
2. Buckingham, A. D. in intermolecular Interactions: From Diatomics to Bipolymers, edited by B. Pullman (Wiley, New York, 1978), p.1.
3. Hanna, D. C.; Yuratich, M. A.; Cotter, D. Nonlinear Optics of Free Atoms and Molecules (Springer, Berlin, 1979)
4. Sekino, H.; Bartlett, R.J.; *J. Chem. Phys.* **1986**, *84*, 2726.
5. Sekino, H.; Bartlett, R. *J. Chem. Phys.* **1991**, *94*, 3665.
6. Karna, S. P.; Dupuis, M. *J. Comput. Chem.* **1991**, *12*, 487.
7. Rice, J. E.; Amos, R. D.; Colwell, S. M.; Handy, N. C.; Sanz, J. *J. Chem. Phys.* **1990**, *3*, 8828.
8. Stott, M. J.; Zaremba, E. *Phys. Rev. A* **1980**, *21*, 12.
9. Mahan, G. D. *Phys. Rev. A* **1980**, *22*, 1780.
10. Deb, B. M.; Ghosh, S. K. *J. Chem. Phys.* **1982**, *77*, 342.
11. Ghosh, S. K.; Deb, B. M. *Chem. Phys.* **1982**, *71*, 295.
12. Torrent-Sucarrat, M.; Solà, M.; Duran, M; Luis, J. M.; Kirtman, B.; J. *Chem. Phys.* **2003**, *118*, 711.
13. Canuto, S. *Int. J. Quant. Chem.: Quantum Chemistry Symposium***1994**, *28*, 265
14. Maroulis, G. *J. Chem. Phys.* **1997**, *108*, 5432.
15. Cohen, E. R.; Birnbaum, G. *J. Chem. Phys.* **1977**, *66*, 2443
16. Collision and Interaction Induced Spectroscopy, edited by Tabisz, G. C. and Neuman, M. N. (Kluwer, Dordrecht, 1995)
17. Moskovits, M. *J. Raman Spectrosc.* **2005**, *36*, 485.
18. Li, X.; Champagne, M. H.; Hunt, K. L.C. *J. Chem. Phys.* **1998**, *109*, 8416.
19. Hohm, U.; Maroulis, G. *J. Chem. Phys.* **2004**, *121*, 10411.
20. Hohm, U.; Loose, A.; Maroulis, G.; Xenides, D. *Phys. Rev. A* **2000**, *61*, 053202.
21. Hohm, U.; Maroulis, G. *J. Chem. Phys.* **2006**, *124* 124312.
22. Maroulis, G.; Xenides, D.; Hohm, U.; Loose, A. *J. Chem. Phys.* **2001**, *115* 7957.
23. Maroulis, G.; Hohm, U. *Phys. Rev A,* **2007**, *76*, 032504.

24. Quinet, O.; Liégeois, V.; Chanpagne, B. *J. Chem. Theory Comput.* **2005**, *1*, 444.
25. Shedge, S. V.; Pal, S.; Köster, A. M. *Chem. Phys. Lett.* **2011**, *510*, 185.
26. A. M. Köster, P. Calaminici, M. E. Casida, R. Flores-Mereno, G. Geudtner, A. Goursot, T. Heine, F. M. Janetzko, J. del Campo, S. Patchkovskii, J. U. Reveles, D. R. Salahub, A. Vela deMon2k, developers, Cinvestav: Mexico City, Mexico 2006.See http://www.demon-software.com
27. Flores-Moreno, R.; Köster, A. M. *J. Chem. Phys.* **2008** *128*, 134015.
28. Sophy, K. B.; Pal, S. *J. Chem. Phys.* **2003**, *118*, 10861.
29. Sophy, K. B.; Shedge, S. V.; Pal, S. *J. Phys. Chem. A* **2008***112*, 11266.
30. Carmona-Espíndola, J.; Flores-Moreno, R.; Köster, A. M. *J. Chem. Phys.* **2010**, *133*, 084102.
31. Köster, A. M.; Reveles, J. U.; del Campo, J. M. *J. Chem. Phys.* **2004**, *121* 3417.
32. Gamboa, G. U.; Calaminici, P.; Geudtner, G.; Köster, A. M. *J. Phys. Chem. A* **2008**, *112*, 11969.
33. Buckingham, A. D. in: J. O. Hirsschfelder (Ed.), Advances in Chemical Physics, Interscience, New York, 1967, p. 107.
34. McLean, A. D.; Yoshimine, M. *J. Chem. Phys.* **1967**, *47*, 1927.
35. Jerphagnon, J. *Phys. Rev. B* **1970**, *2*, 1091.
36. Jerphagnon, J.; Chemla, D. S. *Acta Crystallogr. A* **1972**, *28*, 5231.
37. Chemla, D. S.; Oudar, J. L.; Jerphagnon, *J. Phys. Rev. B* **1975**, *12*, 4534.
38. Sirotin, Y. I. *Soviet Phys. Crystallogr.* **1975**, *19*, 565.
39. Shouten J. A. Tensor Analysis for Physicists (Oxford: Claredon Press) 1964.
40. Coope, J. A. R.; Snider, R. F *J. Math. Phys.* **1970**, *11*, 1003.
41. Coope, J. A. R.; Snider, R. F.; McCourt, F. R. *J. Chem. Phys.* **1965**, *48*, 2269.
42. Jerphagnon, J.; Chemla, D.; Bonneville, R. *Advances in Physics* **1978** *27*, 609.
43. Perdew, J. P.; Burke, K.; Ernzerhof, M. *Phys. Rev. Lett.* **1996**, *77*, 3865.
44. Calaminici, P.; Janetzko, F.; Köster, A. M.; Mejia-Olvera, R.; Zuniga-Gutierrez, B. *J. Chem. Phys.* **2007**, *126*, 044108.
45. Schäfer, A.; Huber, C.; Ahlrichs, R. *J. Chem. Phys.* **1994**, *100*, 5829.

46. Hohm, U.; Loose, A.; Maroulis, G.; Xenides, D. *Phys. Rev. A* **2000**, *61*, 053202.
47. Maroulis, G.; Xenides, D.; Hohm, U.; Loose, A. *J. Chem. Phys.* **2001**, *115*, 7957.
48. Nosé, S. J. *J. Chem. Phys.* **1984**, *81*, 511.
49. Hoover, W. G. *Phys. Rev. A* **1985**, *31*, 1695.
50. McColl, I. H.; Blanch, E. W.; Gill, A. C.; Rhie, A. G. O.; Ritchie, M. A.; Hecht, L.; Nielsen, K.; Barron, L. D. *J. Am. Chem. Soc.* **2003**, *125*, 10019.

CHAPTER 6

Behaviour of density functional theory for electric response properties at distorted geometries of molecules

Abstract:

The role of exchange-correlation is well known for accurate calculations of electric response properties. The exchange-correlation functional in density functional theory (DFT) has been well studied for ground state equilibrium geometry. However, the behaviour of these functionals in stretched geometries, where static correlation play an important role, has not been studied systematically, particularly for response electric properties. Thus we present here the rigorous calculation of electric response properties at distorted geometries of the molecules. We have considered dipole polarizability and dipole quadrupole polarizability for description of role of static and dynamic correlation for electric response properties. The calculations are performed with NIA-CPKS method described in earlier chapters. These DFT results are compared with higher level *ab initio* methods, such as CCSD and fully correlated full CI. We have studied single, double and triple bonded systems at different inter-nuclear separation. We report here the dipole-polarizability and dipole-quadrupole-polarizability of HF, BH, H_2CO, CO and NO^+. We also present the effect of basis and functional on polarizability and dipole-quadrupole polarizability.

6.1 Introduction

The recent developments in theoretical and computational chemistry have made the study of large molecular systems possible. A lot of interest lies in determining structure and properties of systems such as clusters, nano-materials, bio-molecules and periodic systems. DFT has proved to be a good tool for studying such systems efficiently and with reasonable accuracy. The theory is exact in principle for ground states and works well at low computational cost. Thus DFT has been applied broadly in solid state physics and material chemistry for understanding a wide range of phenomenon [1-2]. DFT has also been applied widely for electric and magnetic response properties [3-7]. Static and dynamic electric properties have been studied extensively during last few years [8-11]. A weak electric perturbation affects the electronic distribution of the molecule and it can be analyzed with the study of electric response properties. The newly introduced ADPT and NIA-CPKS are the two non-iterative methods developed for efficient calculation of response of electric perturbation within DFT [14, 15]. These two approaches have been implemented in the master version of deMon2k [16] software for dipole-dipole polarizability. Both the approaches are well tested for dipole-dipole polarizability calculations [17]. Recently, these approaches have been further extended for calculation of dipole-quadrupole polarizabilities and their reliability has been verified by comparison with higher level *ab initio* methods [18]. Both the approaches have provided reasonably accurate and promising results in our earlier studies.

Electron correlation plays an important role in accurate description of binding energies and electric response properties of molecules and materials. Fundamentally DFT gives exact treatment of static and dynamic correlation [19–21]. Though DFT is exact in principle for ground state its success in actual calculation lies in proper formulation of exchange–correlation functional. For ground state equilibrium geometry, a systematic study of exchange-correlation functional has been made in recent years. It is well known from systematic *ab initio* quantum chemical theories that the ground state equilibrium geometry is dominated by dynamic electron correlation. From this, it can be surmised that there exists reliable functional in DFT, which describes dynamic correlation efficiently. However, it is not clear whether the same functionals of DFT can describe the degenerate or near-degenerate states, open-shell systems, breaking of chemical bonds and strongly

correlated systems that are dominated by static correlation. Preliminary studies point to inadequacy of these functionals in representing static correlation leading to incorrect density and energy [22, 23]. The new functional has been developed to cover static correlation in DFT, but it is still beyond the practical application [24]. The single determinant picture of DFT fails to take into account the static correlation. Bally *et al.* have studied the potential energy curve for H_2^+ [25] with DFT method. The H_2^+ potential has showed local minimum at infinity, which should be exactly zero. This wrong behaviour of DFT method is due to the self interaction error [26, 27]. Additionally, DFT gives the incorrect description of dissociation limit of H_2 [28, 29] molecule and some ionic systems such as LiF [30–32]. However, fewer studies are available on behaviour of DFT for response electric properties of molecules [12, 33]. Thus, we present here rigorous calculation of dipole-dipole polarizability and dipole-quadrupole polarizability for a range of internuclear separation and careful analysis of behaviour of DFT for electric properties.

In present chapter, we have considered single bonded, double bonded, triple bonded and charged molecules for our study. The polarizability, quadrupole polarizabilities have been calculated with our NIA-CPKS approach. Different functionals have been employed to observe the consequences of exchange correlation effect on these properties. For comparison the *ab initio* calculations are performed using full CI and CCSD method.

6.2 Theory

The dipole moment and dipole-dipole polarizability are the first and second derivatives of ground state energy with respect to electric field perturbation at zero field respectively. Similarly, dipole-quadrupole polarizability is the second derivative of energy with respect to electric field perturbation, F and field gradient, F' at their zero values.

$$\mu_i = -\left(\frac{\partial E}{\partial F_i}\right)_{F=0} \tag{6.1}$$

$$\alpha_{ij} = -\left(\frac{\partial^2 E}{\partial F_i \partial F_j}\right)_{F=0} \tag{6.2}$$

$$A_{i,jk} = -\left(\frac{\partial^2 E}{\partial F_i \partial F_{jk}}\right)_{F=0,F'=0} \tag{6.3}$$

According to Helmann-Feynman theorem, for the exact wavefunction and variational method, the first derivative of energy with respect to electric field is equal to the expectation value of the derivative of the Hamiltonian. For electric properties, derivative of energy is equal to expectation value of dipole moment operator. When the respective method used for the calculation is variational, then according to Wigner's (2n+1) rule response up to 3^{rd} order can be calculated from the 1^{st} order response of wave function or density. The response properties can be calculated using various methods, such as perturbative method and field-dependent methods. The perturbative methods involve coupling of the excited states for example sum-over states (SOS), whereas field-dependent approaches involve the finite-field and coupled schemes which include CPHF method. In CPHF, Hamiltonian has field-dependence and coupled equations have an implicit dependence on the first-order response thus they need to be solved iteratively. When this approach is implemented in DFT it is known as coupled CPKS. This is the conventional approach used for calculation of first order response of the electric field perturbation. The bottleneck of this approach is the calculation of exchange-correlation kernel derivative which makes it practically difficult to apply for large systems. In NIA-CPKS [12, 13], the derivative of KS matrix is calculated numerically, thus the calculation of functional derivative of Coulomb and exchange correlation is avoided and solution is obtained in single step. Once the perturbed coefficients are calculated from CPKS equation, the response density can be calculated. The components of dipole-dipole polarizability or dipole-quadrupole polarizability can be calculated by taking a trace of the perturbed density matrix and dipole or quadrupole integrals respectively. For the detailed discussion of the implementation of dipole-polarizability and dipole-quadrupole-polarizability, one can refer to previous chapters of this thesis.

6.3 Computational details

We present here the dipole-dipole polarizabilities and dipole-quadrupole polarizabilities of HF, BH, H_2CO, CO and NO^+ molecules for different internuclear separation. For HF and BH, polarizabilities are studied from $0.25R_e$ to $2.5R_e$. In case of formaldehyde, bond is stretched up to 1.75Re and for triple bonded systems CO and NO^+, values are reported up to $1.5R_e$. Here for diatomic molecule R_e is the inter-

nuclear distance at equilibrium geometry and for H_2CO we defined R_e as equilibrium bond length of double bond between carbon and oxygen. For H_2CO, R_e was taken to be 2.27334 a.u [34]. The inter-nuclear distance of single boned HF and BH have been taken as 1.7328 a.u.[35] and 2.3289 a.u. [36] respectively, whereas R_e for triple bonded NO^+ and CO was used as 2.132242 a.u.[37] and 2.00919 a.u. [38] respectively. All calculations have been done using centre of mass coordinate representation. Polarizabilities of BH calculated within DFT have been compared with finite-field (FF) full CI results and for other molecules comparisons have been made with results calculated through (FF) coupled perturbed singles and doubles (CCSD). Here, by finite-field full CI we mean polarizabilities calculated with full CI using finite difference of dipole moments at +0.001 a.u and -0.001 a.u. field values. Similar definition holds for (FF) CCSD. All DFT calculations have been carried out using NIA-CPKS implemented within deMn2k software. The benchmark full CI and CCSD calculations were performed using GAMESS [39]. Three different functionals and three different basis sets were used for the calculation. The functional chosen were local functional, VWN [40] and nonlocal PBE [41] and BLYP [42, 43]. We report here the polarizabilities of HF calculated with aug-cc-pVDZ, Sadlej and DZP basis set. Polarizabilities of BH molecule are calculated with cc-pVDZ basis. We have used Sadlej basis set for calculating polarizabilities of H_2CO molecule. Polarizabilities of CO and NO^+ are reported with cc-pVDZ and aug-cc-pVDZ basis respectively. Chosen basis sets are seen to be working well for the respective molecules. We have employed GEN-A2* [44] auxiliary basis for calculation along with all three functional. In our earlier work it has been observed that PBE functional with GEN-A2* basis works well for polarizability calculation [17]. Atomic units (a.u.) are used to define dipole-dipole polarizability and dipole-quadrupole polarizability throughout this chapter. Diatomic molecules were kept along z axis. For the formaldehyde molecule double bond was aligned along z axis and the molecule was kept in xz plane. Diatomic molecules are of $C_{\infty v}$ symmetry and H_2CO belongs to C_{2v} point group symmetry. According to Buckingham [45] for molecules of $C_{\infty v}$ symmetry there are two independent components of dipole-quadrupole polarizability viz A_{xzx} and A_{zzz}. Molecules of C_2v symmetry have four independent components. Thus, we report here $A_{x,xz}$ $A_{y,yz}$, $A_{z,xx}$, $A_{z,yy}$ components for formaldehyde. The reported components of dipole-quadrupole polaizabilities are traceless quantities.

6.4 Results and discussion

HF and BH molecule are studied thoroughly to understand the effects of exchange and correlation functional in determining dipole-dipole polarizability and dipole-quadrupole polarizability at different inter-nuclear separation. For these two small systems, we have compared the results with extensive *ab initio* calculations in different basis sets. Formaldehyde molecule has double bond between carbon and oxygen atom. It is an interesting molecule for spectroscopic studies and hence the study of electric properties of this molecule is of interest. CO and NO^+ are the simplest triple bonded molecules. CO is significant molecule in astrophysical studies of interstellar molecular clouds [48]. The effect of electron correlation plays key role in determining exact polarizabilities of CO. NO^+ is iso-electronic with CO, yet the electric polarizabilities of the two molecules are markedly different.

The DFT calculations are done with our recently developed NIA-CPKS approach. As stated in the introduction, this approach has been already validated for calculation of dipole-dipole polarizabilities and dipole-quadrupole polarizabilities [12,18]. The considered set of molecules has been studied enormously with different methods for equilibrium and distorted geometries. However, very few of these studies are on the behaviour of DFT for calculation of polarizability at different geometries. In fact, this study represents the first case of dipole-quadrupole polarizability of molecules at different inter-nuclear distances. As pointed out earlier, the static correlation becomes dominant in such cases.

Table 6.1 reports the dipole-quadrupole polarizability of HF molecule with aug-cc-pVDZ basis set. For both HF and BH we report the polarizabilities from 0.25 R_e to 2.5R_e. The benchmarking of the DFT results of HF is done with CCSD results. It is seen from the table 6.1 that from 0.25R_e to 1.75R_e, dipole quadrupole polarizability components of HF, calculated from DFT, are in reasonable agreement with the CCSD values. The difference between CCSD and DFT polarizability increases progressively with increasing inter-nuclear distance from 2R_e to 2.5R_e. The CCSD absolute values of A_{xzx} and A_{zzz} components are generally lower than the DFT absolute value up to 1.5R_e and 1.25R_e respectively. Beyond this, the absolute values of both these components at CCSD level are larger than those at DFT level. However, we find interestingly for A_{zzz} component, that at 2.5R_e absolute value at CCSD level is again lower than DFT level. Similarly, at 0.25R_e the trend of CCSD

and DFT for these two components is different. However, for $0.5R_e$ values of CCSD and DFT are of opposite sign, showing the sensitivity of results to the nature of electron correlation. Within DFT, all the functionals behave more or less the same way. We have also reported the trend of A_{zzz} component of dipole-quadrupole polarizability in Sadlej and DZP basis set. The qualitative results of A_{zzz} component are given in fig. 6.1a and 6.1b. The CCSD results with Sadlej basis confirm the same type of nature observed for aug-cc-pVDZ basis set. For the DZP basis minima is observed for at $2.25R_e$ which was not very clear in Sadlej and aug-cc-pVDZ basis sets. In case of DFT results, such nature is absent for A_{zzz} component**.**

Dipole-dipole polarizabilities of HF and BH molecule were studied earlier with DZ, DZP and Sadlej basis set only up to $2R_e$ [12, 34]. However, we have presented in this chapter the results beyond $2R_e$. The qualitative results of α_{xx} and α_{zz} component are plotted as a function of internuclear distance up to 2.5 R_e, in fig. 6.2a and fig. 6.2b respectively. These results were obtained using aug-cc-pVDZ basis set. The fig. 6.2a for α_{xx} component shows that the DFT results are higher than the CCSD values from $0.25R_e$ to $1.75R_e$. Around $2R_e$, these tend to get closer to CCSD results. Among the DFT functionals, BLYP functional is behaving better for α_{xx} component at stretched internuclear distance of HF molecule. It is known from earlier *ab initio* results that between $2R_e$ to $2.5R_e$ α_{zz} component of dipole-dipole polarizability shows a maximum. The same is observed in fig. 6.2b for CCSD results for α_{zz} with maxima at $2.25R_e$. However, such maximum is missing for DFT results of α_{zz} component. In table 6.2, we report α_{zz} component of HF molecule calculated with Sadlej and DZP basis. For these basis sets relaxed extended (ECCSD) results were available in literature [49] and thus the benchmarking of DFT results is done with the *ab initio* results. DFT results are in agreement with the ECCSD results up to $1.25R_e$, whereas, from $1.5R_e$ to $2.5R_e$ the discrepancy between DFT and ECCSD has been increased. DFT results are almost double the ECCSD at $2.5R_e$. The ECCSD results also show maxima between $2R_e$ and $2.5R_e$ for Sadlej and DZP basis sets, however, for DFT results such maxima is absent even for Sadlej and DZP basis sets. This is due to the missing multireference effects in DFT, which are important at stretched geometry of the molecule. All three functionals are behaving relatively in same manner.

We have selected BH molecule for examining the trend of DFT polarizabilities with fully correlated method i.e. full CI. The calculations were

performed with cc-pVDZ basis set. The plots of A_{xzx} and A_{zzz} component of dipole-quadrupole as a function of internuclear distance are given in fig. 6.3a and 6.3b respectively. It is observed from fig. 6.3a and fig 6.3b, that full CI result of A_{xzx} component shows minima at $0.75R_e$ and A_{zzz} component shows maxima at $2R_e$. The minimum observed for A_{xzx} component of compressed internuclear distance is generated correctly by DFT. For all stretched bond length, A_{xzx} component using DFT is in closer agreement with CCSD results. From fig. 6.3b, it is seen that A_{zzz} components calculated with full CI and DFT are overlapping perfectly up to $1.25R_e$. However, from $1.5R_e$ to $2.5R_e$ DFT and full CI results are extremely different from each other. Full CI results show maxima at $2R_e$. However, DFT values are monotonically increasing from $0.5R_e$ to $2R_e$. fig. 6.4a and 6.4b gives α_{xx} and α_{zz} component of dipole-dipole polarizability respectively, as a function of internuclear separation. The dipole-dipole polarizability shows maxima at $0.5R_e$ for α_{xx} and at $2R_e$ for α_{zz}. Among the three functionals, BLYP results for A_{xzx} and α_{xx} are closer to full CI polarizabilities and VWN is most away and this is observed clearly for $0.5R_e$ to R_e.

Tables 6.3 and 6.4 report four different components of dipole-quadrupole polarizabilities of formaldehyde molecule, viz. A_{xzx}, A_{yzy}, A_{zxx}, A_{zyy}. All four components were calculated up to $1.75R_e$. For equilibrium bond distance, R_e, DFT results are in good agreement with CCSD. In, for compressed and stretched C-O bond length, the agreement between DFT and CCSD results is poor. Exceptionally, for A_{xzx} component DFT results are closer to the CCSD values from $1.25R_e$ onwards. Dipole-dipole polarizabilities of H_2CO are reported in table 6.5. The DFT results of dipole-dipole polarizabilities are also in good agreement with CCSD at R_e. At stretched bond length DFT results are seen to be in closer agreement with CCSD for α_{xx} and α_{yy} components. However, α_{zz} component of polarizability DFT values are in poor agreement with CCSD at $0.25R_e$, $0.5R_e$ and $1.5R_e$. Choice of functionals does not have any significant effect on polarizabilities. All functionals provide similar trends. For dipole-dipole polarizabilities, PBE functional is giving better results than the other two functionals. The same is true for dipole-quadrupole polarizabilities. We had observed same in our earlier work.

Dipole-quadrupole polarizabilities and dipole-dipole polarizabilities of CO are reported in table 6.6 and table 6.7 respectively. We chose cc-pVDZ basis set for CO molecule. Our DFT results are compared with CCSD. Dipole-quadrupole

polarizabilities do not show any kind of maxima or minima for CCSD as well as DFT. A_{xzx} component is getting close to CCSD results at $1.5R_e$. The A_{zzz} component from DFT studies is matching well with CCSD results for $0.75R_e$ to $1.25R_e$. However, at $0.25R_e$ and $1.5R_e$, DFT results are nearly 1.5 a.u. higher than CCSD. Dipole-dipole polarizabilities are also calculated with the same basis. The α_{xx} calculated from CCSD is lower than of DFT, except for $0.5R_e$. For $1.5R_e$ DFT results are close to CCSD results for CO molecule. The α_{zz} component calculated with DFT is very close to CCSD value for 0.5 R_e to R_e, whereas the difference between DFT and CCSD results increases gradually from $1.25R_e$ onwards. The difference between CCSD and DFT polarizability is the highest at $1.5R_e$, which is roughly around 2.2 a. u. For NO^+ molecule, we have chosen aug-cc-pVDZ basis set, which is known to be a good basis set for the charged systems. The dipole-quadrupole polarizabilities and dipole dipole polarizabilities of NO^+ are reported in table 6.8 and table 6.9 respectively. Analogous to earlier observations dipole-quadrupole polarizabilities from DFT are in good agreement with CCSD at equilibrium distance. The agreement between DFT and CCSD results is poor for A_{xzx} component at compressed and stretched bond lengths. However, A_{zzz} component is matching well up to Re and beyond R_e at stretched bond lengths the difference between DFT and CCSD results is progressively increasing. Similarly, it is noted from table 6.9, that dipole-dipole polarizability results of DFT are matching well with CCSD at R_e. PBE results are in better agreement with CCSD. For α_{xx} component, DFT results are higher than CCSD for compressed internuclear distances, whereas at $1.25R_e$ and $1.5R_e$ CCSD and DFT results are showing much closer agreement. The DFT results of α_{zz} component are higher than CCSD for $0.5R_e$ and $0.75R_e$. R_e onwards CCSD results are higher than DFT. The difference between DFT and CCSD result increases from R_e to $1.5R_e$, highest difference is observed at $1.5R_e$. In general higher level *ab initio* methods and DFT results of dipole-quadrupole and dipole-dipole polarizabilities are in good agreement with each other equilibrium bond distance, R_e, for all molecules. However for stretched internuclear distances, DFT failed to produce correct trend of dipole-quadrupole and dipole-dipole polarizabilities.

6.5 Conclusions

In this chapter, we have presented a comprehensive study of the dipole-quadrupole polarizability and dipole-dipole polarizability as a function of internuclear distance of the molecule. The polarizabilities calculated with DFT for all selected molecules are compared with *ab initio* results. In general for all molecules DFT results are in good agreement with higher level *ab initio* results near equilibrium distance. In case of HF molecule DFT results failed to produce the trend shown by CCSD results for dipole-quadrupole polarizabilities at stretched geometry. Dipole-dipole polarizabilities have shown the characteristic maxima along stretched bond length from CCSD calculations. Such trend is absent in DFT calculations. The same is noticed from the comparison between ECCSD and DFT for dipole-dipole polarizability. Variation of the basis does not change the trend remarkably. It merely leads to shift of polarizability values. For BH molecule, our comparison between fully correlated full CI polarizabilities and DFT highlights the significance of electron correlation for determining electric properties. Similarly, for double bonded and triple bonded systems, the correlation effects play important role and this is clear from our observations for H_2CO, CO and NO^+ molecule.

We have also studied the effect of different functionals. Among the three functionals i.e. VWN, PBE and BLYP, PBE shows closer agreement with CCSD and full CI results. This is in general true for all molecules. However, at stretched internuclear distance no functional is showing satisfactory results. These results indicate that while the existing DFT functionals describe dynamic correlation appropriately, these are unable to consider static correlation effects. Thus, DFT is unable to account the multireference effects which are significant for strongly correlated systems. Recently, efforts have been done to include the missing correlation by combining DFT with *ab initio* methods such as multi reference (MR) and CI [48-52]. Such method has been proved to be working excellent for describing energy and density of systems where static correlation effects are important [52-54]. To the best of our knowledge, such combined implementation of multi-reference and DFT methods has not been done for calculation of electric response properties. In near future, we aim to study the behaviour of such combined method for electric property calculation. We expect such implementation would lead to correct

description of electric charge distribution of low lying excited states and open shell systems as well as breaking of chemical bond.

Fig. 6.1: Dipole-quadrupole polarizabilities A_{zzz} component (in a.u.) of HF molecule calculated with Sadlej and DZP basis.

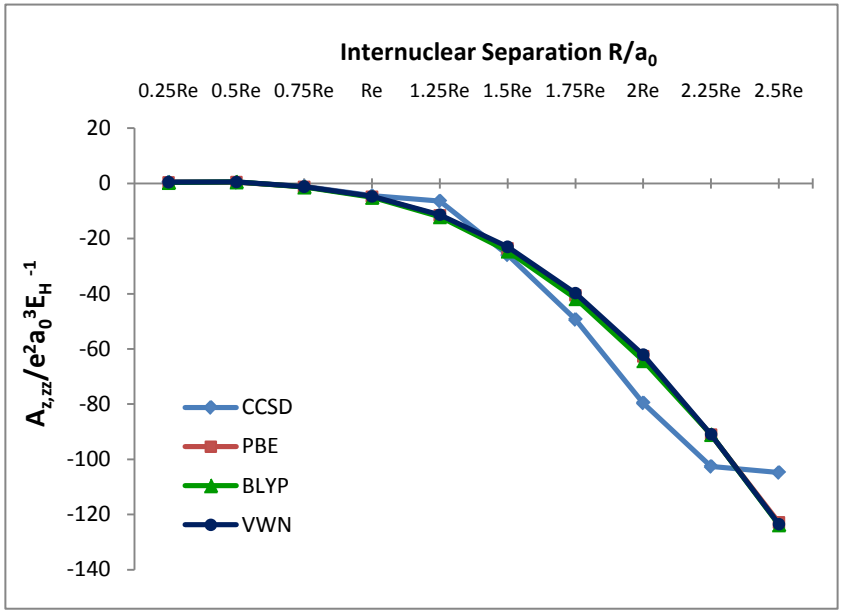

a) Sadlej basis

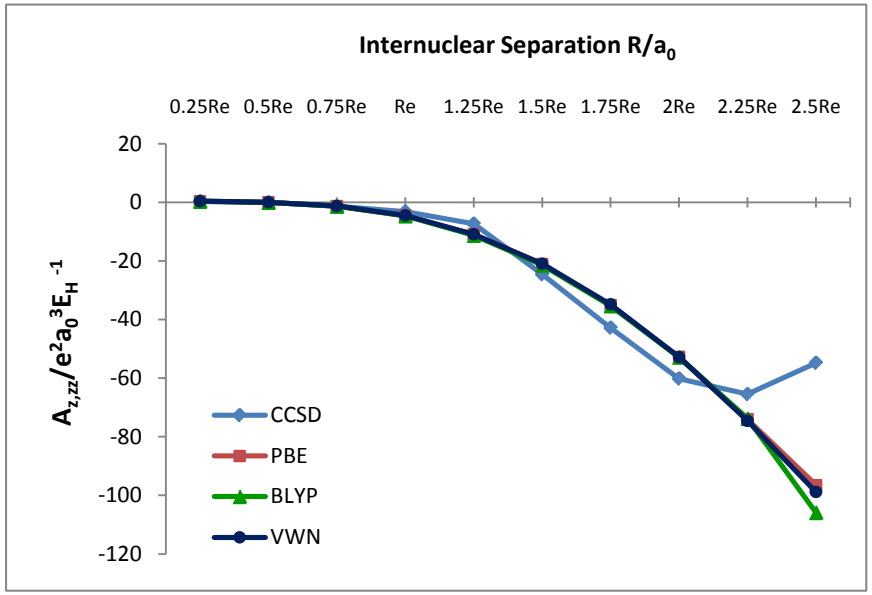

b) DZP basis

Fig 6.2: Dipole-dipole polarizability (α_{xx} and α_{zz} components in a.u.) of HF molecule calculated with aug-cc-pVDZ basis set.

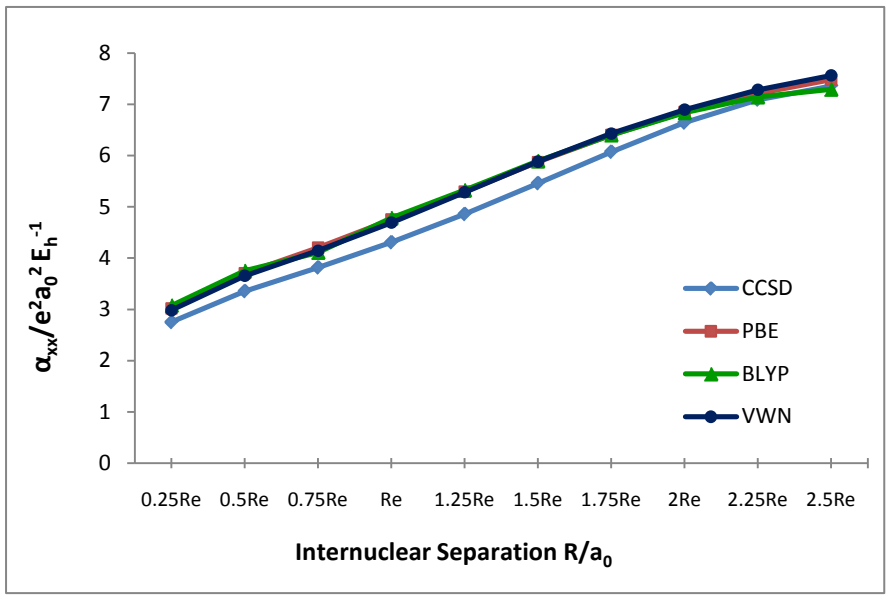

a)α_{xx} component

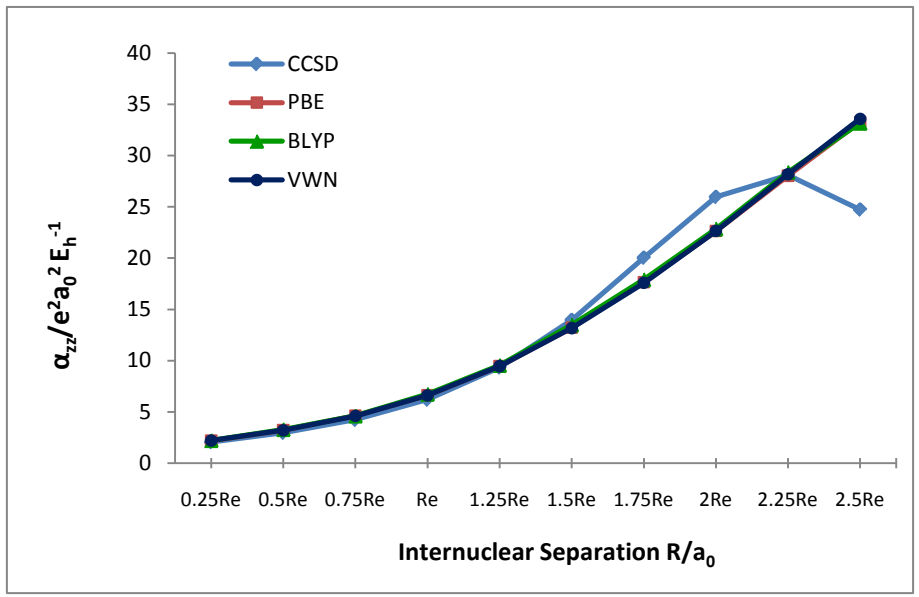

b) α_{zz} component

Fig 6.3: Dipole-quadrupole polarizability (A_{xzx} and A_{zzz} component in a.u.) of BH molecule calculated with cc-pVDZ basis.

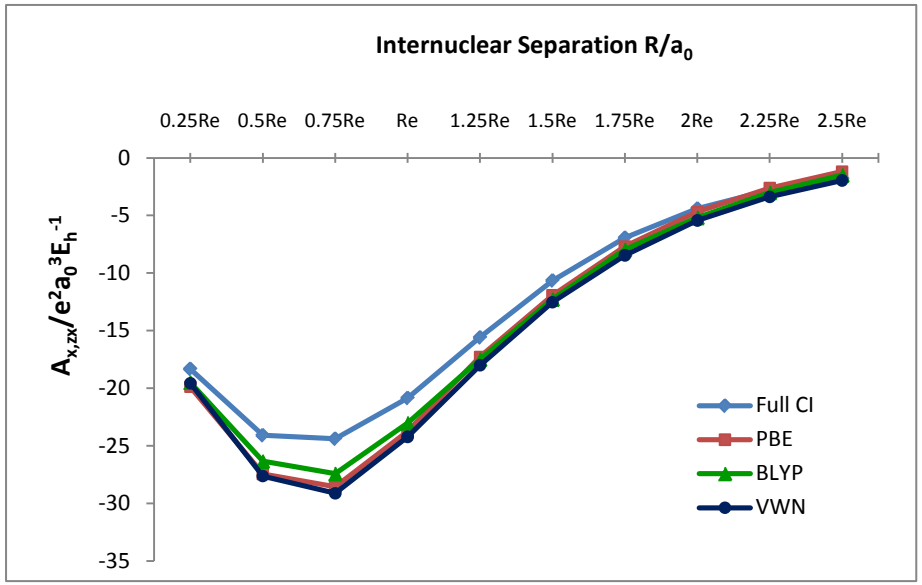

a) A_{XZX}

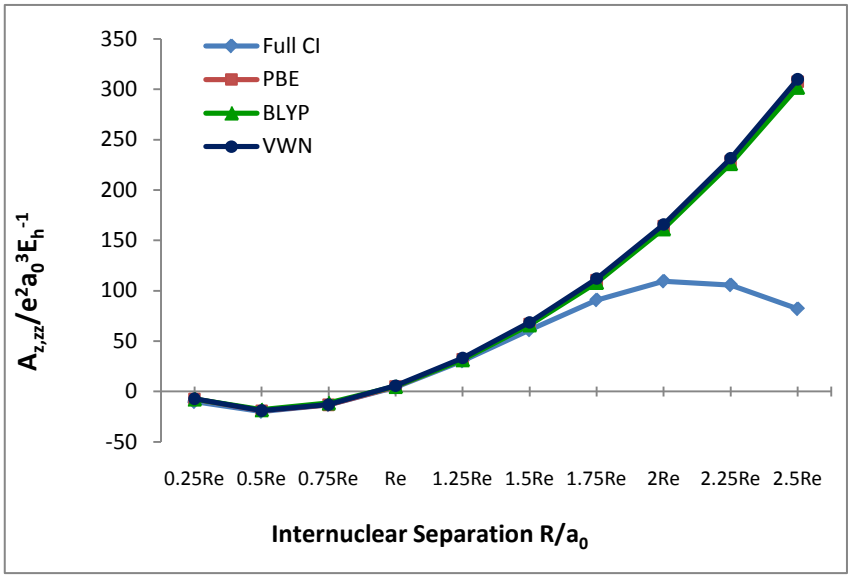

b) A_{ZZZ}

Fig 6.4: Dipole-dipole polarizability (α_{xx} and α_{zz} component in a.u.) of BH molecule calculated with cc-pVDZ basis.

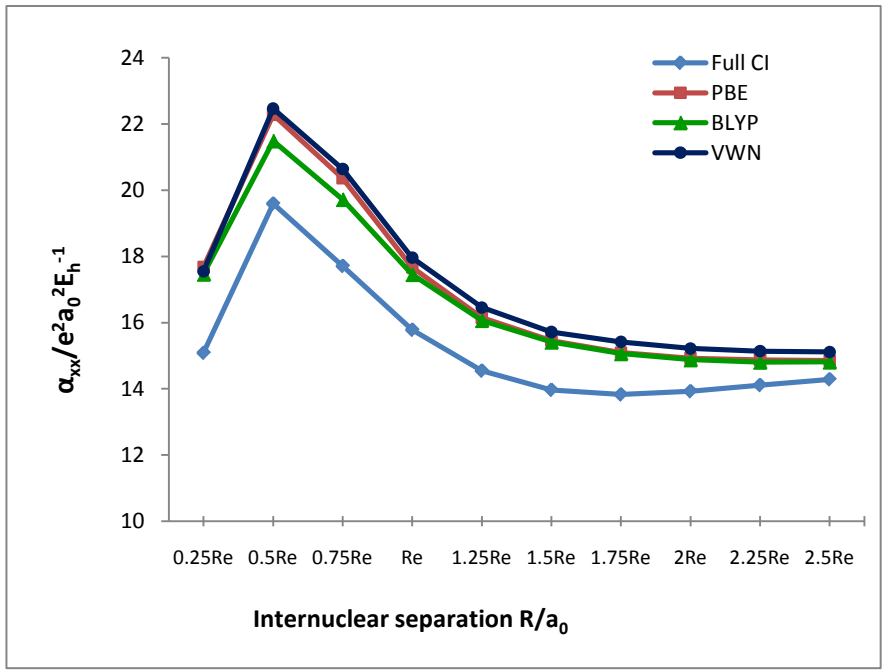

a) α_{xx} component

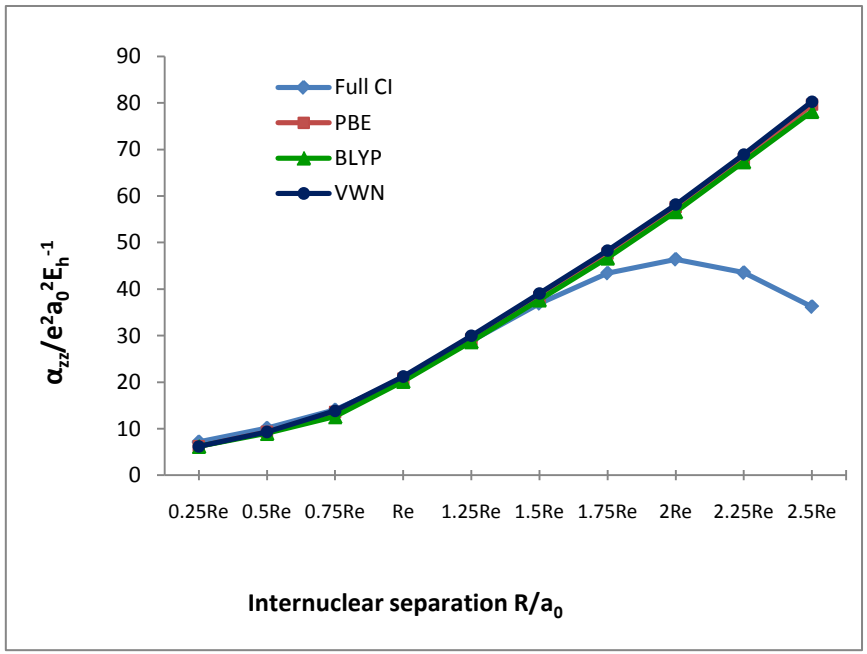

b) α_{zz} component

Table 6.1: Dipole-quadrupole polarizability (A_{xzx} and A_{zzz} component in a.u.) of HF molecule calculated with aug-cc-pVDZ basis set.

	Axzx				Azzz			
R	CCSD	PBE	BLYP	VWN	CCSD	PBE	BLYP	VWN
$0.25R_e$	0.1390	0.1285	0.1023	0.1461	0.5479	0.6004	0.6020	0.6135
$0.5R_e$	-0.0855	-0.2386	-0.3169	-0.2333	0.0814	-0.0531	-0.1146	-0.0177
$0.75R_e$	-0.3903	-0.5777	-0.6200	-0.5786	-1.4773	-1.7959	-1.8405	-1.7490
R_e	-1.1851	-1.4501	-1.5664	-1.4625	-5.1534	-5.7271	-5.8589	-5.6264
$1.25R_e$	-2.5850	-2.8773	-2.9139	-2.9308	-12.8003	-12.9077	-13.1898	-12.7676
$1.5R_e$	-4.7225	-4.9743	-5.0327	-5.0003	-27.0958	-24.8101	-25.3343	-24.5520
$1.75R_e$	-7.7849	-7.4373	-7.4566	-7.4424	-50.508	-41.6793	-43.0311	-41.1576
$2R_e$	-11.7439	-10.2256	-10.2138	-10.2449	-80.8617	-63.8439	-65.2206	-63.6135
$2.25R_e$	-16.1125	-13.1443	-12.9308	-13.2416	-104.5977	-91.6369	-92.7657	-91.7436
$2.5R_e$	-20.0254	-15.9318	-15.1593	-16.1200	-107.2612	-122.809	-122.1649	-123.6400

Table 6.2: Dipole-dipole polarizability (α_{zz} component in a.u.) of HF molecule calculated with Sadlej and DZP basis set.

	(Sadlej) α_{zz}				(DZP) α_{zz}			
R	ECCSD (relaxed)	PBE	BLYP	VWN	ECCSD (relaxed)	PBE	BLYP	VWN
$0.25R_e$		2.5278	2.5733	2.5167		1.2719	1.2660	1.2719
$0.5R_e$		3.5763	3.5851	3.5502		1.6121	1.6013	1.6006
$0.75R_e$	4.555	4.9020	5.0421	4.9207		2.6260	2.5902	2.5858
R_e	6.415	6.8278	7.0402	6.8223	4.32	4.5779	4.5469	4.5049
$1.25R_e$	9.917	9.6270	9.8269	9.6474		7.3926	7.5045	7.3992
$1.5R_e$	14.117	13.4703	13.7561	13.3765	12.83	10.9102	10.9988	10.8783
$1.75R_e$		17.9996	18.3744	17.8898		14.789	14.8353	14.7507
$2R_e$	19.869	22.9549	23.4120	22.9218	20.04	18.9031	18.8927	18.9635
$2.25R_e$		28.5109	28.7059	28.6137		23.1197	23.0268	23.3154
$2.5R_e$	17.532	33.9022	34.1594	34.2550	14.07	26.8402	29.2665	27.5165

Table 6.3: Dipole-quadrupole polarizability (A_{xzx} and A_{yzy} component in a.u.) of H_2CO molecule calculated with Sadlej basis set.

	A_{xzx}				A_{yzy}			
R	CCSD	PBE	BLYP	VWN	CCSD	PBE	BLYP	VWN
$0.5R_e$	-105.3668	-123.3545	-122.5987	-126.9520	-24.0572	-27.6558	-27.2636	-28.3375
$0.75R_e$	-54.6198	-66.9920	-69.7492	-68.3393	-13.9728	-16.1727	-16.1685	-16.3437
R_e	-30.7291	-33.8981	-35.6182	-35.0209	-8.9462	-9.4478	-9.3923	-9.7489
$1.25R_e$	-23.8936	-24.0637	-24.3109	-24.5842	-9.1030	-9.0831	-9.5465	-9.2090
$1.5R_e$	-24.2319	-22.2892	-23.2432	-22.9006	-12.0100	-10.3122	-10.3107	-10.5230

Table 6.4: Dipole-quadrupole polarizability ($A_{z,xx}$ and $A_{z,yy}$ component in a.u.) of H_2CO molecule calculated with Sadlej basis.

	$A_{z,xx}$				$A_{z,yy}$			
R	CCSD	PBE	BLYP	VWN	CCSD	PBE	BLYP	VWN
$0.5R_e$	2.5475	2.7049	2.6317	2.8099	18.9927	23.8598	24.147	24.3599
$0.75R_e$	-1.3386	-2.3637	-3.3004	-2.5537	16.5441	20.4492	21.114	20.7444
R_e	1.6791	1.9273	1.7018	1.9270	13.1453	14.8440	15.6685	15.1748
$1.25R_e$	5.1013	5.4509	5.3992	5.4098	13.8293	12.8652	12.8671	13.2185
$1.5R_e$	10.1629	9.2171	8.1626	8.9939	17.4727	14.5610	14.2680	14.9262
$1.75\ R_e$	17.4084	13.4194	13.2170	13.2467	22.2680	18.4675	18.5861	18.5851

Table 6.5: Dipole-dipole polarizability ($\alpha_{xx,}$, $\alpha_{yy,}$ and α_{zz} components in a.u.) of H_2CO calculated with Sadlej basis set.

R	CCSD	PBE	BLYP	VWN
α_{xx}				
$0.5R_e$	39.0835	45.1711	45.5139	46.3509
$0.75R_e$	21.4087	24.4389	25.0645	24.8203
R_e	17.6397	18.6775	19.0055	18.9713
$1.25R_e$	18.1913	19.1347	19.3387	19.2501
$1.5R_e$	19.5864	20.4541	20.6378	20.6467
$1.75R_e$	20.7258	21.5436	21.8873	21.7621
α_{yy}				
$0.5R_e$	12.9961	14.7552	14.7501	15.0376
$0.75R_e$	10.9896	11.9052	12.0091	11.9825
R_e	12.6302	13.1869	13.0977	13.1946
$1.25R_e$	15.2292	15.6796	15.8382	15.6594
$1.5R_e$	17.6122	17.8411	18.0592	17.7919
$1.75R_e$	18.7842	19.3913	20.0983	19.3205
α_{zz}				
$0.5R_e$	14.3390	16.1506	16.1796	16.3944
$0.75R_e$	18.0182	19.5760	19.7552	19.7753
R_e	22.2218	23.2344	23.6541	23.4099
$1.25R_e$	29.3833	29.5416	30.1213	29.7370
$1.5R_e$	40.3062	38.0035	37.8495	37.9803
$1.75R_e$	51.1393	46.5293	47.6017	47.7805

Table 6.6: Dipole-quadrupole polarizability (A_{xzx} and A_{zzz} component in a.u.) of CO molecule with cc-pVDZ basis set.

	A_{xzx}				A_{zzz}			
R	CCSD	PBE	BLYP	VWN	CCSD	PBE	BLYP	VWN
$0.5R_e$	-11.0405	-10.4939	-10.3742	-10.6007	-8.2220	-7.0801	-7.0195	-7.0728
$0.75R_e$	-12.0212	-12.1767	-11.9978	-12.2982	-9.1283	-9.4075	-9.2772	-9.5038
R_e	-13.3118	-13.6301	-13.4555	-13.8046	-10.4617	-10.6818	-10.5129	-10.8539
$1.25R_e$	-14.7177	-14.9277	-14.8022	-15.1228	-14.0259	-13.5037	-13.3065	-13.7329
$1.5R_e$	-16.0352	-16.0960	-16.0392	-16.2166	-19.7852	-18.6237	-18.4403	-18.8481

Table 6.7: Dipole-dipole polarizability (α_{xx} and α_{zz} component in a.u.) of CO molecule with cc-pVDZ basis set.

	α_{xx}				α_{zz}			
R	CCSD	PBE	BLYP	VWN	CCSD	PBE	BLYP	VWN
$0.5R_e$	7.2040	6.9793	6.9296	7.0406	6.2551	6.0944	6.0739	6.1183
$0.75R_e$	7.8068	8.009	7.9379	8.0837	8.5195	8.6137	8.5890	8.6199
R_e	8.1849	8.4058	8.3384	8.4759	12.8212	12.5540	12.4860	12.5440
$1.25R_e$	8.3037	8.3956	8.3358	8.4534	19.1591	18.0385	17.8870	18.0425
$1.5R_e$	8.1660	8.1345	8.0870	8.1617	26.5255	24.2463	23.9985	24.1973

Table 6.8: Dipole-quadrupole polarizability (A_{xzx} and A_{zzz} component in a.u.) of NO^+ molecule calculated with aug-cc-pVDZ basis set

	A_{xzx}				A_{zzz}			
R	CCSD	PBE	BLYP	VWN	CCSD	PBE	BLYP	VWN
$0.5R_e$	-2.0460	-2.2025	-2.2710	-2.2386	-1.6587	-1.5884	-1.61	-1.6137
$0.75R_e$	-2.5754	-2.6514	-2.5200	-2.6942	-2.0282	-2.0689	-2.0938	-2.1063
R_e	-2.988	-2.9464	-2.9551	-2.9464	-2.7018	-2.4991	-2.4492	-2.4991
$1.25R_e$	-3.4824	-3.2025	-3.3465	-3.2653	-4.7649	-3.6084	-3.7038	-3.6577
$1.5R_e$	-4.2482	-3.4906	-3.6329	-3.6227	-8.4365	-5.5060	-5.5161	-5.5545

Table 6.9: Dipole-dipole polarizability (α_{xx} and α_{zz} component in a.u.) of NO^+ with aug-cc-pVDZ basis set.

	α_{xx}				α_{zz}			
R	CCSD	PBE	BLYP	VWN	CCSD	PBE	BLYP	VWN
$0.5R_e$	3.6746	3.8647	3.9193	3.9104	3.6528	3.7685	3.8301	3.8084
$0.75R_e$	4.7381	4.8782	4.9021	4.9397	5.7138	5.7306	5.7638	5.7468
R_e	5.8408	5.8988	5.9239	5.8988	9.0726	9.0687	9.1008	9.0687
$1.25R_e$	6.7481	6.7742	6.8255	6.8245	13.4070	13.5208	13.6330	13.5564
$1.5R_e$	7.3740	7.3709	7.3439	7.4319	18.7690	18.3360	18.2351	18.3893

References:

1. Gutsev, G.L.; O'Neal, R. H. Jr.; Belay, K. G.; Weatherford C.A. *Chem. Phys.* **2010**, *368*, 113.
2. Jha, P. C.; Seal, P.; Sen, S.; Ågren, H.; Chakrabarti, S. *Comput. Mater. Sci.* **2008,** *44*, 728.
3. Champagne, B.; Eric, A.; Perpète, E.A.; Jacquemin, D. *J. Phys. Chem. A* **2000**, *104*, 4755.
4. Pereiro, M.; Baldomir, D. *Phys. Rev. A* **2007**, *75*, 033202.
5. Calaminici, P.; Jug, K.; Köster, A. M. *J. Chem. Phys.* **1998**, *109*, 7756.
6. Pradhan, K.; Reveles, J. U.; Sen, P.; Khanna, S. N. *J. Chem. Phys.* **2010**, ***132***, 124302.
7. Berlanga-Ramírez, E.O.; Aguilera-Granja, F.; Montejano-Carrizales, J. M.; Díaz-Ortiz, A.; Michaelian, K.; *Phys. Rev. B* **2004** , *70*, 014410.
8. Hohm, U.; Maroulis, G. *J. Chem. Phys.* **2006**, *124*, 124312.
9. Karamamanis, P.; Maroulis, G. *J. Chem. Phys.* **2006**, *124*, 071101.
10. Maroulis, G.; Hohm, U. *Phys. Rev. A* **2007**, *76*, 032504.
11. Quinet, O.; Liégeois, V.; Chanpagne, B. *J. Chem. Theory. Comput.* **2005** *1*, 444.
12. Sophy, K. B.; Pal, S. *J. Chem. Phys.* **2003**, *118*, 10861.
13. Sophy, K. B.; Shedge, S. V.; Pal, S. *J. Phys. Chem. A* **2008** *112*, 11266.
14. Flores-Moreno, R.; Köster, A. M. *J. Chem. Phys.* **2008** *128*, 134015.
15. Flores-Moreno, R. Ph.D. Thesis, **2006** Cinvestav, Mexico City, Mexico.
16. Köster, A. M.; Calaminici, P.; Casida, M. E.; Flores-Mereno, R.; Geudtner, G.; Goursot, A.; Heine, T. Janetzko, F. M.; del Campo, J.; Patchkovskii, S.; Reveles, J. U.; Salahub, D. R.; Vela, A. deMon2k developers, Cinvestav: Mexico City, Mexico **2006**. See http://www.demon-software.com
17. Shedge, S. V.; Carmona-Espíndola, J.; Pal, S.; Köster, A. M. *J. Phys. Chem. A* **2010** *114*, 2357.
18. Shedge, S. V.; Pal, S.; Köster, A. M. *Chem. Phys. Lett.* **2011**, ***510,*** **185.**
19. Hohenberg, P.; Kohn, W. *Phys. Rev.* **1964**, *136*:B864
20. Kohn, W.; Sham, L. J. *Phys. Rev.* **1965**, *140*:A1133

21. Parr, R. G.; Yang, W. Density Functional Theory of Atoms and Molecules, 1989, New York.
22. Savin, A.; In: Seminario JM (ed) Recent Developments and Applications of Modern Density Functional Theory, 1996, p. 327, Elsevier, Amsterdam.
23. Baerends, E. J. *Phys. Rev. Lett.* **2001** *87*, 133004.
24. Becke, A. D. *J. Chem. Phys.* **2003**, *119*, 2972.
25. Bally, T.; Sastry, G. N. J. *Phys. Chem. A* **1997** *101*, 7923.
26. Zhang, Y.; Yang, W. *J. Chem. Phys.* **1998**, *109*, 2604.
27. Perdew, J. P.; Leavy, M. *Phys. Rev. B* **1997**, *56*, 16021.
28. Gunnarsson, O. Lundqvist, B. I. *Phys. Rev. B* **1976** *13*, 4274.
29. Perdew, J. P.; Savin, A.; Burke, K. *Phys. Rev. A* **1995** *51*, 4531.
30. Perdew, J. P. In: Dreizler RM(ed) Density Functional Methods in Physics, 1985, pp. 265, Plenium, New York.
31. Dutoi, A. D.; Head-Gordon, M. *Chem. Phys. Lett.* **2006,** *422*:230.
32. Ruzsinszky, A. Perdew, J. P.; Csonka, G. I.; Vydrov, O. A.; Scuseria, G. E. *J. Chem. Phys.* **2006**, *125*, 194112.
33. Sophy, K. B.; Pal, S. () *J. Mol. Struc. THEOCHEM.* **2004,** *676*, 89.
34. Fowler, P. W. *Mol Phys* **1982**, *47*, 355
35. Bishop, D. M.; Pipin, J.; Kirtman, B. *J. Chem. Phys.* **1995**, *102*, 6778.
36. Huber, K. P.; Herzberg, G. Constants of diatomic molecules Van Nostrand, Princeton, 1979.
37. Kobayashi, R.; Koch, H.; Jorgensen, P. *Chem. Phys. Lett.* **1993**, *211*, 94.
38. Mérawa, M.; Bégué, D.; Pouchan, C. *J. Mo.l Struc. THEOCHEM* **2003**, *633*, 157.
39. Gamess :: Schmidt, M. W.; Baldridge, K. K.; Boatz, J. A.; Elbert, S. T.; Gordon, M. S.; Jensen, J. J.; Koseki S.; Matsunaga, N.; Nguyen, K. A.; Su, S.; Windus, T. L.; Dupuis, M.; Montgomer, J. A. *J.Comput. Chem.* **1993**, *14*, 1347.
40. Vosko, S. H.; Wilk, L.; Nusair, M. *Can. J. Phys.* **1980** , *58*, 1200.
41. Perdew, J. P.; Burke, K.; Ernzerhof, M. *Phys. Rev. Lett.* **1996**, *77*, 3865
42. Becke, A. D. *Phys. Rev. A* **1988**, *38*, 3098
43. Lee, C.; Yang, W.; Parr, R. G. *Phys. Rev. B* **1988**, *37*, 785
44. Calaminici, P.; Janetzko, F.; Köster, A. M.; Mejia-Olvera, R.; Zuniga-Gutierrez, B. *J. Chem. Phys.* **2007**, *126*, 044108.
45. van der Bout, P.; Steed, J. M.; Bernstein, L. S.; Klemperer, W. *Astrophys. J.* **1979,** *234*, 503.

46. Buckingham, A. D. In: Hirsschfelder JO (ed) Advances in chemical physics. 1967 Interscience, New York, p 107

47. Vaval, N.; Pal, S. *Chem. Phys. Lett.* **2004**, *398*, 194.
48. Gusarov, S.; Malmqvist, P. A.; Lindh, R.; Roos, B. O. *Theor. Chem. Acc.* **2004**, *112*, 84.
49. Gräfenstein, J.; Cremer, D. *Chem. Phys. Lett.* **2000**, *316*, 569.
50. Kusakabe, K. *J. Phys. Soc. Jpn.* **2001** *70*, 2038.
51. Yamanaka, S.; Nakata, K.; Takada, T.; Kusakabe, K.; Ugalde, J. M.; Ymaguchi, K.; *Chem. Lett.* **2006**, *35*, 242.
52. Wu, Q.; Cheng, C.; Voorhis, T. V.; *J. Chem. Phys.* **2007**, *127*, 164119.
53. Nakata, K.; Ukai, T.; Yamanaka, S.; Takada, T.; Ymaguchi, K. *Int. J. Quant. Chem.* **2006,** *106*, 3325.
54. Yamanaka, S.; Nakata, K.; Ukai, T.; Takada, T.; Yamaguchi, K. *Int. J. Quant. Chem.* **2006**, *106*, 3312.

CHAPTER 7

Future work and the conclusions

Abstract:

This chapter focuses mainly on the future scope of the NIA-CPKS method. The methodology and the implementation of the NIA-CPKS, discussed so far were limited to the closed shell molecules only. The newer implementation of the NIA-CPKS in SCP formalism facilitates further development of the method for open shell molecules. This implementation will make the NIA-CPKS more inclusive for calculation of static response properties. Further the derivative of dipole-dipole polarizabilities, dipole-quadrupole polarizabilities and electric–magnetic dipole polarizability with respect to normal coordinates can be calculated within deMon2k. In this chapter we have discussed the methodology for implementation of polarizability derivatives. We finally concluded the work presented in this thesis.

7.1 NIA-CPKS for open shell systems

The open shell systems can be studied within DFT either with unrestricted Kohn-Sham (UKS) or with restricted open shell Kohn-Sham (ROKS) approach. For UKS the total electronic density is represented as a sum of α spin density and β spin density.

$$\rho(r) = \rho^{\alpha}(r) + \rho^{\beta}(r) \tag{7.1}$$

Both UKS and ROKS had been implemented in dMon2k. We mainly discuss here the way ROKS and UKS have been implemented in deMon2k. As discussed in chapter1, within ADFT the auxiliary functions are used to fit the charge density. The auxiliary density is also separated into two spin densities contributions as above and from equation (1.36) of auxiliary density we get the following equation,

$$\tilde{\rho}(r) = \tilde{\rho}^{\alpha}(r) + \tilde{\rho}^{\beta}(r) = \sum_{\bar{k}} \left(x_{\bar{k}}^{\alpha} + x_{\bar{k}}^{\beta} \right) \bar{k}(r) \tag{7.2}$$

Here $x_{\bar{k}}^{\alpha}$ and $x_{\bar{k}}^{\beta}$ are spin polarized fitting coefficients which are obtained from separate fitting equations for $\alpha \; and \; \beta$ densities. The spin polarized KS matrix is given as,

$$K_{\mu\nu}^{\sigma} = H_{\mu\nu} + \sum_{\bar{k}} \langle \mu\nu \| \bar{k} \rangle \left(x_{\bar{k}}^{\alpha} + x_{\bar{k}}^{\beta} + z_{\bar{k}}^{\sigma} \right) \tag{7.3}$$

The symbol σ represents the spin, either α or β. In UKS, the two decoupled sets of KS equations are solved similar to unrestricted HF (UHF) method [1]. The α and β Fock matrices are individually diagonalized and the solutions iterated until self-consistency is achieved.

For calculation of response properties within SCP theory for open shell case, the response of the spin polarized density matrix has to be calculated [2-8]. The spin polarised perturbed density is given as:

$$(P^{\sigma})^{\lambda} = \sum_{i,a} \frac{(\mathcal{K}^{\sigma})_{ia}^{\lambda}}{\varepsilon_i^{\sigma} - \varepsilon_a^{\sigma}} \left(c_i^{\sigma} c_a^{\sigma^{\dagger}} + c_a^{\sigma} c_i^{\sigma^{\dagger}} \right) \tag{7.4}$$

The perturbed KS matrix $(\mathcal{K}^{\sigma})_{ia}^{(\lambda)}$ is given in the molecular orbital representation as,

$$\mathcal{K}^{\sigma}{}_{ia}^{(\lambda)} = \sum_{\mu,\nu} c_{\mu i}^{\sigma}\, c_{\mu i}^{\sigma}\, K^{\sigma}{}_{\mu\nu}^{(\lambda)} \tag{7.5}$$

Within NIA-CPKS for UKS the perturbed KS matrix for each spin is calculated by finite difference method. Under this approximation the perturbed KS matrix in atomic orbitals is given as,

$$K^{\sigma}{}_{\mu\nu}^{(\lambda)} = \frac{K^{\sigma}{}_{\mu\nu}(+\Delta F_{\lambda}) - K^{\sigma}{}_{\mu\nu}(-\Delta F_{\lambda})}{2\,\Delta F} \tag{7.6}$$

This perturbed KS matrix calculated from eq. (7.6) can be substituted in eq. (7.5) to calculate the corresponding perturbed densities. The final perturbed density is obtained by adding corresponding perturbed densities of α and β spin. Once the total perturbed density matrix is calculated the dipole-dipole polarizability and dipole quadrupole polarizability components can be obtained from the trace of product of perturbed density matrix and respective moment integrals as shown in formula (3.4) and (3.5).

The other method to deal with open shell systems is ROKS [6, 9, 10]. This is a DFT analogue of Roothaan's open-shell method for Hartree-Fock theory [11]. For ROKS implementation in deMon2k the α and β density matrices (and densities) are used as in the case of UKS case. However, these are built from only one set of MO coefficients. Thus the differences of these two matrices arise solely from the different occupation numbers. As a result, α and β Coulomb and exchange-correlation fitting coefficients are calculated as for UKS. However, in contrast to UKS, only one KS matrix is diagonalized. This KS matrix is built from the α and β Kohn-Sham matrices which are both generated in ROKS [12]. Thus only one set of coefficients is generated using this KS matrix. These coefficients are used to build the density matrix (and density) as described above. Thus for electric properties calculation only one perturbed KS matrix can be generated by finite-field method and thereby the perturbed density can be built for calculation of polarizabilities. The polarizabilities are calculated as per the trace formula. We can follow the same perturbation branch for NIA-CPKS scheme in which the ADPT [8] has been implemented for open-shell case except that the KS matrix is calculated directly by finite-field method.

7.2 Implementation and simulation of VROA in deMon2k

The vibrational Raman optical activity is an important field of research due to its application in determination of the absolute configuration of chiral molecules and the enantiomeric excess of stereoisomer in a given enantiomeric mixture [13-20]. Experimentally, the presence of enantiomer and enantiomeric excess in a mixture can be identified with optical rotation and circular dichroism [21]. These conventional techniques have practical difficulties and these methods are time consuming. Thus ROA has gained attention among all other spectroscopic techniques of studying the structural characteristics of molecule. Compared to NMR, ROA has a significant advantage in structural studies of biomolecules as the much shorter time scale is accessible here due to which short-lived conformers can also be investigated. In contrast to crystallographic methods, it is possible to study the molecules in an aqueous environment with the ROA technique. The first evidence of the scattering mechanism responsible for ROA was observed by Atkins and Barron [22]. In 1971, Barron and Buckingham presented the theoretical background for ROA phenomenon [23]. They defined the dimensionless circular intensity difference (CIDi) to describe the effect of scattering in VROA, which is given as,

$$\Delta = \frac{I^R - I^L}{I^R + I^L} \tag{7.7}$$

where $I^R \; and \; I^L$ are the scattered intensities in right- and left-circularly polarized incident light respectively. For a sample of randomly oriented molecules, the expressions for CIDi of forward and backward Rayleigh (elastic) scattering are

$$\Delta(0^\circ) = \frac{4[45\alpha G' + \beta(G')^2 - \beta(A)^2]}{c[45\alpha^2 + 7\beta(\alpha)^2]} \tag{7.8}$$

and

$$\Delta(180^\circ) = \frac{24\left[\beta(G')^2 + \frac{1}{3}\beta(A)^2\right]}{c[45\alpha^2 + 7\beta(\alpha)^2]} \tag{7.9}$$

The isotropic and anisotropic invariants defined in above equations are given as,

$$\alpha = \frac{1}{3}\alpha_{\alpha\alpha} \; and \; G' = \frac{1}{3}G'_{\alpha\alpha} \tag{7.10}$$

$$\beta(\alpha)^2 = \frac{1}{2}\left(3\alpha_{\alpha\beta}\alpha_{\alpha\beta} - \alpha_{\alpha\alpha}\alpha_{\beta\beta}\right) \tag{7.11}$$

$$\beta(G')^2 = \frac{1}{2}\left(3\alpha_{\alpha\beta}G'_{\alpha\beta} - \alpha_{\alpha\alpha}G'_{\beta\beta}\right), \tag{7.12}$$

$$\beta(A)^2 = \frac{1}{2}\omega\alpha_{\alpha\beta}\varepsilon_{\alpha\gamma\delta}A_{\gamma,\delta\beta} \tag{7.13}$$

where $\varepsilon_{\alpha\gamma\delta}$ is the Levi–Civita tensor (the unit third-rank antisymmetric tensor). In the above equations, α is the electric dipole–dipole polarizability, G' is the linear polarization of the electric dipole moment by the magnetic field component of the incident light (the electric dipole–magnetic dipole polarizability), and A is the electric dipole–quadrupole polarizability. The definition and the formula to evaluate α *and* A have been already specified in earlier chapters of this thesis. The elements of the electric dipole–magnetic dipole polarizability tensor can be defined either with respect to the electric dipole moment or the magnetic dipole moment as [24],

$$G'_{i,j}(-\omega,\omega) = \frac{\partial\mu_i}{\partial B_j(\omega)} \tag{7.14}$$

$$= \frac{\partial m_i}{\partial F_j(\omega)} \tag{7.15}$$

And it can be calculated by the trace formula,

$$G'_{i,j}(-\omega,\omega) = -Tr\left[P_i^{(\lambda)}(-\omega)\cdot\boldsymbol{m}_j\right] \tag{7.16}$$

$$G'_{i,j}(-\omega,\omega) = -Tr\left[\boldsymbol{\mu}_i\cdot P_j^{(\kappa)}(\omega)\right] \tag{7.17}$$

where $P_i^{(\lambda)}$ *and* $P_j^{(\kappa)}$ is the first order derivative of the density matrix with respect to electric field and magnetic field respectively. $\boldsymbol{m}_j$ represents the component of magnetic dipole moment integrals and electric $\boldsymbol{\mu}_i$ the electric dipole moment integrals.

The CIDi mentioned in equation (7.8 and 7.9) account for the Rayleigh scattering of the incident light. The CIDi arising from the Raman scattering, are determined by the vibrational transition moments. These transition moments are generated due to the interaction of scattered light with molecular vibrations, inducing excitations or de-excitations in the different vibrational modes of the molecule. The transition moments can be represented as follows,

$$\langle \nu_{0p}|\alpha_{\alpha\beta}|\nu_{1p}\rangle\langle \nu_{1p}|\alpha_{\alpha\beta}|\nu_{0p}\rangle = \frac{1}{2\omega_p}\left(\frac{\partial \alpha_{\alpha\beta}}{\partial Q_p}\right)\left(\frac{\partial \alpha_{\alpha\beta}}{\partial Q_p}\right) \tag{7.18}$$

$$\langle \nu_{0p}|\alpha_{\alpha\beta}|\nu_{1p}\rangle\langle \nu_{1p}|G'_{\alpha\beta}|\nu_{0p}\rangle = \frac{1}{2\omega_p}\left(\frac{\partial \alpha_{\alpha\beta}}{\partial Q_p}\right)\left(\frac{\partial G'_{\alpha\beta}}{\partial Q_p}\right) \tag{7.19}$$

$$\langle \nu_{0p}|\alpha_{\alpha\beta}|\nu_{1p}\rangle\langle \nu_{1p}|\varepsilon_{\alpha\gamma\delta}A_{\gamma\delta\beta}|\nu_{0p}\rangle = \frac{1}{2\omega_p}\left(\frac{\partial \alpha_{\alpha\beta}}{\partial Q_p}\right)\varepsilon_{\alpha\gamma\delta}\left(\frac{\partial A_{\gamma\delta\beta}}{\partial Q_p}\right) \tag{7.20}$$

Where, $\nu_{0p} and\ \nu_{1p}$are the vibrational ground and excited-state wave functions respectively, for mode p and the corresponding normal coordinate Q_p. $\omega_p$is the harmonic frequency. Thus the transition moments can be calculated from the geometric derivatives of the three tensors $\alpha, A\ and\ G'$. [25, 26],

The above discussion highlights the importance of the electric dipole-dipole and dipole-quadrupole polarizabilities for the study of VROA spectra. In recent years, attempts are made to investigate VROA with *ab initio* techniques. The first HF level calculations of molecular tensors significant in determining ROA intensities were carried out by Amos *et al.* [27]. Using the static approximation of Amos *et al*. CIDis observed in ROA spectra were reported by Polavarapu [28]. This was the first complete theoretical study of ROA. Some studies have reported results calculated with correlated methods such as MCSCF wave functions [29]. An analytical method for evaluating the derivatives of polarizabilities at TDHF level was presented by Quinet and Champagne [30]. The methods have also been developed using TDDFT for calculation of ROA intensities for some small molecules [31, 32]. The theoretical simulation of VROA spectra is time consuming and the calculations demand reasonable accuracy. Thus there is a need for efficient methodology for calculation of ROA CIDi for realistic molecules which overcome the practical difficulties of experimental methods. The main challenge in simulation of the VROA spectra is efficient and accurate calculation of polarizabilities and their geometric derivatives. We have already discussed the implementation NIA-CPKS method for calculation of static dipole-dipole polarizabilities and dipole-quadrupole polarizabilities. It has been observed that the method is reasonably accurate and efficient and hence can be applied for large molecules. However, calculation of

VROA spectra requires the dynamic polarizabilities, which can be calculated with ADPT method. Thus the VROA spectra can be calculated by implementing the methodology to calculate the geometric derivatives of these polarizabilities within deMon2k. The components of the dipole-dipole and dipole-quadrupole polarizabilities can be calculated with ADPT method at given experimental frequency. Similarly, it is possible to calculate the electric dipole–magnetic dipole polarizability using equation (7.16). The first order perturbed density matrix is generated for calculation of dipole-dipole and dipole-quadrupole polarizabilities and magnetic dipole integrals are available in deMon2k. Hence, it is easy to implement electric-magnetic dipole polarizability with ADPT. For calculation of geometric derivatives of these polarizabilities, it is more convenient to calculate the derivatives with respect to Cartesian coordinates first and then transform them into normal coordinates. The derivative of $\alpha, A \; and \; G'$ with respect to atomic Cartesian coordinate a is given as,

$$\alpha_{ij}^{a}(-\omega,\omega) = \frac{\partial \alpha_{ij}(-\omega,\omega)}{\partial a} \tag{7.21}$$

$$A_{i,jk}^{a}(-\omega,\omega) = \frac{\partial A_{i,jk}(-\omega,\omega)}{\partial a} \tag{7.22}$$

$$G'^{a}_{i,jk}(-\omega,\omega) = \frac{\partial G'_{i,jk}(-\omega,\omega)}{\partial a} \tag{7.23}$$

The geometric derivative of these polarizabilities can be calculated numerically by small geometric distortion. The central difference formula with suitable step size can be used for derivative calculation of each component of polarizability.

$$\alpha_{ij}^{a}(-\omega,\omega) = \frac{\alpha_{ij}(+\Delta a) - \alpha_{ij}(-\Delta a)}{2\,\Delta a} \tag{7.24}$$

The values $+\Delta a$ and $-\Delta a$ in the parentheses denote the symmetrically chosen coordinate value and Δa is the magnitude of the geometric displacement. Other two derivatives given in equation (7.22) and (7.23) can be obtained using same formula. Similarly, the derivatives of static polarizabilities obtained from NIA-CPKS can be calculated. The static polarizability derivatives calculated from NIA-CPKS and ADPT can be compared to test the exactness of the implementation. The method can be validated by the assessment of these results with higher level results. Thus progressively we can develop a methodology for simulation of VROA spectra.

7.3 Conclusions

In this thesis we discussed the electric repose properties in detail. We presented here the new method for efficient calculation of dipole-dipole and dipole-quadrupole polarizabilities. This approach can be further extended for calculation of non-linear response properties such as hyperpolarizability. Our method can be applied to lager systems; hence, it is possible to study the NLO properties of some experimentally important molecules. The results of polarizabilities presented here have validated our method for calculation of reasonably accurate values. In first chapter we have defineded the electric response properties and a brief overview of the literature have been presented. We have also discussed various electronic structure methods available for calculation of various properties. In chapter 1, we have focussed on the methods which have been used for this work. In our discussion we have emphasised mainly on DFT. The structure of the deMon2k program and the LC-GTO approach has been discussed in detail. The earlier implementation of NIA-CPKS and ADPT formalism for calculation of electric response properties have been presented in this chapter. The chapter ends with the short discussion on MD simulation and property calculation within MD. In chapter 2 we have reported dipole-polarizabilities for azoarene molecule and its di-substituted derivatives. The aim of this chapter is to validate our implementation and compare the NIA-CPKS and ADPT method. We have successfully produced the trend of the polarizabilities supposed to be observed for these push-pull systems, hence both the methods have been validated. Chapter3 is more technical chapter where the newer implementation of the NIA-CPKS version of SCP for calculation of dipole-dipole and dipole-quadrupole polarizabilities has been given described. The newer implementation of the NIA-CPKS has been validated by calculation of dipole-quadrupole polarizabilities of tetrahedral molecules, these results are reported in chapter 4. In chapter 5, we have presented thorough study of temperature and frequency effects on dipole-quadrupole polarizabilities of the P_4 and admantane molecule. The effect of temperature for accurate calculation of dipole-quadrupole polarizability of adamantane molecule has been highlighted by our calculation. In chapter 6, we have discussed results of the dipole-dipole polarizabilities and dipole-quadrupole polarizabilities at distorted geometries calculated using various functionals. We have argued here the need of better functional or the new methodology such as MR-DFT

to take into account the static correlation for calculation of electric response properties of the molecules at distorted geometries. In present chapter we have discussed the methodology for extending our NIA-CPKS implementation for open-shell molecules. The implementation of polarizability derivatives using ADPT method will facilitate the simulation of VROA spectra within deMon2k.

References

1. Pople, J. A.; Nesbet, R. K. *J. Chem. Phys.* **1954**, *22*, 571.
2. Diercksen, G.; McWeeny, R. *J. Chem. Phys.* **1966**, *44*, 3554.
3. Dodds, J. L.; McWeeny, R.; Raynes, W. T.; Riley, J. P. *Mol. Phys.* **1977**, *33*, 611.
4. Dodds, J. L.; McWeeny, R.; Sadlej, A. J. *Mol. Phys.* **1977**, *34*, 1779.
5. McWeeny, R. *Phy. Rev.* **1962**, *126*, 1028.
6. McWeeny, R. in: Sekino, H. (Ed.), Methods of Molecular Quantum Mechanics, Academic Press, London, 2001
7. Flores-Moreno, R. Ph.D. Thesis, Cinvestav, Mexico City, Mexico, 2006.
8. Flores-Moreno, R.; Köster, A. M. *J. Chem. Phys.* **2008**, *128*, 134105.
9. Okazaki, I.; Sato, F.; Yoshihiro, T.; Ueno, T.; Kashiwagi, H. *J. Mol. Struct. (THEOCHEM)* **1998,** *451*, 109.
10. M. Filatov and S. Shaik, Chem. Phys. Lett. 288, 689 (1998).
11. C. C. J. Roothaan, Rev. Mod. Phys. 32, 179 (1960).
12. Russo, T. V.; Martin, R. L. Hay, P. J. *J. Chern. Phys.* **1994**, *101*, 7729.
13. Barron, L. D.; Hecht, L.; Gargaro, A. R.; Hug, W. *J. Raman Spectrosc.* **1990**, *21*, 375.
14. Hug, W. *Handbook of Vibrational Spectroscopy* (Wiley, Chichester, 2002), Vol. 1, p. 175.
15. Ruud, K.; Helgaker, T.; Bour, P. *J. Phys. Chem. A* **2002**, *106*, 7448.
16. Zuber, G.; Hug, W. *Helv. Chim. Acta* **2004**, *87*, 2208.
17. Barron, L. D.; Hecht, L.; McColl, I. M.; Blanch, E. W. *Mol. Phys.* **2004**, *102*, 731.
18. Zuber, G.; Goldsmith, M. R.; Beratan, D. N.; Wipf, P. *ChemPhysChem* **2005** , *6*, 595.
19. Haesler, J.; Schindelholz, I.; Riguet, E.; Bochet, C. G.; Hug, W. *Nature (London)* **2007**, *446*, 526.
20. McColl, I. H.; Blanch, E. W.; Gill, A. C.; Rhie, A. G. O.; Ritchie, M. A.; Hecht, L.; Nielsen, K.; Barron, L. D. *J. Am. Chem. Soc.* **2003**, *125*, 10019.
21. Djerassi, C. Optical Rotatory Dispersion: Applications to Organic Chemistry; McGraw-Hill: New York, 1960.

22. Barron, L. D. Molecular Light Scattering and Optical Activity; Cambridge University Press: Cambridge, 1982.
23. Barron, L. D.; Buckingham, A. D. *Mol. Phys.* **1971**, *20*, 1111.
24. A. D. Buckingham, *Adv. Chem. Phys.* **1967**, *12*, 107.
25. Placzek, G. *Handb. Radiol.* **1934**, *6*, 205.
26. Liégeois,v.; Ruud,K.; Champagne, B. *J. Chem. Phys.* **2007**, *127*, 204105.
27. Amos, R. D. *Chem. Phys. Lett.* **1982,** *87*, 23.
28. Polavarapu, P. L. *J. Phys. Chem.* **1990**, *94*, 8106.
29. Helgaker, T.; Ruud, K.; Bak, K. L.; Jørgensen, P.; Olsen, *J. Faraday Discuss* **1994**, *99*, 165.
30. Quinet, O.; Champagne, B. *J. Chem. Phys.* **2001**, *115*, 6293.
31. Ruud, K.; Helgaker, T.; Bouř, P. *J. Phys. Chem. A* **2002**, *106*, 7448.
32. Bouř, P. *J. Comput. Chem.* **2001**, *22*, 426.

Appendix A

Input I : Calculation of dipole-quadrupole polarizability using NIA-CPKS within deMon2k.

```
TITLE Dipole-quadrupole polarizability componenents of P4
#
GRID FIXED
AUXIS (GEN-A2*)
VXCTYPE PBE
POLARIZABILITY NIACPKS DQ FFS=0.001
SCFTYPE CDF=1.E-7 TOL=1.E-9
MATINV ANALYTICAL DIA TOL=1.E-12
#
BASIS (aug-cc-pVDZ)
#
END
GEOMETRY  ANGSTROM
P  -0.776334   0.776334  -0.776334
P   0.776334  -0.776334  -0.776334
P  -0.776334  -0.776334   0.776334
P   0.776334   0.776334   0.776334
```

Note: For calculation dipole-dipole polarizability keyword DQ should be replaced by DD.

Input II : Calculation of dipole-quadrupole polarizability using ADPT within deMon2k.

```
TITLE Dipole-quadrupole polarizability componenents of P4
#
GRID FIXED
AUXIS (GEN-A2*)
VXCTYPE PBE
POLARIZABILITY DQ w=0.088558
SCFTYPE CDF=1.E-7 TOL=1.E-9
MATINV ANALYTICAL DIA TOL=1.E-12
#
BASIS (aug-cc-pVDZ)
#
END
GEOMETRY  ANGSTROM
P  -0.776334   0.776334  -0.776334
P   0.776334  -0.776334  -0.776334
P  -0.776334  -0.776334   0.776334
P   0.776334   0.776334   0.776334
```

Note: Frequency value (w) is in atomic unit.

Input III : Calculation of MD trajectories within deMon2k.

```
Title P4 BOMD with VWN
#
LPCONSERVE ON
VISUALIZE MOLDEN MD
VELOCITIES RANDOM LP=0 T=1000
BATH NOSE NHC=3 FREQ=1500 T=1000
DYNAMICS STEP=1.0 MAX=100000 INT=10
#
# Optimized Z-Matrix coordinates
#
END
GEOMETRY  ANGSTROM
P  -0.776334   0.776334  -0.776334
P   0.776334  -0.776334  -0.776334
P  -0.776334  -0.776334   0.776334
P   0.776334   0.776334   0.776334
```

Input IV: Calculation of dynamic dipole-quadrupole polarizabilities along MD trajectories using ADPT within deMon2k.

```
TITLE pole-quadrupole polarizability along MD trajectory for
P4
#
GRID FIXED
AUXIS (GEN-A2*)
POLARIZABILITY DQ w=0.088558
SCFTYPE CDF=1.E-7 TOL=1.E-9
VXCTYPE PBE
MATINV ANALYTICAL DIA TOL=1.E-12
SIMULATION CALCULATE POLARIZABILITY INT=100
#
BASIS (aug-cc-pVDZ)
#
#
END
GEOMETRY  ANGSTROM
P  -0.776334   0.776334  -0.776334
P   0.776334  -0.776334  -0.776334
P  -0.776334  -0.776334   0.776334
P   0.776334   0.776334   0.776334
```